RESULTS AND DISCUSSION

Eichhornia crassipes (Mart.) Solms, an aquatic weed was chosen in the present work considering the immediate need of attention the plant requires. Isolation, structure elucidation of compounds from various extracts of the dried plant and its bio-, pharma activity screening has been carried out. The results of the work along with relevant discussions are given in this chapter.

4.1 Extraction of plant material

Extraction involves the use of an inert solvent which actively separates the molecules from the plant parts. Reflux method and percolation was used for the bulk extraction of metabolites from *E. crassipes*.

4.1.1 Alkaline ethanolic extraction of dried *E. crassipes*

Dried *E. crassipes* (1.5 kg) was extracted by reflux with petroleum ether for 6 h which yielded 8 g of petroleum ether extract. The residual plant material was then extracted twice with 2 N ethanolic potassium hydroxide for 6 h. The alkaline ethanol extract was desolvetised and refluxed thrice with acetone for 1 h which yielded 300 g of acetone extract.

4.1.2 Sequential extraction of dried *E. crassipes*

Percolation technique was adopted for the sequential extraction of metabolites from *E. crassipes.* Percolation depends on the size of the plant material, types and temperature of the solvent (**Sarker *et al,* 2006**). In the present study, a temperature of 74 °C was maintained throughout the extraction. The coarsely ground plant material (28 kg) was extracted by percolation with ethyl acetate twice for 6 h and then with water twice for 6 h yielding 300 g and 1.2 kg of ethyl acetate and aqueous extract respectively.

4.1.3 Fractionation of aqueous extract

A crude extract may contain a number of metabolites clubbed together. These metabolites can be separated by simple fractionation with solvents of diverse polarity. Liquid-liquid fractionation was adopted for fractionating the aqueous extract of *E. crassipes*. The aqueous extract (200 g) was fractionated with ethanol yielding 150 g of aqueous fractionate (AFE) and 50 g of ethanol fractionate (EFA). The aqueous extract (600 g) was also fractionated with methanol yielding 400 g of aqueous fractionate (AFM) and 150 g of methanol fractionate (MFA).

4.1.4 Extraction of fresh and dried *E. crassipes* by different methods

Resurgence in plant derived chemicals in the past few decades necessitates the need of optimizing a suitable extraction method. The extraction of metabolites from dried material is typically a two step process that involves steeping the plant material in solvent to facilitate swelling and hydration processes and the mass transfer of soluble constituents from the material to solvent by diffusion and osmotic processes (**Vinatoru, 2001**).

Extraction of dried leaves and shoot portion of *E. crassipes*

The yield of the extraction of *E. crassipes* (20 g) by various methods of extraction for 3 h in ~250 mL solvent is given in Table 8. Reflux method gave a higher yield of the extract compared to the other methods. A unique feature noted during extraction was, that the dried plant material floated over the solvent in the extracting vessel. This might be due to the presence of large number of wax like compounds as noted in certain other plants (**Amaral *et al,* 1990**). The observed increase in the yield of extraction by the reflux method may probably be due to the rapid evaporation and condensation of the solvent at its boiling point onto the floating plant material thus catalyzing the extraction. Furthermore, temperature of extraction condition affects many physical properties including viscosity, diffusivity, solubility and surface tension (**Yang *et al,* 2008; Boonkird *et al,* 2008**). In reflux method, an increased temperature is obvious which allows the solvent to have higher capacity to solubilize analytes, while surface tension and solvent viscosity decreases with temperature, which improves sample wetting and matrix penetration, respectively (**Amirah *et al,* 2012**).

Table 8. Yield (g) of extracts obtained in different extraction methods for dried *E. crassipes* (3 h)

S.No	Solvent used for extraction	Method		
		Reflux	Ultrasonic homogenizing	Sonication
		Yield (g)		
1	Ethyl acetate	0.405	0.369	0.410
2	Ethanol	**1.649**	1.116	1.012
3	Methanol	0.719	0.643	0.394
4	Water	1.503	0.818	0.714

A comparison of the yield obtained in various solvents for dried *E. crassipes* revealed that the yield of ethyl acetate extract obtained in extraction using ultrasonic

bath was comparable with that of the reflux method and homogenizer assisted sonic extraction. The higher yield of ethyl acetate extract can be due to the agitation in the sonic bath that might have caused efficient steeping of ethyl acetate due to its less viscosity compared to the other solvents used for extraction (**Pires *et al,* 2007**). On agitation, the solvent penetrates through the dried plant material providing an efficient extraction. Similar observations are reported in the extraction of ginseng using sonic probe and sonic bath (**Wu *et al,* 2001**). The authors have noted better yields of extraction using sonic bath than with probe and have claimed agitation and higher temperature obtained in the sample container as the cause. Extraction of dried *E. crassipes* using ethanol has given better yield than other solvents in all the methods. This shows that large quantities of relatively polar compounds are present in the plant material that gets extracted in ethanol in the sequential extraction process.

Extraction of fresh leaves and shoot portion of *E. crassipes*

The yield of the extracts obtained from extraction of 350 g fresh *E. crassipes* in three selected solvents by three different methods is given in Table 9. It is apparent from the table that ultrasonic homogenization gives high yield of the extract compared to other methods of extraction. The yield of ethyl acetate extract obtained in ultrasonic homogenizing was approximately 4 times more than reflux method and 3 times more than the yield from extraction using ultrasonic bath. Similar trend has been noted with other two solvents where the yield of extract obtained by ultrasonic homogenizing was approximately 2-3 times more than sonication and reflux method. Hence, it is obvious from the results that ultrasonic homogenization best suits extraction of fresh *E. crassipes*.

Table 9. Yield of the extract obtained by conventional and sound assisted extractions for fresh *E. crassipes*

S.No	Solvent used for extraction	Method and Yield of the extracts (mg)		
		Reflux	Ultrasonic homogenizing	Sonication
1	Ethyl acetate	80	360	121
2	Ethanol	1490	4630	1539
3	Water	590	1330	770

Several researchers have reported the advantage of the use of ultrasonic homogenizer (**Paniwnyk *et al,* 2001; Sheu *et al,* 2009; Alupului *et al,* 2009; Yang**

***et al,* 2009**) and ultrasonic bath (**Boonkird *et al,* 2008; Zhang *et al,* 2009**) for extracting the plant metabolites. Sonic extraction in most cases has proved to improve the extraction yield (**Vintoru, 2001, Wang and Weller, 2006**) and this was found to hold good for the extraction of fresh *E. crassipes*. Ultrasound can facilitate swelling and hydration and so cause an enlargement in the pores of the cell wall. This involves the diffusion process and therefore enhances mass transfer (**Vinatoru, 2001**). The enhancement of extraction efficiency by ultrasound is partially due to its efficacy in breaking down cell walls by the mechanical waves. These waves formed by the ultrasound enable generation locally of micro-cavitations in the solvent surrounding the plant material and therefore, a heating of this plant material, enhancing the release of the extract (**Alupuli *et al,* 2009**). Cavitation bubbles produced, collapse at or near walls or interfaces thus improving the mass transfer across the solid-liquid interface thus introducing a kinetic energy in the whole volume (**Alupului *et al,* 2009**). The solvent diffuses through the cell wall and washes out the cell contents once the cell wall is broken and this phenomenon is greatly affected by ultrasonic irradiation.

Furthermore, a high yield was noted in ultrasonic homogenization than from sonication in a bath. The joint action of the cavitations and the efficient breaking of the cell walls (**Torti *et al,* 1995**), higher ultrasound energy provided using ultrasonic homogenizer (**Wu *et al,* 2001**) might have contributed to the higher yield of extracts. Several studies have reported the higher extraction efficiency of ultrasonic homogenizer extraction (probe) compared to sonic bath extraction (**Torti *et al,* 1995; Salgado *et al,* 2006; Pereira *et al,* 2010**).

Extraction of fresh *E. crassipes* with ethyl acetate by ten different methods

The yields of extraction of fresh *E. crassipes,* with ethyl acetate by ten different methods *viz.,* reflux, sonication using ultrasonic bath, ultrasonic homogenizing, hot continuous extraction (soxhlet), microwave assisted extraction, percolation, maceration, infusion, digestion, hot aqueous extraction (decoction) is given in Table 10. The aim of the use of different extraction methods for extracting the active components is to increase the yield of extraction and reduce the hours of extraction normally required. To adjudge the suitability of the better extraction method, it was aimed at choosing a single solvent and hence ethyl acetate, a medium polar solvent was chosen for the present study. Extraction was continued till the solvent became colourless indicating the completion of the process and hence the variation in time of extraction in different

methods.

It is conspicuous from Table 10 that the yield of the extract obtained from infusion was more (750 mg) than the yield obtained from other techniques. The yield of the extract obtained in refluxing, sonication, decoction, maceration and digestion was almost one-third the yield obtained from infusion method. Ultrasonic homogenising, soxhlet extraction and microwave method gave almost equal amounts of yields (around 400-500 mg). Infusion involves grinding the plant material with minimum amount of solvent and then dissolving the soluble portion in solvent. This might have resulted in complete extraction of soluble matter, hence the highest yield compared to all other methods adopted.

Table 10. Time and yield of ten different methods of extraction of fresh *E. crassipes* with ethyl acetate

Method of extraction	Time (h)	Yield (mg)
Reflux	6	170
Sonication	5	130
Ultrasonic Homogenising	2	525
Soxhlet	1	540
Microwave Extraction	1.40	400
Percolation	600 (h.c)*	500
	600 (c.c)*	400
Maceration	72	200
Infusion	½	**750**
Digestion	1	250
Decoction	1	200

*hot condition; cold condition

4.2 Secondary metabolite profiling

Profiling of the metabolites isolated from *E. crassipes* was carried out using GC-MS. Mass spectral library search is the first step in any mass spectral interpretation. The aim of a library search is either to obtain a correct structure hit of compounds already in the library or to obtain partial structural insights from compounds that nearly match. For that purpose, an experimental mass spectrum is searched against a large collection of already recorded mass spectra that are stored in a database (**Kind and Fiehn, 2010**).

4.2.1 Isolation and profiling of sterols

The sterol mixture (Yield- 300 mg) isolated from *E. crassipes* by the procedure of **Wang *et al*** (**2002**) tested positive in Liebermann-Burchard and Salkowski's test. TLC of the sterols in 1:1 petroleum ether:ethyl acetate followed by detection with 10% sulphuric acid and anisaldehyde reagent revealed two distinct brown spots and a trailing spot indicating a mixture of sterols. The observed brown colour of the spots may perhaps be due to the mixture of sterols rather than a specific sterol. The colour of the spot varies with the nature of sterol. β-sitosterol and stigmasterol gives pink and greyish violet colour respectively when sprayed with 10% sulphuric acid and anisaldehyde reagent (**Archana *et al,* 2011**) and this, as a mixture might probably be responsible for the brown colour spots of the isolated sterols. Functional groups that form coloured products include double bonds and cyclic ethers (**http://www.sigmaaldrich.com**).

The GC data of the isolated sterol indicated the presence of 12 components (Figure 1). The GC separated peak at RT 13.96 showed the presence of an ion at *m/z* 253 and 209 suggesting the presence of Δ^5 sterols. The peaks at *m/z* 255 and 211 are indicative of Δ^5 sterols (**Li *et al,* 2007**). The presence of oxo sterols in the isolated sterol fraction was noted from ions at *m/z* at 55 and 98 in the GC separated fraction at RT 16.17. These peaks are due to the cyclo-hexanone-type rearrangement which starts with α-cleavage and ends with the formation of ions of *m/z* 55 and 98 (**Kasal *et al,* 2010**). The presence of peak at *m/z* 283 was noted in the MS of the GC separated fraction at RT 18.42 and 19.69 indicating the presence of Δ^{23} as noted by **Wretensjo and Karlberg** (**2002**).

The results indicated the fragmentation of the side chain together with the cleavage of the rings. The fragmentation pattern of sterols is rather complex involving breakdown processes followed by complex hydrogen transfers. This complexity implies that a given structural unit may give rise to a set of typical fragmentation patterns in one type of sterol, but not in another (**Wretensjo, 2004**). **Goswami *et al* (1983)** has reported the presence of stigmasterol, sitosterol and campesterol in sterol mixture of *E. crassipes* analysed by GLC. The present study also reveals the presence of such type of sterols in *E. crassipes*.

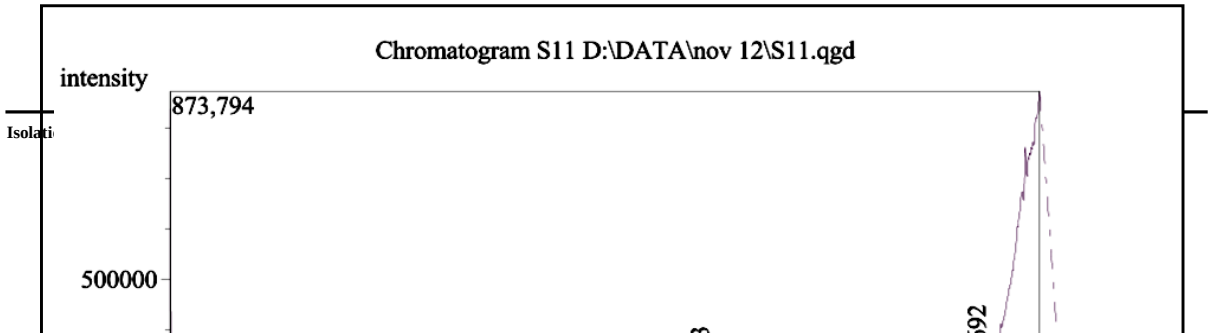

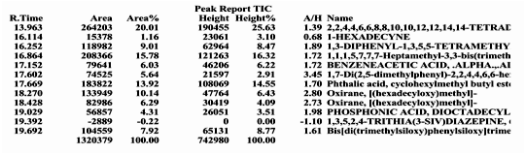

Peak Report TIC

R.Time	Area	Area%	Height	Height%	A/H	Name
13.963	264203	20.01	190455	25.63	1.39	2,2,4,4,6,6,8,8,10,10,12,12,14,14-TETRAE
16.114	15378	1.16	23061	3.10	0.68	1-HEXADECYNE
16.252	118982	9.01	62964	8.47	1.89	1,3-DIPHENYL-1,3,5,5-TETRAMETHY
16.864	208366	15.78	121263	16.32	1.72	1,1,1,5,7,7,7-Heptamethyl-3,3,3-bis(trimeth
17.152	79641	6.03	46206	6.22	1.72	BENZENEACETIC ACID, .ALPHA.,.AI
17.602	74525	5.64	21597	2.91	3.45	1,7-Di(2,5-dimethylphenyl)-2,2,4,4,6,6-he
17.669	183822	13.92	108069	14.55	1.70	Phthalic acid, cyclohexylmethyl butyl est
18.270	133949	10.14	47764	6.43	2.80	Oxirane, [(hexadecyloxy)methyl]-
18.428	82986	6.29	30419	4.09	2.73	Oxirane, [(hexadecyloxy)methyl]-
19.029	56857	4.31	26051	3.51	1.98	PHOSPHONIC ACID, DIOCTADECYL
19.392	-2889	-0.22	0	0.00	-1.10	1,3,5,2,4-TRITHIA(3-SIV)DIAZEPINE,
19.692	104559	7.92	65131	8.77	1.61	Bis[di(trimethylsiloxy)phenylsiloxy]trime
	1320379	100.00	742980	100.00		

Figure 1. Gas chromatogram of sterols isolated from *E. crassipes*

4.2.2 Isolation and profiling of alkaloids in methanol fractionate of aqueous extract of *E. crassipes*

The alkaloids in the methanol fractionate of aqueous extract of *E. crassipes* was isolated by slight modification of the method of **Shekar** (**2008**). The isolated fraction (Yield- 300 mg) tested positive for Dragendorrf's test, Mayer's test and Wagner's test. The alkaloids chromatographed on TLC [Methanol:NH_4OH (200:3)], gave three distinct spots of bright blue, blue and orange colour with an R_f 0.8, 0.7 and 0.5 respectively. Bright blue and blue spots obtained in UV indicate cytisine and quinine respectively (**Harborne, 1973**). TLC detection of cytisine, nicotine, tomatine, codeine, thebaine and quinine in the aqueous extract of *E. crassipes* is reported (**Lata and Dubey, 2010**). The isolated alkaloid fraction in the present study, may probably contain cytisine and quinine.

The GC-MS profiling of alkaloids indicated the presence of one compound in major quantity (RT 12.95) along with 17 other compounds in minor quantity (Figure 2). The compound at RT 12.95 showed a base peak at *m/z* 61 in mass spectra indicating the presence of a nitromethane group. The other fragments at *m/z* 73, 87, 123, 193, 207, 219, 235, 252, 281 might be due to the loss of H_2O, CH_2 and C≡N indicating of the presence of alkaloids. Similar type of fragmentation pattern has been observed in indole alkaloids (**Ogalde *et al,* 2009**). Hence, the isolated fraction might contain indole alkaloids. The other compounds at RT 12.34 and 17.20 had a base peak

at *m/z 55* and fragmentation pattern that indicated the presence of hydrocarbons in the alkaloids isolated from the methanol fractionate of aqueous extract of *E. crassipes*.

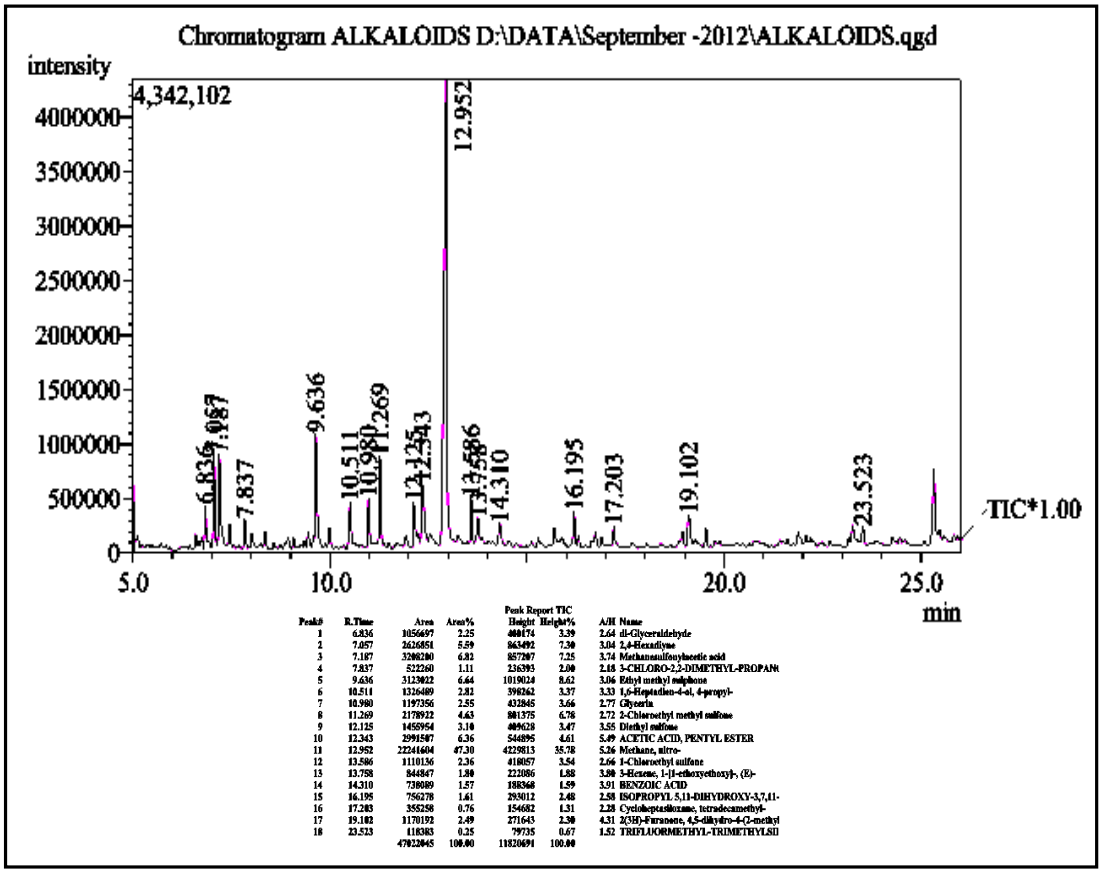

Figure 2. Gas Chromatogram of alkaloids isolated from methanol fractionate of aqueous extract of *E. crassipes*

4.2.3 Isolation and profiling of terpenoids

The terpenoids (Yield- 4 mL) isolated from the ethyl acetate extract of *E. crassipes* by flash column chromatography gave a positive chloroform test for terpenoids. The TLC of the terpenoids in 8.5:1.5 petroleum ether:ethyl acetate showed two major spots in UV at R_f 0.90 and 0.64 which showed a blue and red fluorescence respectively. Detection with 10 % sulphuric acid in ethanol gave purple and brown colour spot correspondingly.

GC chromatogram of the terpenoids indicated the presence of eight major components. The gas chromatogram with retention time and the percentage area are given in Figure 3. The mass spectral fragmentation pattern of the compound eluted at RT 3.05 showed a base peak at *m/z* 56 and the other fragment was noted at *m/z* 72. This indicated the presence of hydrocarbon and the library match showed it to be of 3-Amino-2,2-dimethyl-1-propanol. The compound eluted at RT 5.05 in GC showed a base peak at *m/z* 57 (due to acylium ion) and fragment ions at *m/z* 71 and *m/z* 99

denoted the presence of alkane and the compound was identified as 3,5-dimethyl heptane.

The compound eluted at RT 23.54 in GC gave fragment ions at *m/z* 413, 341, 327, 281, 207, 147 and 73 (base peak) and this corresponded to 3-Butoxy-1,1,1,7,7,7-hexamethyl-3,5,5-tris(trimethylsiloxy) tetra siloxane. The compound eluted at RT 25.32 gave fragment ions at *m/z* 55, 60, 73, 83, 115, 129, 157, 253 and the library match indicated the compound to be hexadecanoate. The compounds eluted at RT 29.97 and 31.34 were identified as dodecene-L-ribofuranose (base peak at *m/z* 253) and 1,2 benzenedicarboxylic acid (base peak 149) respectively based on its fragmentation pattern and mass spectral library match.

The compound eluted at RT 32.59 and 35.83 from GC gave a base peak at *m/z* 73 and 81 indicating the presence of hexadecanoic acid and 6-octen-1-ol respectively from the mass spectral library match. The isolated terpenoids from *E. crassipes* was found to contain mono terpenoids which is obvious from the GC-MS profiling.

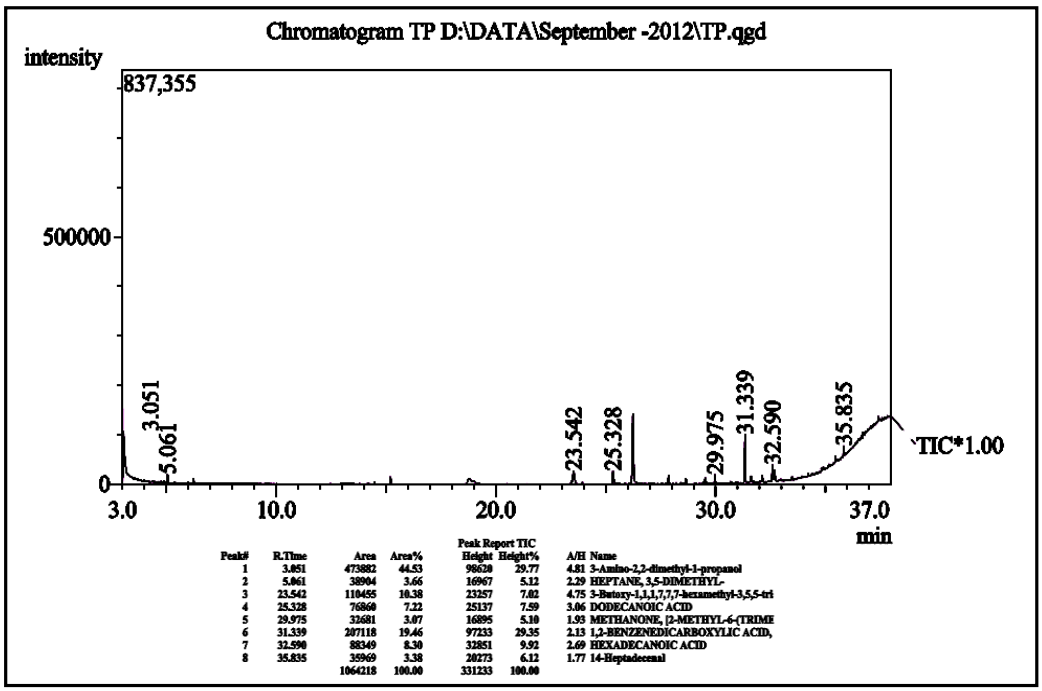

Peak Report TIC

Peak#	R.Time	Area	Area%	Height	Height%	A/H	Name
1	3.051	473882	44.53	98628	29.77	4.81	3-Amino-2,2-dimethyl-1-propanol
2	5.061	38904	3.66	16967	5.12	2.29	HEPTANE, 3,5-DIMETHYL-
3	23.542	110455	10.38	23257	7.02	4.75	3-Butoxy-1,1,1,7,7,7-hexamethyl-3,5,5-tri
4	25.328	76860	7.22	25137	7.59	3.06	DODECANOIC ACID
5	29.975	32681	3.07	16895	5.10	1.93	METHANONE, [2-METHYL-6-(TRIME
6	31.339	207118	19.46	97233	29.35	2.13	1,2-BENZENEDICARBOXYLIC ACID,
7	32.590	88349	8.30	32851	9.92	2.69	HEXADECANOIC ACID
8	35.835	35969	3.38	20273	6.12	1.77	14-Heptadecenal
		1064218	100.00	331233	100.00		

Figure 3. Gas Chromatogram of terpenoids isolated from ethyl acetate extract of *E. crassipes*

4.3 Phytochemical screening of the plant extracts

Phytochemical screening of the plant extracts provides an understanding of the nature of the metabolites present in that particular extract thereby helping in choosing appropriate isolation procedure. The phytochemical screening of the petroleum ether

(PE), acetone (Ac), ethyl acetate (EA), aqueous (AQ), acid (HE), the aqueous fractions *viz.* chloroform (CF), ethanol (EF), and aqueous (AF), aqueous fractionate (AFE) and ethanol fractionate (EFA), aqueous fractionate (AFM), methanol fractionate (MFA), chloroform (CE), ethanol (EE) and methanol (ME) extracts are summarized in Table 11. The results obtained show the presence of flavonoids, alkaloids, terpenoids, sterols, tannins, phenol carbohydrates, anthraquinone, anthocyanins and proteins in different extracts.

Phytochemicals synthesized by plants are used for long in the treatment of many ailments. Understanding the nature of phytochemicals becomes an integral part in any study involving these metabolites. A large number of phytochemicals possessing innumerous activity have been isolated from plants.

Alkaloids are heterocyclic indole compounds which have established pharmacological properties (**Gao *et al,* 2012; Nagappan *et al,* 2011; Cherney and Baran, 2011; Ignacimuthu and Shanmugam, 2010; Nantachit *et al,* 2010; Ismail *et al,* 2009; Frederich *et al,* 2008; Grycova *et al,* 2007; Mallikharjuna *et al,* 2007; Molyneux *et al,* 2002; Luca and Pierre, 2000; Henry, 1949**). The presence of flavonoids and tannins in all the plants is likely to be responsible for the free radical scavenging effects observed. Flavonoids and tannins are phenolic compounds and plant phenolics are a major group of compounds that act as primary antioxidants or free radical scavengers (**Polterait *et al,* 1997**).

Flavonoids exhibit pharmaceutical activities (**Nessa *et al,* 2012; Sandhar *et al,* 2011; Shohaib *et al,* 2011; Buer *et al,* 2010; Lafuente et al, 2009; Tapas *et al,* 2008; Safi *et al,* 2007; Andersen and Markham, 2006; Grotewold, 2006; Cushnie and Lamb, 2005; Bylka *et al,* 2004; Ren *et al,* 2003; Chao *et al,* 2002; Nijveldt *et al,* 2001**) like antiallergic, anti-inflammatory, antimicrobial and anticancer activity (**Yamato and Gayor, 2002**). Steroids (anabolic steroids) have been observed to promote nitrogen retention in osteoporosis and in animals with wasting illness (**Aliu and Nwude, 1982**). Triterpenoids are a large class of natural isoprenoids present in higher plants, which exhibit a wide range of biological activities (**Chen *et al,* 2012; Leandro *et al,* 2012; Yoo and Park, 2012; Gupta *et al,* 2011; Thoppil and Bishayee, 2011; Devappa *et al,* 2010; Goto *et al,* 2010; Nassar *et al,* 2010; Yermakov *et al,* 2010; Ajikumar *et al,* 2008; Zwenger and Basu, 2008; Omara *et al,* 2007; Isvett *et al,* 2002**).

Anthocyanins exhibit important antioxidant and anti-inflammatory actions as well as chemotherapeutic effects (**Lee *et al,* 2009**). Anthraquinones are a main source of

natural dye, which are gaining importance due to the environmental pollution caused by synthetic dyes (**Ledwani and Singh, 2005**). Carbohydrate is reported to have numerous roles in living things, such as the storage and transport of energy (starch, glycogen) and structural components (cellulose in plants, chitin in animals). Additionally carbohydrates and their derivatives play major role in the working process of the immune system, fertilization, pathogenesis, blood clotting and development (**Madziga *et al,* 2010**).

Secondary metabolites like alkaloids, reducing compounds, polyoses, saponins, glycosides, tannins etc are reported in *E. crassipes* (Table 12) by phytochemical screening (**Baral and Vaidya**, **2011a,b**; **Lata and Dubey, 2010a**; **Sharshar and Haroon**, **2009; Vasu *et al,* 2009**; **Nduibuisi *et al,* 2007**).

In the present study, extracts obtained by different extraction methods have been screened for the presence of phytochemicals. Additionally, there are no reports on the phytochemical screening of the petroleum ether, ethyl acetate, acetone, ethanol extract and fractionates of *E. crassipes*. The presence of phytochemicals such as anthocyanins, quinones and proteins was noted in extracts of *E. crassipes* which have not been previously reported. The phytochemical screening of the aqueous extract of *E. crassipes* revealed the absence of terpenoids whereas its presence has been reported by **Lata and Dubey** (**2010a**). **Nduibuisi *et al*** (**2007**) has reported the presence of alkaloids and anthraquinones in the chloroform extract of *E. crassipes* whilst the absence of these phytochemicals was noted in the chloroform extract in this study. **Vasu *et al*** (**2009**) and **Shanab *et al*** (**2011**) have reported the presence of alkaloids, triterpenes, phenolics and sterols in the methanol extract of *E. crassipes* whereas these phytochemicals were absent in the methanol extract in the present study. This might be due to the variation in extraction procedures, geographical location of the collection of the plant and other factors like harvest time, climate conditions and age (**Mossi *et al,* 2009)**. Phytochemicals in the extract also depends on the method, conditions and solvent used for the extraction and hence, the variation in the phytochemical constituents.

Aqueous extract was found to contain relatively more number of metabolites than other extracts. In an attempt to minimize the complexity of the extract, liquid-liquid fractionation has been adopted for partitioning aqueous extract with ethanol and methanol. Presence of flavonoids, anthraquinones, anthocyanins and carbohydrates were noted in MFA whereas AFM tested positive for alkaloids and quinones. EFA showed the presence of alkaloids, flavonoids, anthraquinones, anthocyanins and

quinones whereas it's aqueous fractionate AFE showed the presence of quinones and carbohydrates. Rather than employing a single isolation procedure for the isolation of compounds from the cocktail of metabolites, solvent fractionation might be employed prior to any isolation technique. The results obtained also confirm that solvent fractionation aids in simplifying the process of isolation of compounds. The affirmative results of the phytochemical screening test of the extracts of *E. crassipes* prompted us to isolate the metabolites from the plant extracts.

Table 12. Phytochemicals in various extracts of *E. crassipes*

S.No	Plant part	Extract	Phytochemicals	Reference
1 A	Shoot portion of dry plant	Aqueous	Tannin, phlobtannin, alkaloid, flavonoid, steroid, terpenoid, phenolics quinone, anthraquinone, cardiac glycosides	Lata and Dubey, 2010a
B	Rhizome portion of dry plant	Aqueous	Tannin, alkaloid, flavonoid, steroid, terpenoid, phenolics quinone, anthraquinones	Lata and Dubey, 2010a
2	Dried plant (Part of the plant-not mentioned)	Hexane Methanol Aqueous	Alkaloids Reducing compound Polyoses, saponins and alkaloid salts	Baral and Vaidya, 2011a
3	Whole plant (Dry)	Hexane Methanol Aqueous	Alkaloids Reducing compound Polyoses, saponins and alkaloid salts	Baral and Vaidya, 2011b
4	Dried plant (Part of the plant-not mentioned)	Methanol	Alkaloids, phenolic compounds, terpenoids	Shanab *et al*, 2011
5	Leaves of dried plant	Not mentioned	Glycosides, tannins, flavonoids, sterols, terpenes and alkaloids	Sharshar and Haroon, 2009
6	Whole plant (Dry)	Methanol	Alkaloid, ellagic acid, phenol, steroid, triterpenoids tannin and saponin	Vasu *et al*, 2009
7	Leaves	Chloroform	Saponin, alkaloid, glycoside and anthraquinone	Ndubuisi *et al*, 2007

Table 11. Preliminary phytochemical screening of the solvent extracts and solvent fractionates of aqueous extracts of *E. crassipes*

S.No	Phytochemicals	PE	Ac	EA	AQ	HE	CF	EF	AF	EFA	AFE	MFA	AFM	CE	EE	ME
1	**Alkaloids**															
A	Mayer's test	-	+	-	+	+	+	+	-	-	-	-	+	-	-	-
B	Wagner's test	-	+	-	+	+	-	+	+	+	+	-	-	-	-	-
C	Hager's test	-	+	-	+	+	-	+	-	-	-	-	-	-	-	-
2	**Flavonoids**															
A	NaOH Test	+	-	-	+	-	-	-	-	-	-	-	-	-	+	-
B	H_2SO_4 test	+	-	-	+	+	-	+	-	+	-	+	-	-	+	-
3	**Sterols**															
A	Liebermann-Burchard test	-	+	-	+	+	+	+	+	-	-	-	-	-	-	-
4	**Terpenoids**															
A	Liebermann-Burchard test	-	+	-	-	-	-	+	-	-	-	-	-	-	-	-
5	**Anthraquinones**															
A	Borntrager's test	-	+	+	+	+	+	+	+	+	-	+	-	-	+	+
6	**Anthocyanins**															
A	NaOH test	-	+	-	+	-	-	+	+	+	-	+	-	+	-	-
7	**Proteins**															
A	Ninhydrin test	-	-	-	+	-	-	+	-	-	-	-	-	+	+	+
8	**Phenolics**															
A	Ferric chloride test	-	-	-	-	-	-	+	-	-	-	-	-	+	+	-
B	Libermann's test	-	-	+	-	-	+	+	+	-	-	-	-	+	+	-
9	**Quinones**															
A	HCl test	-	-	-	+	+	-	-	+	+	+	-	+	-	-	-
10	**Carbohydrates**															
A	Molisch test	-	-	-	-	+	-	-	-	-	-	-	-	+	+	+
B	Fehling's test	-	-	-	-	+	-	-	-	-	+	+	-	-	+	+

The study subsequent to the present work with ethanol extract of fresh *E. crassipes* stated the presence of alkaloids, flavonoids, sterols, terpenoids, anthraquinones, proteins, phenols and quinones (**Thamaraiselvi *et al,* 2012**). Presence of alkaloids, flavonoids, sterols, terpenoids, anthraquinones, anthocyanins, phenols and quinones in the ethyl acetate extract of fresh *E. crassipes* are documented (**Sujitha *et al,* 2012**).

4.4 Isolation of compounds from *E. crassipes*

4.4.1 Isolation of compounds from acetone extract of *E. crassipes*

4.4.1.1 Structure elucidation of A5

Column chromatography of acetone extract on elution with 99:1 petroleum ether: ethyl acetate furnished a compound designated as A5 (Yield- 8.5 g).

Physical description

(i) Appearance- Orange viscous liquid.

Chemical characteristics

(i) Liebermann Burchard test- Red ring indicating the presence of terpenoids.

(ii) TLC - R_f - 0.6 (5:1 petroleum ether:ethyl acetate), strong iodine absorption.

(iii) Solubility- Miscible with petroleum ether, acetone, ethyl acetate, chloroform, ethanol and methanol.

Spectral interpretation

UV ($CHCl_3$) λ_{max} : 256, 261 and 293 nm.

FTIR : 3443, 1713, 1673, 1624, 1577, 1131, 1060 and 950 cm^{-1}.

Mass : 334 $[M^+]$, 316 $[M\text{-}H_2O]^+$, 252 $[M\text{-}C_6H_{10}]^+$, 238 $[M\text{-}C_6H_{10}\text{-}CH_2]^+$, 225 $[M\text{-}C_6H_{10}\text{-}C_2H_3]^+$, 211 $[M\text{-}C_6H_{10}\text{-}C_2H_3\text{-}CH_2]^+$, 197 $[M\text{-}C_6H_{10}\text{-}C_2H_3\text{-}CH_2\text{-}CH_2]^+$, 160 (100) $[M\text{-}C_6H_{10}\text{-}C_2H_3\text{-}CH_2\text{-}C_4H_3]^+$, 142 $[M\text{-}C_6H_{10}\text{-}C_2H_3\text{-}CH_2\text{-}C_4H_3\text{-}H_2O]^+$, 126 $[M\text{-}C_6H_{10}\text{-}C_2H_3\text{-}C_7H_{15}]^+$.

The UV spectrum (Figure 4) (chloroform, λ_{max}) exhibited absorption bands at 256, 261 and 293 nm corresponding to n→π* transitions. The IR spectrum (Figure 5) showed presence of hydroxyl –OH (band at 3443 cm^{-1}), carbonyl (1713 cm^{-1}), C–O moiety (1131 cm^{-1}, 1060 cm^{-1}) as well as olefinic (1673 cm^{1}, 1624 cm^{-1}, 1577 cm^{-1} and 950 cm^{-1}) functionalities.

NMR interpretation

The ^1H NMR spectrum of A5 is given in Figure 6. The signal at δ_H 0.92 was attributed to the methyl protons. The singlets at δ_H 1.82, δ_H 1.84, δ_H 1.94, δ_H 1.97 and

the quartet at δ_H 2.05 corresponds to methine proton resonance. The signal at δ_H 2.69 indicated the presence of methylene proton adjacent to olefinic proton. The deshielded proton signal at δ_H 5.94, δ_H 5.86, δ_H 5.78 and δ_H 7.36 corresponds to the methine protons adjacent to double bond. The doublet at δ_H 2.17 might be due to the deshielded methyl protons, adjacent to carbonyl group.

Interpretation of the ^{13}C NMR spectrum (Figure 7a) together with DEPT 45 spectrum (Figure 7b) and DEPT 135 (Figure 7c) exhibited a conjugated structure consisting of four methyl carbons (δ_C 28.30, δ_C 28.10, δ_C 31.80; δ_C 31.98) of which two are deshielded (δ_C 31.80; δ_C 31.98), one methylene (δ_C 39.45), nine methine (δ_C 24.56, δ_C 24.70, δ_C 39.44, δ_C 45.05, δ_C 45.67, δ_C 45.92, δ_C119.80, δ_C 121.07 and δ_C 125.29) and six quarternary carbons (δ_C 31.00, δ_C 31.61, δ_C 147.84, δ_C 148.76, δ_C 151.66 and δ_C 153.35). The characteristic carbon resonances at δ_C 199.298, δ_C 198.668 suggest the presence of two quaternary oxygenated carbons in the compound. The ^{13}C NMR spectrum of A5 revealed the presence of more than 20 carbon atoms.

In the ^{1}H-^{1}H COSY spectrum (Figure 8) of the compound, the key couplings indicated connectivity between the proton at δ_H 7.36 → δ_H1.97, δ_H 7.36 → δ_H1.84, δ_H 5.86 → δ_H1.94 and δ_H 5.86 → δ_H1.82. The cross peaks between the proton at δ_H 5.94 and δ_H 2.69 indicated the coupling between the two protons. Off-diagonal peaks between the singlet at δ_H 5.78 and the quartet at δ_H 2.05 were observed. The HSQC spectrum (Figure 9) revealed the short range ^{1}H-^{13}C coupling in the molecule.

Mass fragmentation of A5 involves the loss of $–(CH_2)_n–$ and the loss of H_2O. Owing to the difficulty in recording HMBC spectrum and processing of peaks for HSQC spectrum beyond 150, the coupling between carbonyl could not be established. From the spectral analysis, the presence of the following groups –CH=CH–CH–C–C=; –CH–CH–CH–; –CH=CH–; $–CH_2–$CH= and eight quarternary carbons inclusive of two carbonyl carbons is evident. Thus, the compound is characterized to be diterpene which was further confirmed by Liebermann-Burchard's test.

Diterpenes occuring in all plant families have limited therapeutic importance and are used in the formulation of expectorants; cough sedatives and antispasmodics. Taxol, an anticancer drug, Forskolin, a weight reduction drug, Stevioside, a sweetener and many pharmacologically active compounds belong to the class of diterpenes. Hence, the isolation of diterpene from *E. crassipes* in quantitative yield (9 g compound from 100 g acetone extract) is noteworthy and the plant can be considered as a good source of pharmacologically active diterpenes.

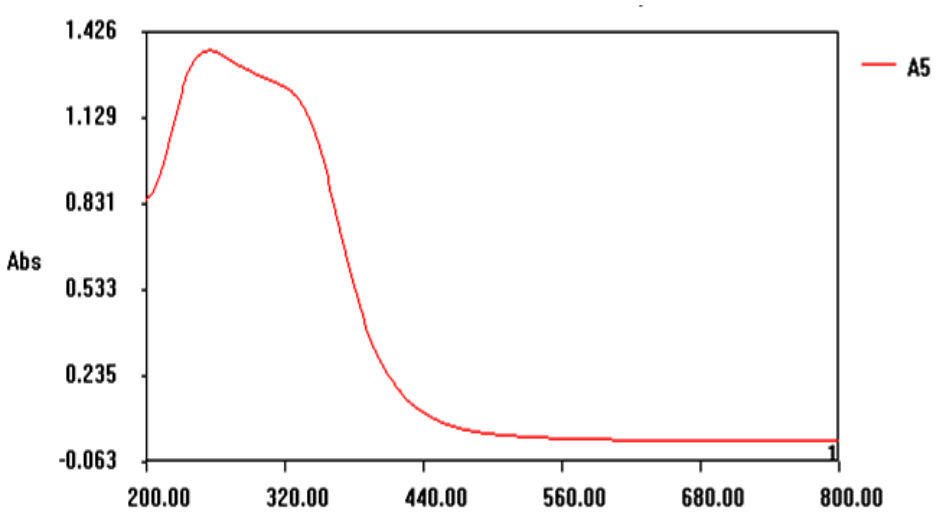

Peak Pick		Valley Pick	
293.6	1.281	459.2	0.067
234.8	1.260	203.6	0.855
261.2	1.353	384.8	0.477
224.0	1.108	209.6	0.895
256.4	1.359	374.0	0.638

Figure 4. UV spectrum of A5

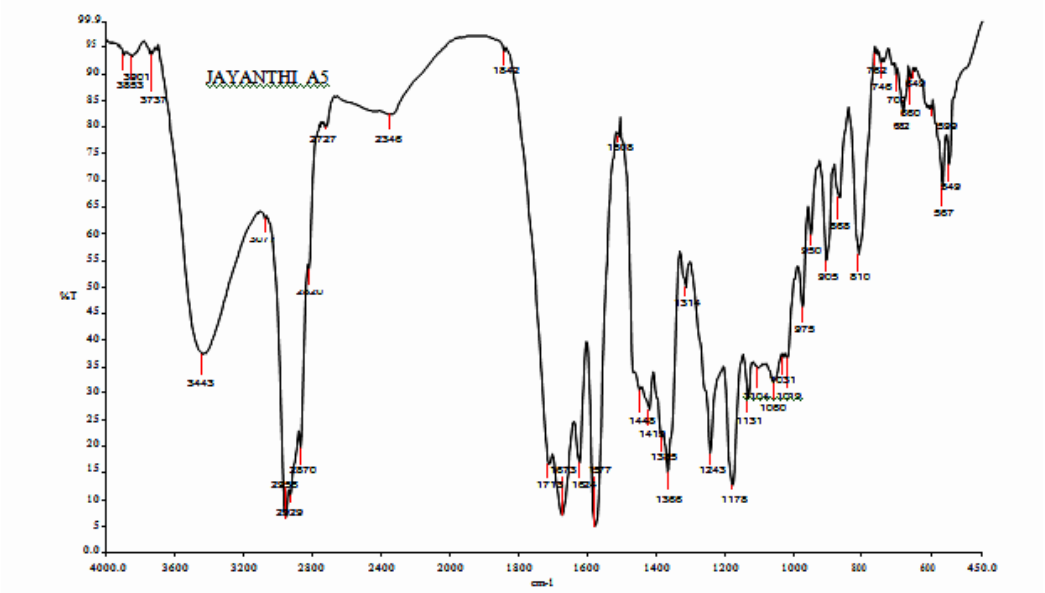

Figure 5. IR spectrum of A5

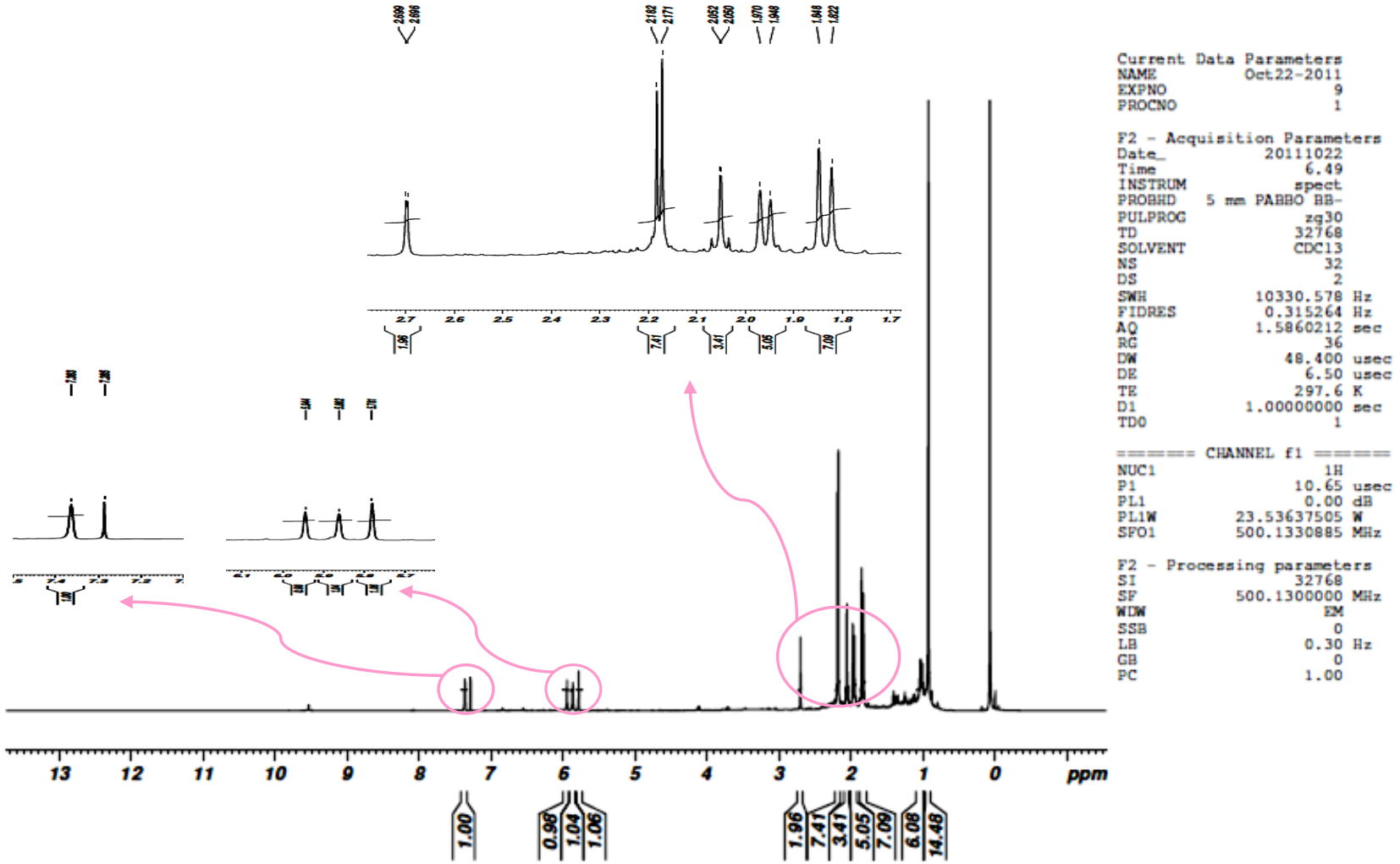

Figure 6. ^{1}H NMR spectrum of A5

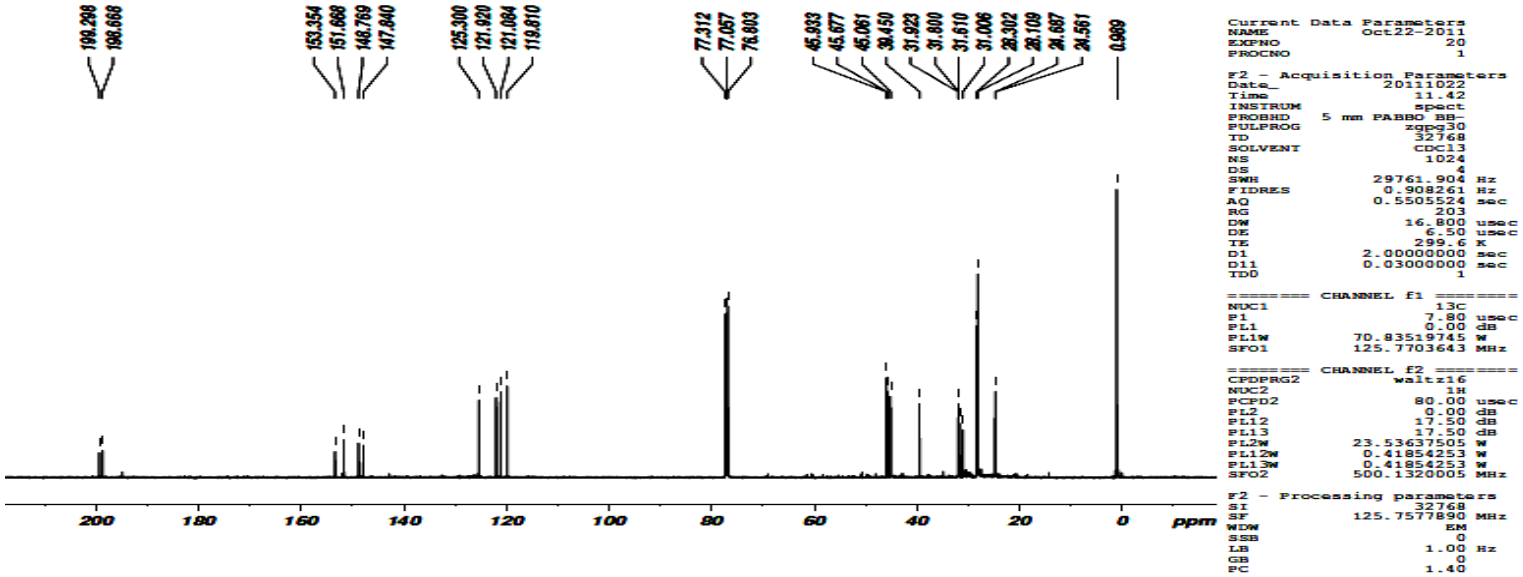

Figure 7a. ^{13}C NMR spectrum of A5

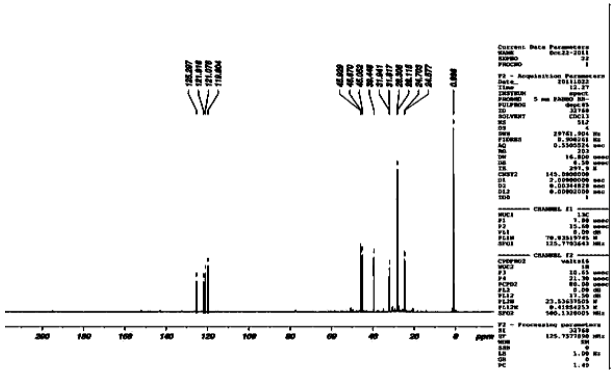

Figure 7b. DEPT 45 spectrum of A5

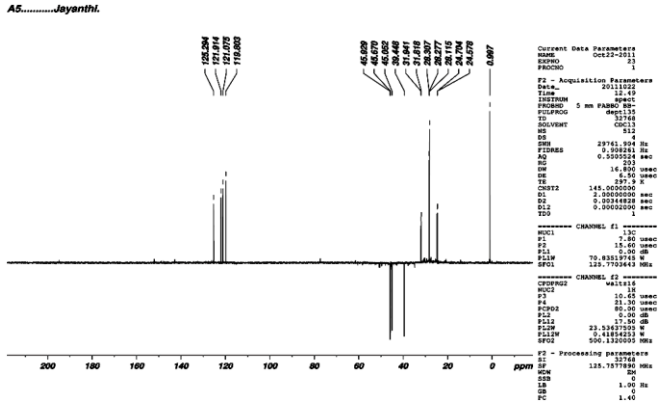

Figure 7c. DEPT 135 spectrum of A5

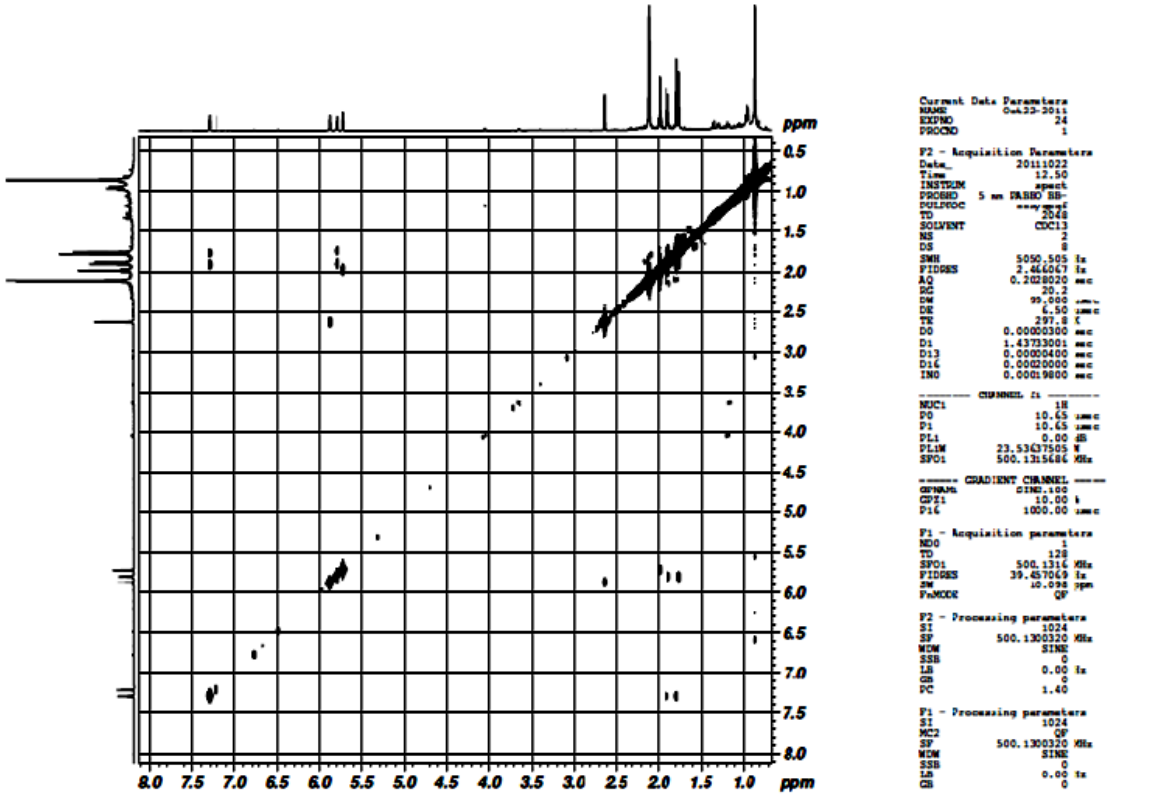

Figure 8. ^{1}H-^{1}H COSY spectrum of A5

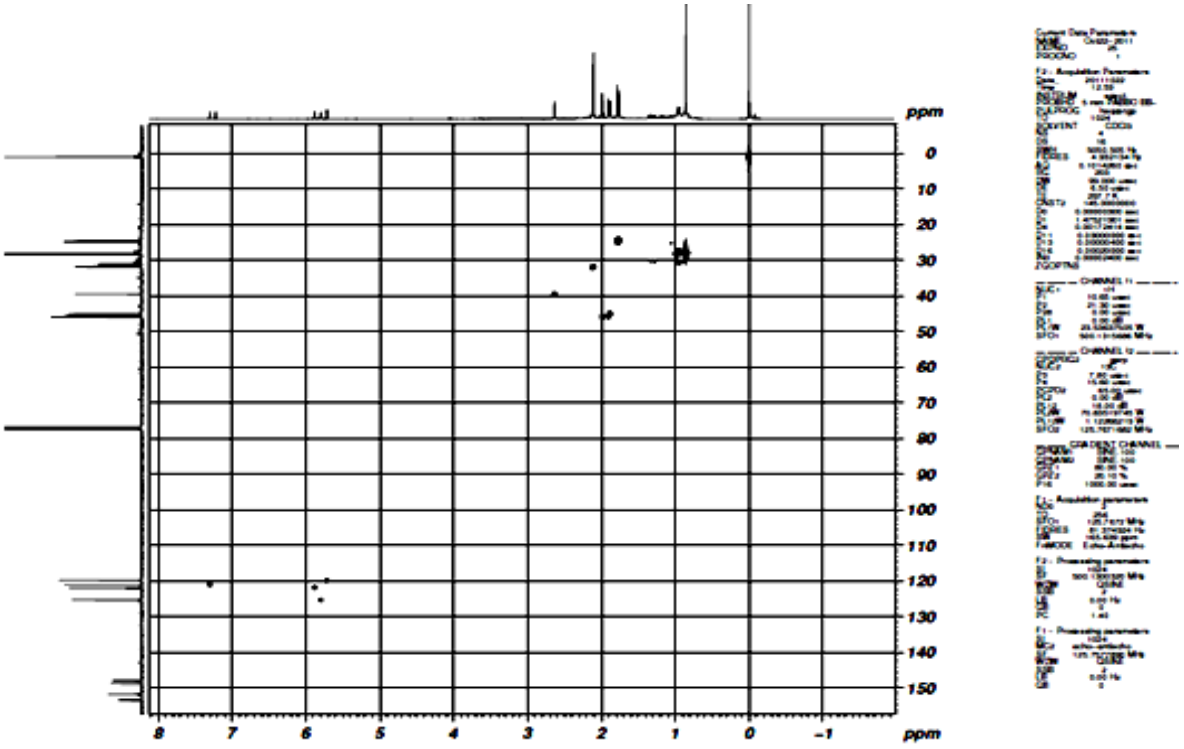

Figure 9. HSQC spectrum of A5

4.4.1.2 Structure elucidation of A15

Column chromatography of acetone extract on elution with 80:20 petroleum ether:ethyl acetate yielded a compound cognominated as A15 (Yield- 2 g).

Physical description

(i) Appearance-Orange liquid.
(ii) Pleasant odour.

Chemical characteristics

(i) Hydroxylamine hydrochloride test- Formation of wine red colour indicates the presence of ester moiety.
(ii) TLC-R_f - 0.6 (5:1 petroleum ether: ethyl acetate).
(iii) Solubility- Miscible with organic solvents like petroleum ether, acetone, ethyl acetate, chloroform, ethanol and methanol.

Spectral interpretation

The UV spectrum (chloroform, λ_{max}) exhibited absorption bands at 279 nm that provided the evidence of n-π* transition. The IR spectrum showed the presence of carbonyl (1820 cm^{-1}, 1658 cm^{-1}), C–CH–O– (1377 cm^{-1}, 1261 cm^{-1}, 1067 cm^{-1}, 1047cm^{-1}) group as well as long aliphatic chain (879 cm^{-1} and 736 cm^{-1}).

NMR spectra interpretation

The ^{1}H NMR spectrum of A15 is shown in Figure 10. The two triplets at δ_H 0.90 is ascribed to the methyl group in the aliphatic region and broad peak at δ_H 1.27 is attributed to the methylene groups. The ^{1}H NMR spectrum displayed a methoxy group as a well defined triplet at δ_H 4.07 (J=6.5 Hz), two –CH_2–groups as finely resolved triplets at δ_H 2.36 and δ_H 2.30 with J=7.5 Hz referring to the hydrogens α to the carbonyl moiety. The multiplet generated by the hydrogen β to the carbonyl was observed at lower field δ_H 1.64. The assignment of the protons is in agreement with the ^{13}C NMR spectrum (Figure 11) which contained resonances from two methyl and twenty one methylene carbons and three oxygenated carbon of which two were quaternary and the other, an oxymethylene carbon (δ_C 64.42). The DEPT 45 spectrum (Figure 11) showed the presence of twenty three proton attached carbon atoms. DEPT 135 spectrum (Table 13) showed the presence of one methyl at δ_C 14.12 and twenty three methylene carbons.

The ^{1}H-^{1}H COSY spectrum (Figure 12) of A15 showed a coupling between δ_H 0.88 and δ_H 1.27. The cross peaks noted between the carbomethoxy proton δ_H 4.07

and δ_H 1.64 indicated a coupling between these two protons. HSQC spectrum (Figure 13) aided in the assignment of the protons to the corresponding carbons. The carbon resonances at δ_C 174.07 and δ_C 178.34 were assigned by the use of HMBC spectrum. The 2D HMBC spectrum (Figure 14) revealed two bond and three bond correlations between the terminal methyl δ_H 0.90 and δ_C 31.96 $(CH_2)_n$ group and δ_C 22.69 and between δ_C 22.69 and δ_H 1.27. The carbonyl group of the ester moiety δ_C 178.34 revealed HMBC interactions to the methylene proton δ_H 1.64 and δ_H 2.36. The latter showed long range coupling with δ_C 24.75 whereas the former showed HMBC correlation with δ_C 64.42. Furthermore, long range correlations between δ_H 2.30 and δ_C 174.07 was also observed showing the proximity of methylene and carbonyl group. The ^1H-^1H COSY and HMBC correlations are given in Table 13 and Figure 15.

In mass spectra, there were peaks at *m/z* 369 $[M\text{-}C_2H_3]^+$, 312 $[M\text{-}C_2H_3\text{-}C_2H_5C{=}O]^+$, 284 $[M\text{-}C_2H_3\text{-}C_2H_5C{=}O\text{-}CO]^+$, 193 $[M\text{- }M\text{-}C_2H_3\text{-}C_2H_5C{=}O\text{-}CO\text{-}COOCH_3C_4H_7]^+$. Peaks due to the loss of CO_2, $C_4H_9COCH_2$, O, H_2O were also observed. α cleavage and McLafferty rearrangement also indicated the presence of an oxo group. From the spectral analysis we were able to arrive at the probable structures:

A.

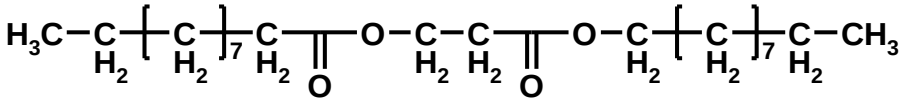

B.

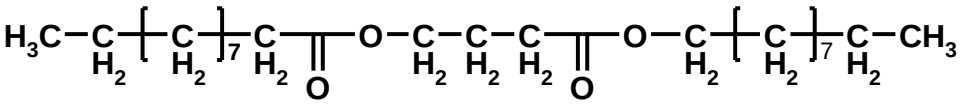

C.

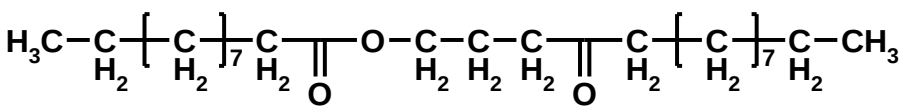

.

The ^1H NMR spectrum of the compound showed an unresolved multiplet at δ_H 1.64 which corresponded to a deshielded methylene group. The presence of two methylene group in between two ester functionality warrants the multiplicity of the methylene group to be a triplet and not multiplet. Therefore, structure A has been ruled out bringing down the probablility between structure B and C.

The IR spectrum of the compound showed a peak at 1820 cm^{-1} and 1658 cm^{-1} which indicated the presence of a ketone and ester moiety (C=O) and the peak at

1377 cm^{-1} and 1261 cm^{-1} denoted the **–**C–O group. Furthermore, the λ_{max} at 279 nm indicated the presence of a ketone carbonyl group (**Al-Khateeb *et al*, 2008**). Since structure B had only ester groups, it was ruled out and narrowed down to structure C.

Based on the previous observations, the compound A15 was unequivocally assigned as structure C, **Undecanoic acid 4-oxo-tetradecyl ester** ($C_{25}H_{48}O_3$). The predicted ^{1}H NMR for the proposed structure for A15 also conformed to the experimental ^{1}H NMR spectrum.

The ethyl ester of pelargonic acid has been identified in *E. crassipes* by GC-MS (**Muthunarayanan *et al,* 2011**). The compound A15 might have been formed from pelargonic acid ethyl ester present in the plant due to the esterification by ethanolic KOH and acetone used for the extraction.

Table 13. ^{1}H NMR, ^{13}C NMR, DEPT 135, ^{1}H-^{1}H COSY and HMBC data of A15

C no	^{1}H (ppm)	^{13}C (ppm)	DEPT 135	^{1}H-^{1}H COSY	HMBC
1		178.34			H-2; H-3
2	2.36 (t, 2 H)	33.77	33.77*		
3	1.64 (m, 8 H)	25.04	25.04*		
4	1.64	24.71	24.71*		H-2
5	1.27 (s, 28 H)	29.71	29.71*		
6	1.27	29.17	29.17*		
7	1.27	29.28	29.28*		
8	1.27	29.25	29.25*		
9	1.27	22.69	22.69*		H-8
10	1.27	31.93	31.93*		
11	0.90 (t, 6 H)	14.12	14.12		H-10; H-9
1'	4.07 (t, 2 H)	64.42	64.42*	H-2'	
2'	1.64	28.66	28.66*		
3'	2.30 (t, 2 H)	34.43	34.43*		
1''		174.07			H-3'
2''	1.64	25.94	25.94*	H-3''	
3''	1.27	29.66	29.66*		
4''	1.27	29.61	29.61*		
5''	1.27	29.60	29.60*		
6''	1.27	29.54	29.54*		
7''	1.27	29.48	29.48*		
8''	1.27	29.44	29.44*		
9''	1.27	29.37	29.37*		
10''	1.27	31.93	31.93*		
11''	0.90	14.12	14.12	H-10''	H-10'';H-9''

* Downward peak

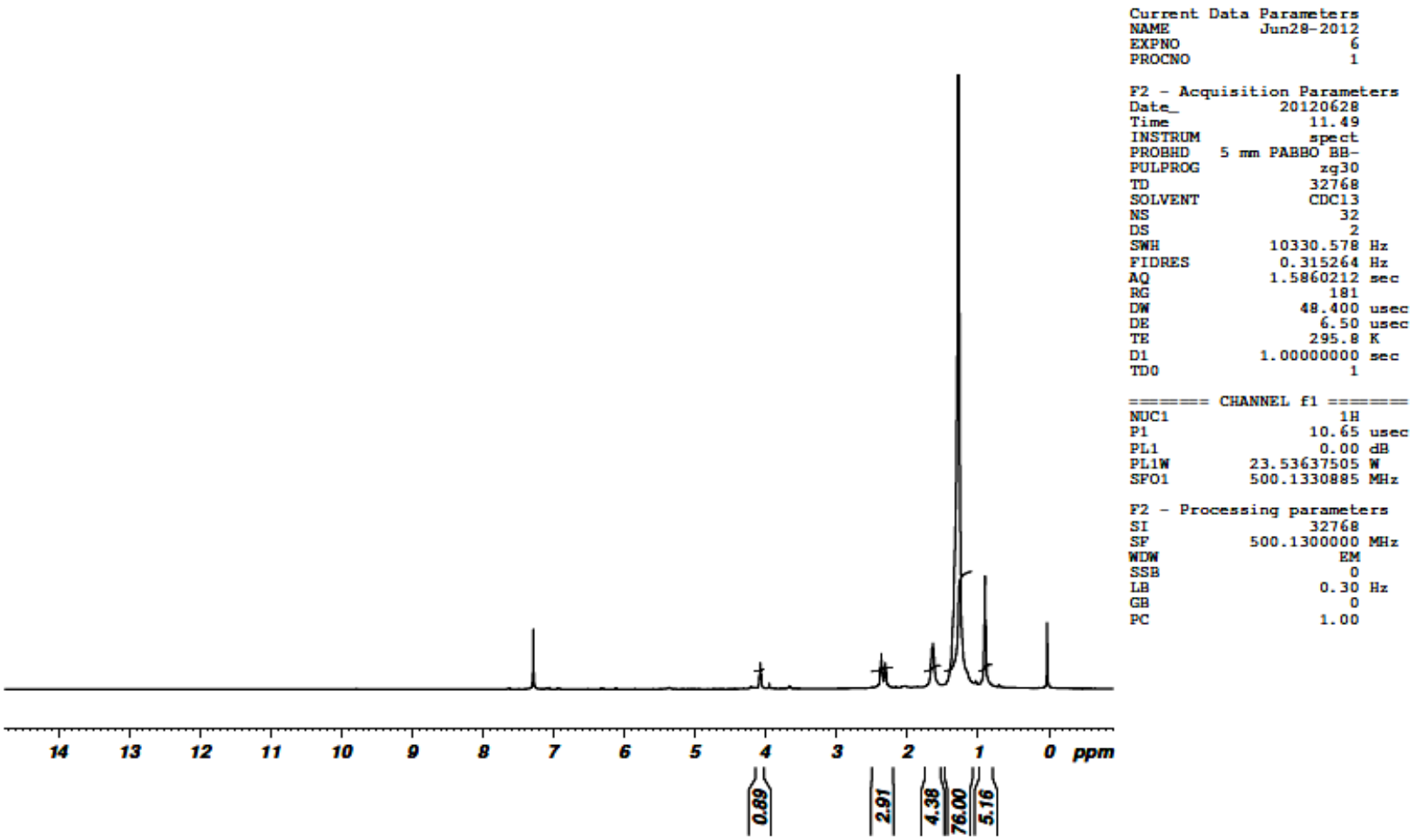

Figure 10. ^{1}H NMR spectrum of A15

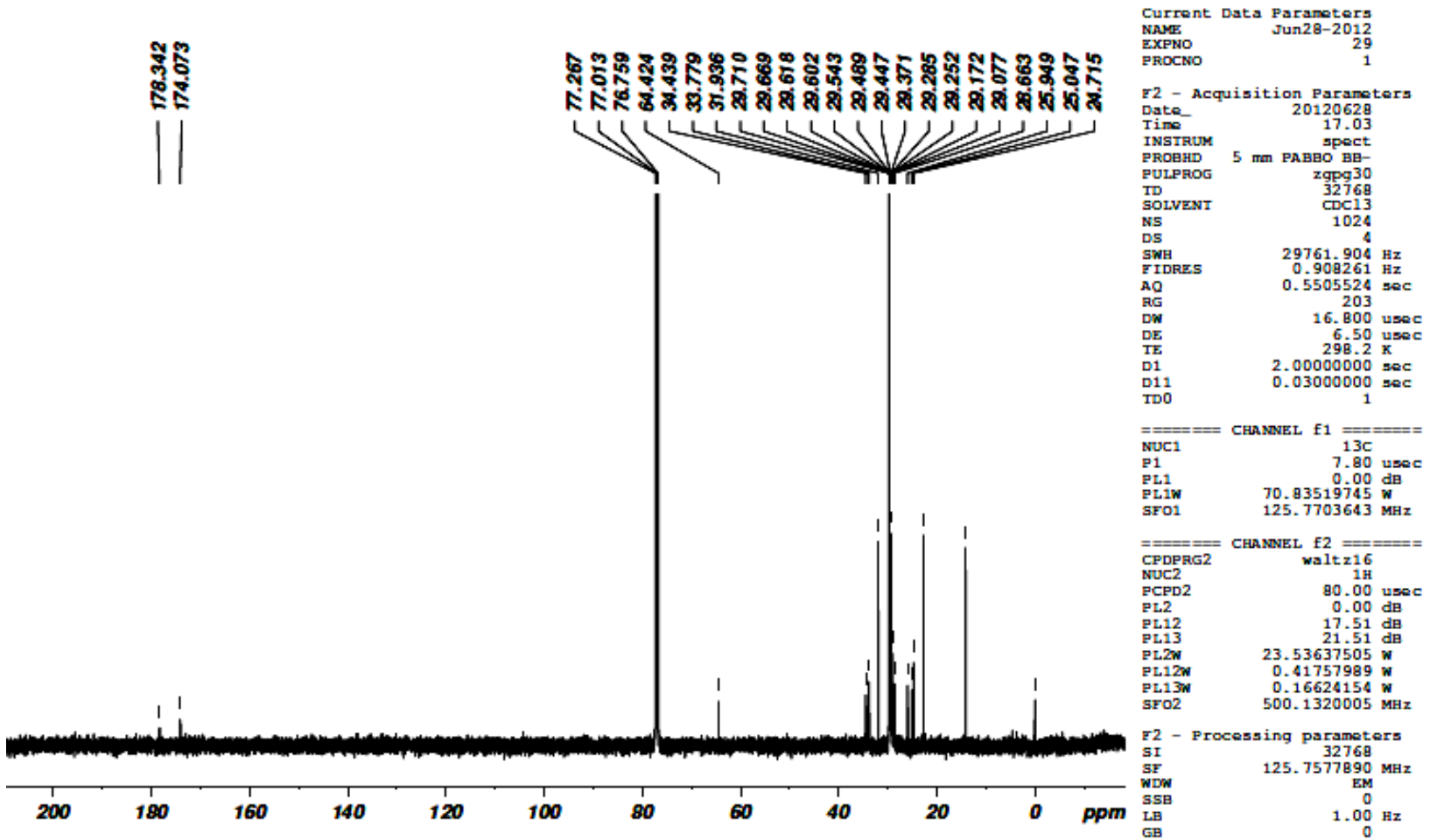

Figure 11. ^{13}C NMR spectrum of A15

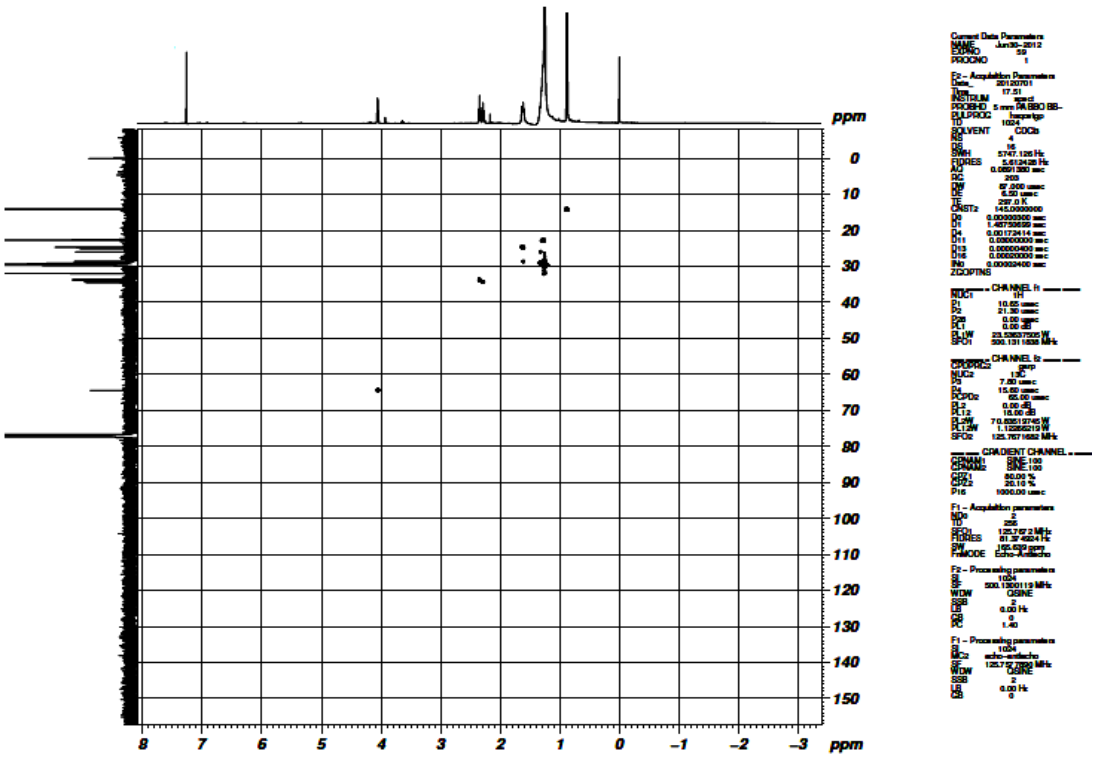

Figure 12. ^{1}H-^{1}H COSY spectrum of A15

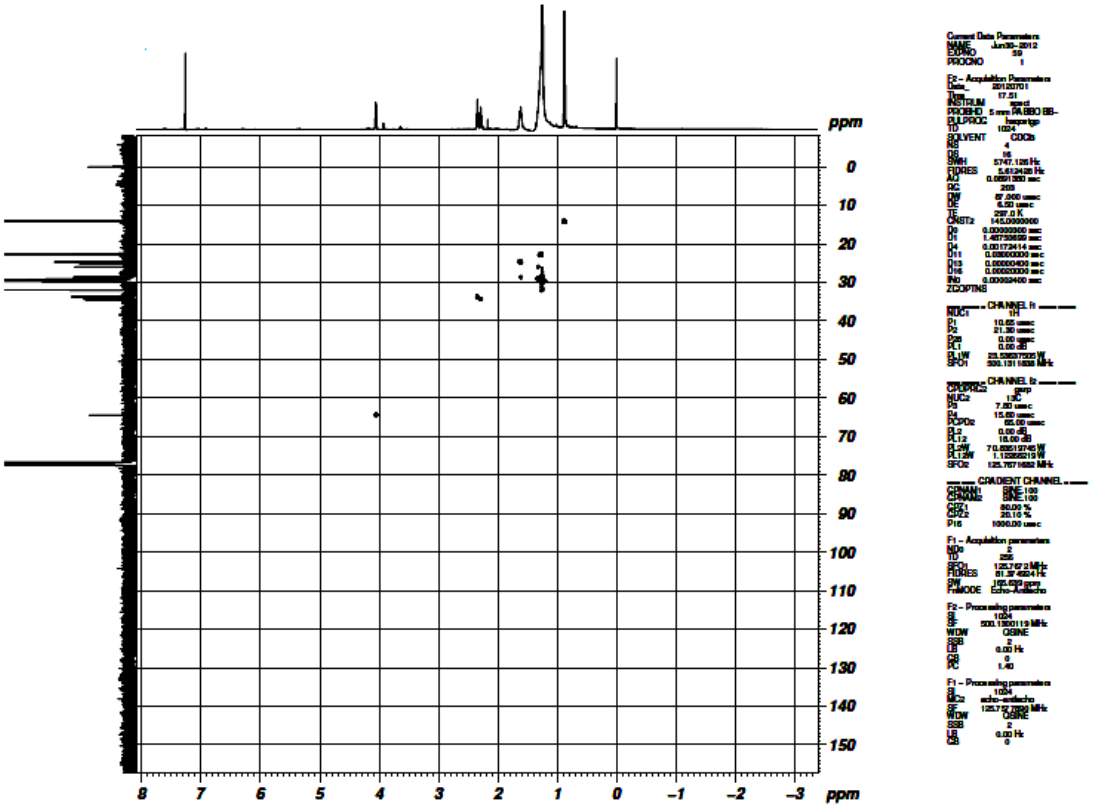

Figure 13. HSQC spectrum of A15

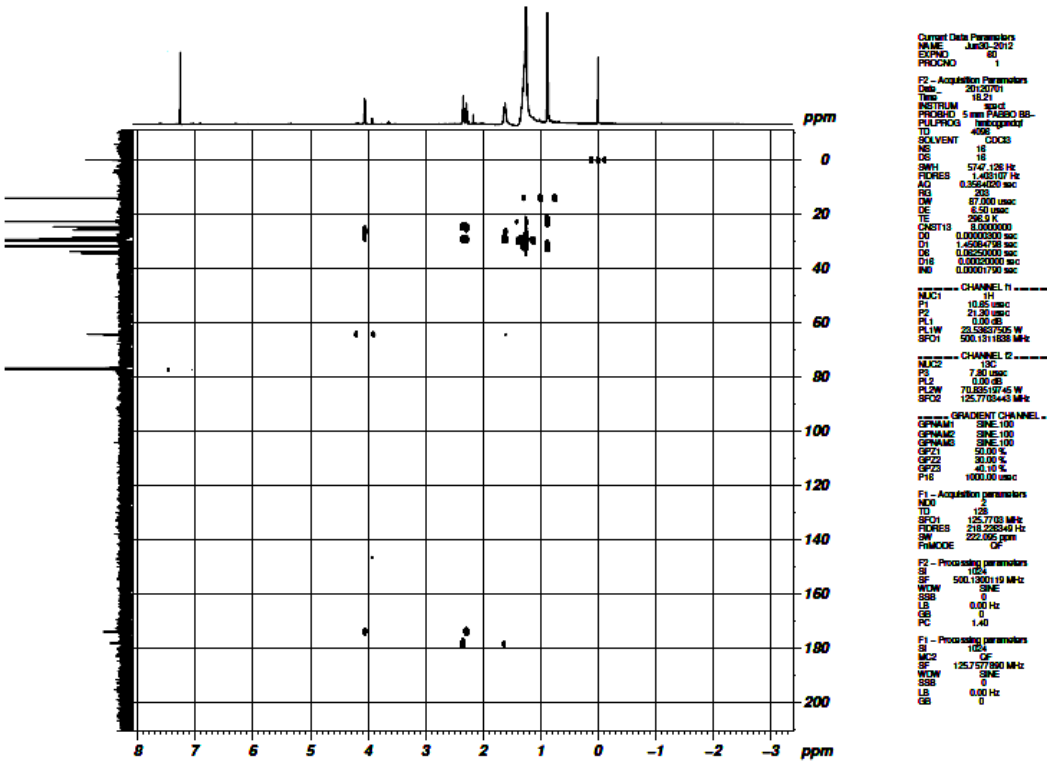

Figure 14. HMBC spectrum of A15

Isolation of fatty acid esters from plants is reported (**Wandji *et al*, 2002; Shen *et al,* 2003; Wu *et al,* 2006; Alam *et al,* 2011; Saha *et al,* 2011; Santana *et al,* 2012**). Liquid wax esters from *Simmondsia chinensis* provide superior oxidative stability, excellent emolliency (**Alvarez and Rodríguez, 2000**), and are used as bioadhesives (**Hansen *et al,* 1999**), reactive diluents (**Bloom, 2006**), lubricants, cosmetics, biofuel additives, surface active agents and plasticizers (**Lerin *et al,* 2011**). Fatty acid esters as a formulation with amphotericin B and other therapeutic agents provide bioavailability at the low pH in gastric fluid (**Wasan and Wasan, 2010**).

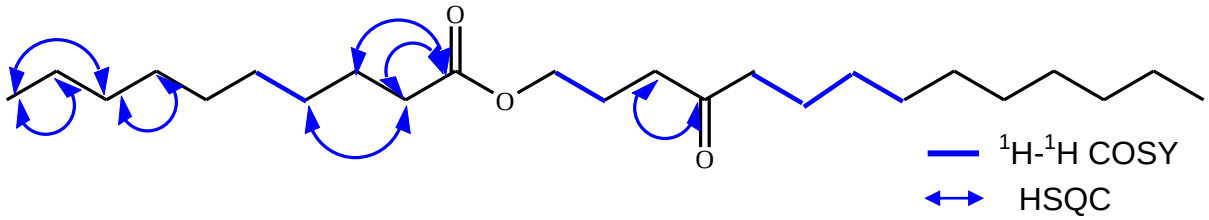

Figure 15. ^{1}H-^{1}H COSY and HMBC correlations of A15

A range of fatty acid esters is now being produced commercially using immobilized lipase in non-aqueous solvents. Enzyme catalysed fatty acid ester synthesis has been adopted in most cases due to its regioselectivity (**Yoo *et al,* 2007**), reusability of the

enzyme and lower operating temperatures (**Meng *et al,* 2011**). Different methods of preparation of fatty acid esters have been adopted by several researchers (**Cert *et al,* 2000; Nithya and Koria, 2012**). In the present study 100 g of acetone extract has yielded 2 g of Undecanoic acid 4-oxo-tetradecyl ester. The isolation of fatty acid ester in good yields from *E. crassipes* is ecofriendly and economical.

4.4.1.3 Structure elucidation of A20

A reddish orange liquid obtained by the column chromatography of acetone extract on elution with petroleum ether:ethyl acetate was designated as A20 (Yield- 8 g).

Physical characteristics

(i) Appearance- Reddish Orange liquid.

(ii) Odour- Pleasant odour.

Chemical characteristics

(i) TLC- R_f - 0.74 (7:3 ethyl acetate:petroleum ether).

(ii) Solubility- Soluble in petroleum ether, chloroform, ethanol and methanol.

Spectral determination

The UV spectrum of A20 displayed a main absorbance with a shoulder at 252 nm. The IR spectrum exhibited absorption bands at 1724 cm^{-1} (C=O of unsaturated ester), 1381 cm^{-1} (≡C–O stretching) and 1450 cm^{-1}, 745 cm^{-1}, 700 cm^{-1} (aromatic ring system).

NMR spectral analysis

^{1}H and ^{13}C NMR spectral values of A20 are given in Table 14. The proton NMR spectrum of A20 exhibited an AA'BB' system at δ_H 7.69 and δ_H 7.51 indicative of a disubstituted aromatic ring. The spectrum displayed a triplet of oxymethylene proton at δ_H 4.32. The pentet at δ_H 1.70 and a multiplet at δ_H 1.41 corresponds to methylene group in two different environments and a triplet at δ_H 0.93 was that of the terminal methyl groups. This was consistent with ^{13}C NMR spectrum which displayed resonances for:

- 1 carbonyl carbon - δ_C 167.69 (C-1)
- 2 quarternary carbons- δ_C 132.28 (C-2; C-7),
- 4 methine carbons - δ_C130.91 (C-4; C-5) and δ_C 128.82 (C-3; C-6),
- 6 methylene carbons - δ_C 65.54 (C-1'; C-1''), δ_C 30.54 (C-2'; C-2''), δ_C 19.16 (C-3'; C-3'') and
- 2 methyl carbons - δ_C 13.72 (C-4'; C-4'').

The multiplicities of the carbon were further confirmed with DEPT 45 and DEPT 135. Each carbon signal was accounted to two carbons based on the intensity of the signal. The connectivities within the molecule were recognized with ^{1}H - ^{1}H COSY which showed all possible proton-proton correlations, ^{1}H -^{13}C HSQC spectrum which displayed short range ^{1}H -^{13}C correlations and ^{1}H -^{13}C HMBC spectrum which demonstrated long-range ^{1}H -^{13}C correlations. ^{1}H-^{1}H COSY and HMBC correlations are shown in Figure 16. The ^{1}H-^{1}H COSY spectrum revealed correlations between δ_H 7.69 →δ_H 7.51; δ_H 4.28 → δ_H 1.70 and δ_H 1.41; δ_H 1.41→0.93. In the HMBC plot, the carbonyl carbon δ_c 167.69 correlated with δ_H 4.26 and the latter correlated with δ_C 30.54 and δ_C 19.16. Long range correlations were observed between δ_H 1.41 to δ_C 65.54, δ_C 30.54 and δ_C 13.72 in HMBC spectrum. The DEPT spectral values, ^{1}H-^{1}H COSY and ^{1}H -^{13}C HMBC correlations are given in Table 14.

The spectral analysis led to the characterisation of A20 to be **phthalic acid dibutyl ester (dibutyl phthalate) and was confirmed by comparison of NMR values with those reported in the literature** (**Khatiwora *et al,* 2011**). **This is the first report of isolation of this compound in good yield (8 g) from *E. crassipes*.**

Table 14. ^{1}H NMR, ^{13}C NMR, DEPT 45, DEPT 90, DEPT 135, ^{1}H-^{1}H COSY and HMBC data of A20

C no	^{1}H (ppm)	^{13}C (ppm)	DEPT 45	DEPT 90	DEPT 135	^{1}H-^{1}H COSY	HMBC
1		167.69	-	-			H-1'
2		132.28	132.28	132.28	132.28		
3	7.69 (dd, 2 H)	128.82	128.82	128.82	128.82	H-4	
4	7.51(dd, 2 H)	130.91	130.91	130.91	130.91		H-3
5	7.51	130.91	130.91	130.91	130.91	H-6	H-6
6	7.69	128.82	128.82	128.82	128.82		
7		132.30	132.30	132.30	132.30		
1'	4.26 (t, 4 H)	65.54	65.54	-	65.54*	H-4'	H-2'
2'	1.70 (m, 4 H)	30.56	30.56	-	30.56*		H-1'; H-3'; H-4'
3'	1.41 (m, 4 H)	19.18	19.18	-	19.18*	H-4'	H-1'; H-2'; H-4'
4'	0.93 (t, 6 H)	13.72	13.72	-	13.72		H-2'; H-4'

* Downward peak

Dibutyl phthalate has been isolated from the chloroform extract of *Polyalthia rumphii* stem (**Wang *et al,* 2012**), *Dendropanax chevalieri* roots (**Ren *et al,* 2012**), whole plant of *Blumea aromatica* (**Lan *et al*, 2012**), *Mimusops elengi* (**Ruikar *et al,* 2011**) and from root exudates of *A. adenophora* (**Zhang, 2005**).

Figure 16. HMBC and ^{1}H-^{1}H COSY correlations of A20

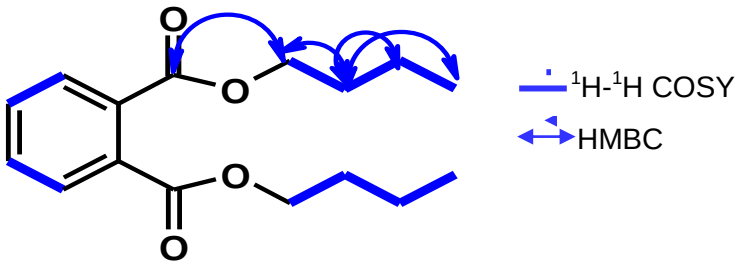

Dibutyl phthalate (DBP) finds use mainly as a plasticizer in combination with nitrocellulose cellulose ether, polyacrylate and polyacetate dispersions. DBP when used as a plasticizer do not chemically bind in the matrix and used in a wide range of end products in addition to interior and outdoor polymer applications such as in advanced textile products, dental materials, military propelling charges, explosives, equipments for nuclear installations, catalysts for the production of polypropylene, elastomers, lacquers, explosives, printing inks, perfume oil solvents, paper coatings, adhesives, solid rocket propellant (**www.npi.gov.au**), safety glass, cellophane, dyes, pesticides, deodorants solvents, lubricating agents and rubber fabric softener (**www.chinaplasticizer.com**), nail, hair care formulations (**www.national-toxic-encephalopathy-foundation.org**), medicinal products and active pharmaceutical substances (**http://echa.europa.eu**). DBP has been used in lamb-marking dressings in prolonged wound healing to protect the wound from fly strikes (**Johnstone and Southcott, 1954**).

DBP has also been demonstrated to possess antibacterial activity against *Klebseilla pneumonia, Proteus mirabilis Pseudomonas erogenous* and *Pseudomonas aeruginosa* (**Khatiwora *et al,* 2012**) and exhibits cytotoxicity against K562 (**Wang *et al,* 2012**). DBP selectively deteriorates leukaemia cells with less harmful effect on the growth of normal hemopoietic progenitors (**Chu-tse *et al,* 1993**).

Feasible synthesis of dibutyl phthalate using alkyl sulphate as a catalyst (**Gon *et al,* 1994**) has been patented. Giving consideration to the industrial importance of DBP, many methods have been developed for the synthesis of this compound. The cost of organic synthesis of dibutyl phthalate is high. Cost for 1 g dibutyl phthalate (Fluka) is 2,230 INR. In the present work, 8 g of dibutyl phthalate has been obtained from 100 g of acetone extract which may cost 17,000 INR (approximately). This compound has been isolated from plants like *Polyalthia rumphii* stem (Yield- 32 mg from 9.7 kg plant) (**Wang *et al,* 2012**). In the present study, it is obtained from *E. crassipes* in high yields.

4.4.1.4 Structure elucidation of A22

Column chromatography of acetone extract of *E. crassipes* with ethyl acetate and ethanol gave a compound designated as A22 (Yield- 4 g).

Physical characteristics

(i) Appearance- Dark Brown Powder.
(ii) Odour- Pleasant odour.
(iii) Melting point- 124 °C.

Chemical characteristics

(i) TLC - Rf -0.6 (2:8 chloroform : methanol).
(ii) Solubility- Soluble in methanol.

Spectral analysis

The UV spectrum showed an absorption maximum (chloroform, λ_{max}) at 288 nm. The IR spectrum showed the presence of carboxyl group at 1715 cm^{-1} (C=O), ≡C–O stretching at 1381 cm^{-1} and aromatic system at (1456 cm^{-1}, 745 cm^{-1}, 700 cm^{-1}).

NMR spectral interpretation

^{1}H and ^{13}C NMR spectral values are given in Table 15. The proton NMR spectrum (Figure 17) of A22 showed the presence of two an unresolved singlet's at δ_H 7.73 and δ_H7.55 that pointed out the existence of AA'BB' system of a disubstituted aromatic ring. A well defined triplet at δ_H 4.32 indicated the existence of an oxygenated methylene group. This was supported by the presence of a peak at δ_C 65.59 in the ^{13}C NMR spectrum (Figure 18). Unresolved doublet at δ_H 2.34 corresponded to deshielded methylene groups. All the peaks within the range δ_H 1.7 to 1.26 were that of the methylene protons. The methylene protons at two different environment resonated as triplets at δ_H 0.97 and 0.89.

The ^{13}C NMR spectrum displayed a peak at at δ_c 167.75, typical for carbonyl carbon. The aromatic carbons gave signals at δ_C 132.30, δ_C 130.92 and δ_C 128.84. All the other methylene carbons were obtained within δ_C 34. Further the ^{13}C NMR spectra together with DEPT 45 (Figure 19), 90 (Table 15) and 135 (Figure 20) indicated the presence of one quarternary carbon, six methine carbon, twenty four methylene carbon and four methyl carbon, based on the intensity and the number of the signals.

The ^{1}H - ^{1}H COSY spectrum (Figure 21) displayed six possible correlations: δ_H 7.73- δ_H 7.55 ; δ_H 4.32 - δ_H 1.73 ; δ_H 2.34 - δ_H 1.62 ; δ_H 1.73 - δ_H 1.45 ; δ_H 1.45 - δ_H *0.97* ; δ_H 1.26 - δ_H 0.89. The ^{1}H -^{13}C HSQC spectrum (Figure 22) revealed all ^{1}H -^{13}C direct (^{1}J) correlations and thus affirmed the ^{1}H- ^{13}C assignments.

The ^{1}H -^{13}C HMBC spectrum (Figure 23) revealing all key ^{2}J-^{3}J long-range ^{1}H -^{13}C correlations, played a significant role in elucidation of structure of compound A22. The carbonyl carbon δ_c 167.75 displayed ^{2}J correlation with δ_H 4.32 and the latter correlated with δ_c 30.56, which correlated with δ_H 1.45 and δ_H 0.97. From this correlation, it was possible to establish the following sequence –COO–CH_2–CH(CH_3)–CH_2–. Furthermore, the deshielded methylene proton at δ_H 2.34 showed connectivities to δ_C 24.75, δ_C 31.43 and δ_C 29.69. The compound A22 was deduced as **phthalic acid bis-(2-methyl-tridecyl) ester** with the molecular formula $C_{36}H_{62}O_4$. Thus, the structure of compound A22 composes of an *o*, *p* disubstituted aromatic ring and branched long chain. **This is the first report of isolation of this compound from *E. crassipes* and its family Pontederiaceae.** Ethylhexyl phthalate, methyl-dioctyl phthalate and dioctyl phthalate has been identified by GC-MS in the fractions of the methanol extract of *E. crassipes* separated by TLC (**Shanab and Shalaby, 2012**).

Table 15. ^{1}H NMR, ^{13}C NMR, DEPT 90, ^{1}H-^{1}H COSY and HMBC data of A22

C no	^{1}H (ppm)	^{13}C (ppm)	DEPT 90	^{1}H-^{1}H COSY	HMBC
1		167.75			H-1'
2		132.30			
3	7.73 (dd, 2 H)	128.84	128.84	H-4	
4	7.55 (dd, 2 H)	130.78	130.78		H-3
5	7.55	130.78			H-6
6	7.73	128.84			
7		132.30			
1'	4.32 (t, 4 H)	65.59			H-2'; H-3'
2'	1.73 (t, 2H)	30.56	30.56	H-1'; H-3'	H-1'''
3'	1.45 (m, 4 H)	19.18			
4'	1.62 (m, 4 H)	24.75		H-5'	
5'	2.34 (m, 4 H)	33.8			H-4';H-6';H-7'
6'	1.27 (s, 28 H)	31.43			
7'	1.27	29.69			
8'	1.27	29.46			
9'	1.27	29.35			
10'	1.27	29.26			
11'	1.27	29.09			
12'	1.27	22.68		H-12'	H-13'
13'	0.89 (t, 6 H)	14.12			
1'''	0.97 (t, 6 H)	13.72			

There are only fewer reports on the occurrence of phthalates from plants (**Srinivasan *et al,* 2009**). Phthalic acid esters like o-phthalic acid bis(2-ethylnonyl) ester methanolic extract of the whole plant of *Periploca aphylla* (**Aziz-Ur-Rehman *et al,* 2004**), 1,2-benzenedicarboxylic acid bis(2S-methyl heptyl) ester from the hexane extract of the whole plant of *Ajuga bracteosa* (**Singh *et al*, 2006**), bis(2-methylheptyl)phthalate from the ethanol extract of *Pongamia pinnata* (**Rameshthangam and Ramasamy, 2007**), dibutyl phthalate from butanol extract of the leaves of *Torreya grandis* (**Saeed *et al,* 2007**) and the dried stem of *Ipomoea carnea* (**Khatiwora *et al,* 2011**), 1,2-benzenedicarboxylic acid bis(2-ethylhexyl) ester from the methanol extract of leaves of the variety minor seeds of *Ricinus communis* (**Sani and Pateh, 2009**), dibutyl phthalate and phthalic acid bis-(2-ethylhexyl) ester from 95% ethanol extract of pine needles of *Cedrus deodara* (**Zhang *et al,* 2010**), 1,2-benzenedicarboxylic acid bis(2S-methyl heptyl)ester from the hexane extract of the whole plant of *Ajuga bracteosa* (**Upadhyay *et al,* 2011**), dioctylphthalate from methanolic extract of aerial parts of *Chaerophyllum macropodum* (**Shafaghat *et al,* 2012**), diethyl phthalate, phthalic acid, butyl dodecyl ester and 1,2- benzene dicarboxylic acid, mono(2-ethylhexyl)ester from the ethyl acetate fraction of root bark of *Psidium guajava* (**Velmurugan *et al,* 2012**) has been isolated.

GC-MS identification of diisooctyl phthalate in *Euphorbia hirta* (**Ogunlesi *et al,* 2009**), phthalic acid, butyltetradecylester in essential oil of stem of *Chasmanthera dependens* (**Ogunlesi *et al,* 2009**), dibutyl phthalate in *Urtica dioica* leaves (**Dar *et al*, 2012**), bis (2-ethyl hexyl) phthalate in the ethanol extract of leaves of *Mallotus tetracoccus* (**Ramalakshmi and Muthuchelian, 2011**) are reported.

Phthalate esters exhibit antibacterial, antifungal and antialgal properties (**Shanab and Shalaby, 2012**; **Srinivasan *et al,* 2012**) and antiviral activity against white spot syndrome virus of *Penaeus monodon* Fabricius (**Rameshthangam and Ramasamy, 2007**).

Phthalate esters are used in nonplasticizer products such as perfumes and cosmetics like eye shadow, toilet waters, other fragrances, and mainly in plasticized products such as vinyl swimming pools, plasticized vinyl seats on furniture and in cars, and clothing including jackets, raincoats and boots. These esters are used in the production of lacquers, dispersion, cellulose, polystyrole, colours, synthetic and natural rubber, lubricants, polyamides, insect repellents, fixatives for perfumes, congealing

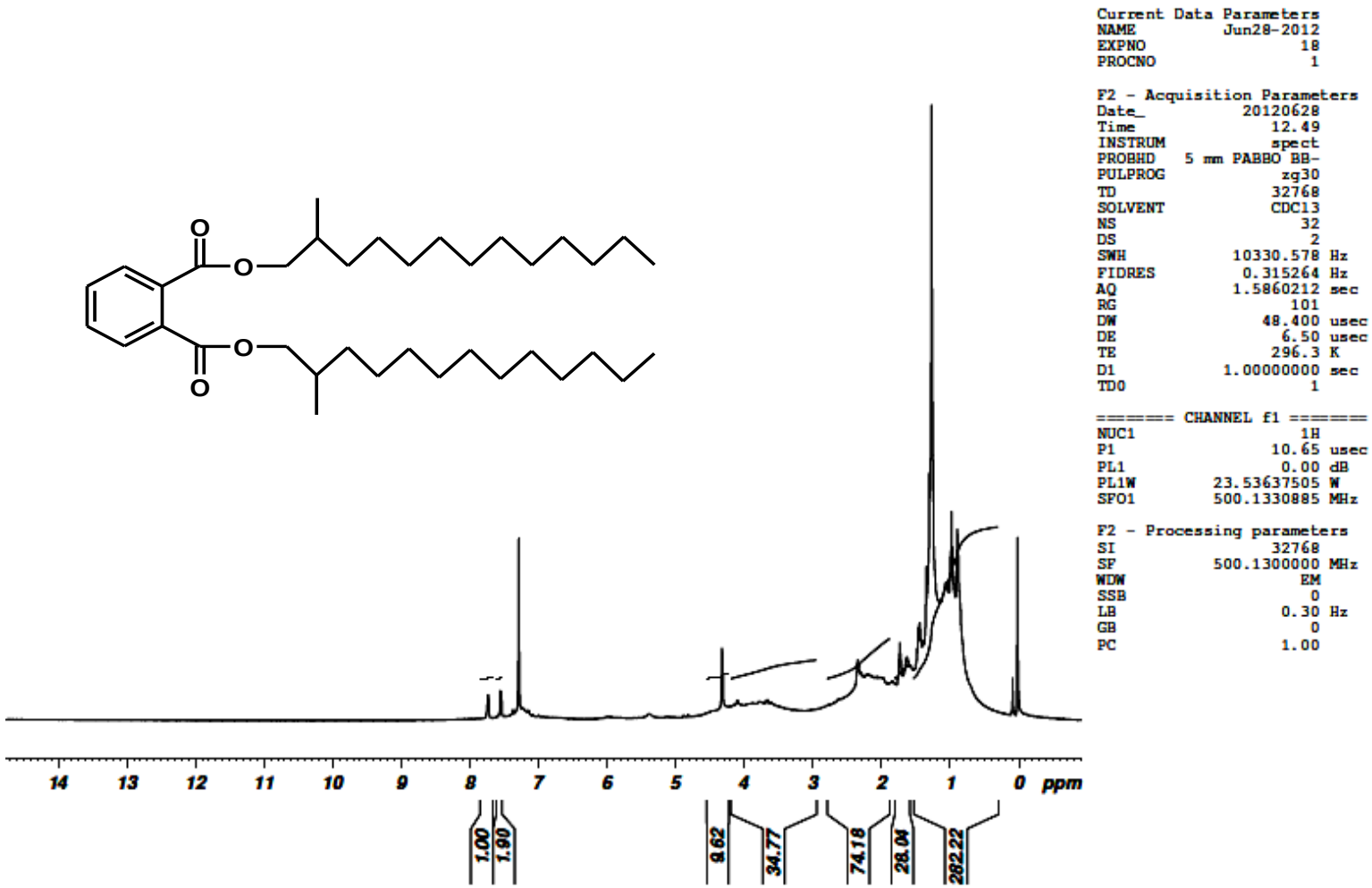

Figure 17. ^{1}H NMR spectrum of A22

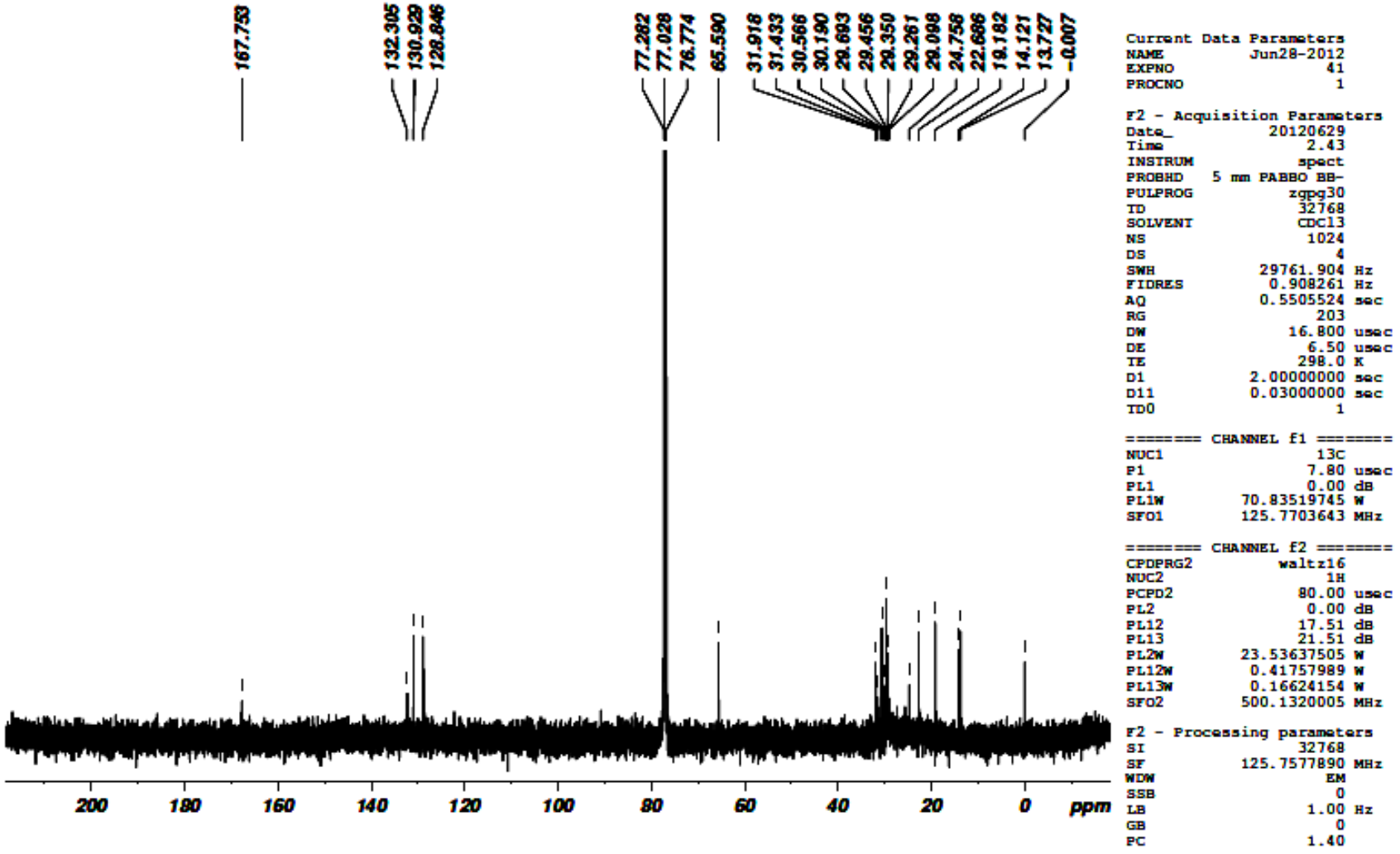

Figure 18. ^{13}C NMR spectrum of A22

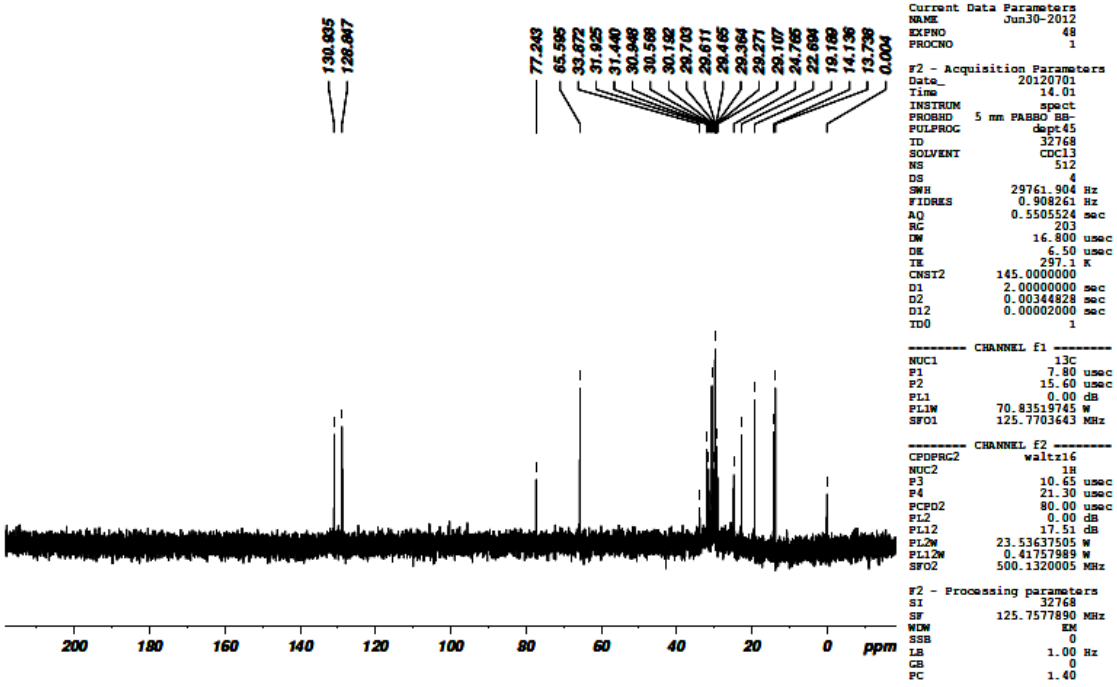

Figure 19. DEPT 45 spectrum of A22

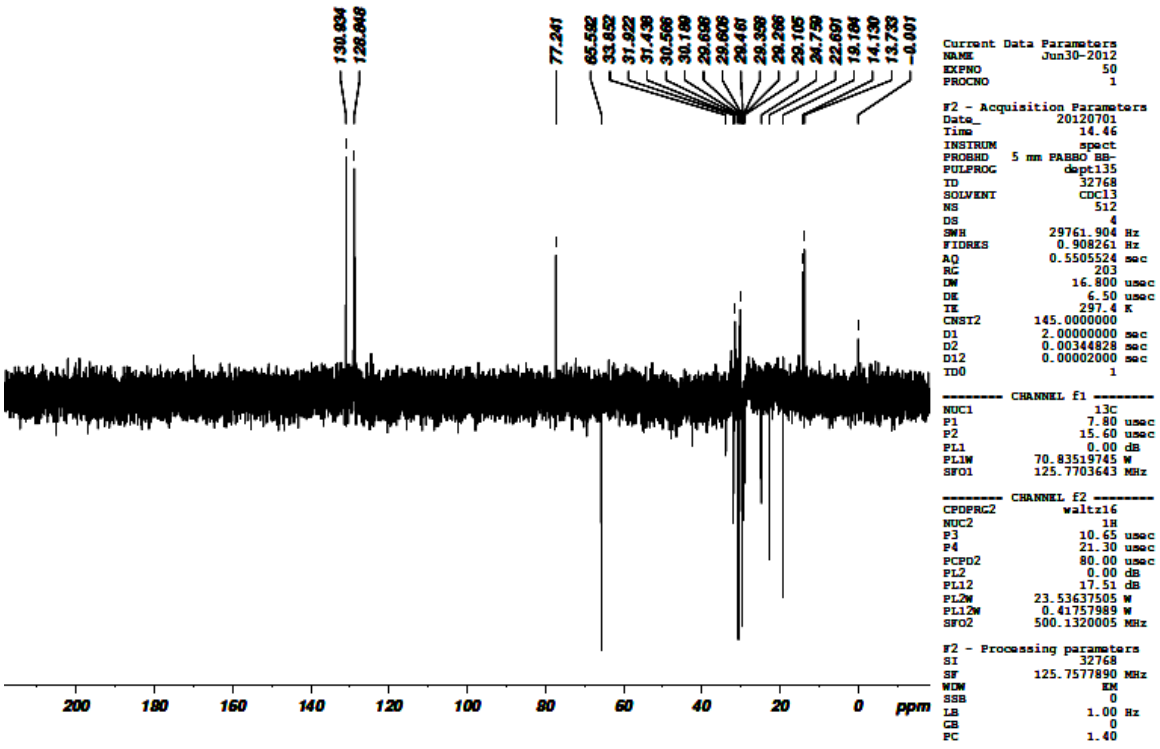

Figure 20. DEPT 135 spectrum of A22

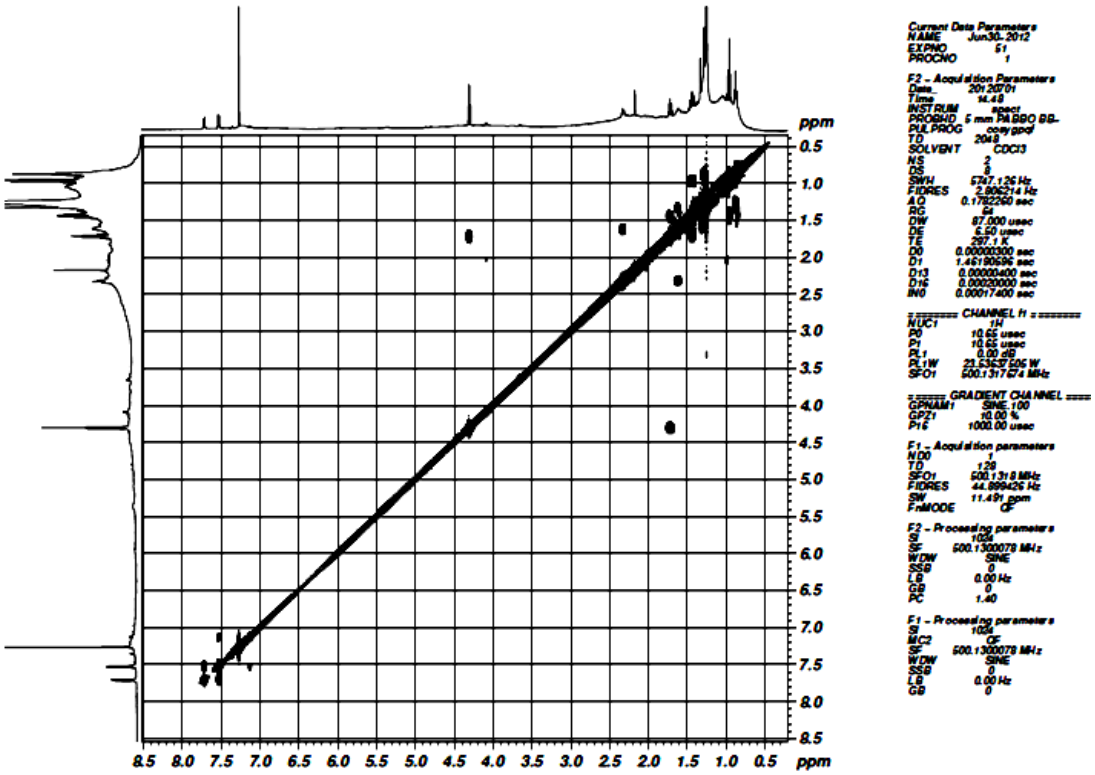

Figure 21. ^{1}H-^{1}H COSY spectrum of A22

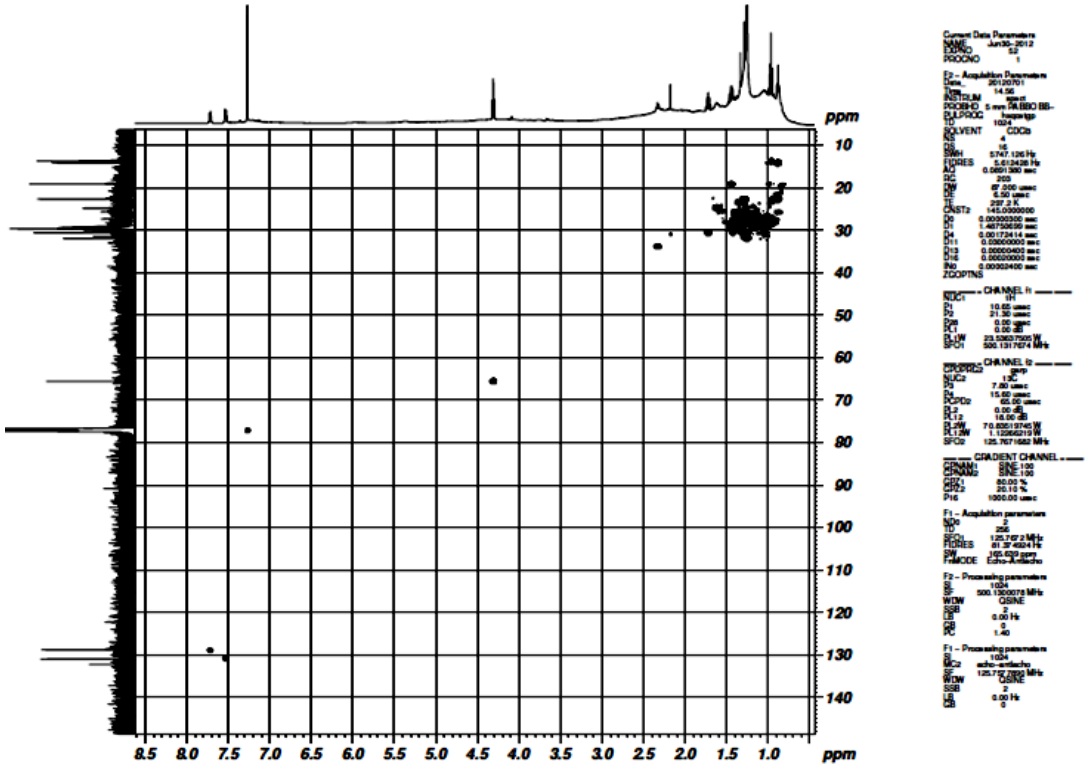

Figure 22. HSQC Spectrum of A22

agents for explosives and working fluids for high-vacuum pumps (**www.ilo.org; Velanganni and Kadamban, 2011; CDER, 2012**). Phthalate esters are also used in making medical devices like blood circuit tubes, infusers, catheters and endotracheal tubes. Phthalate esters give vinyl gloves the strength and durability to resist tears, protecting both doctors and patients (**www.ping.be/chlorophiles**). Phthalic acid diesters are used in magnetic recording medium (**Ohya and Hayakawa, 1992**). Phthalic acid diester derivative capable of donating electron has been patented (**Tashino *et al,* 2003**).

There are no reports on the synthetic preparation of this compound. Acetone extract (100 g) of *E. crassipes* has yielded 4.8 g of the compound. Hence, this plant may be considered as an excellent source of phthalic acid bis-(2-methyl-tridecyl) ester.

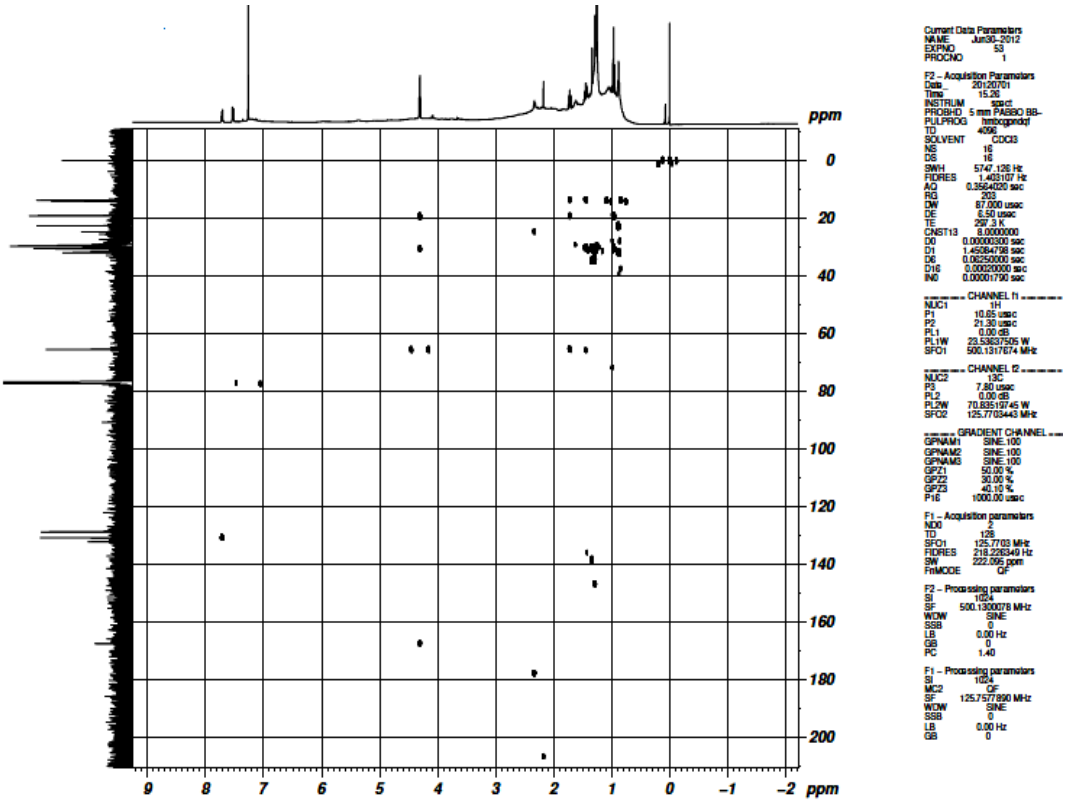

Figure 23. HMBC spectrum of A22

Biosynthesis of fatty acid esters

Biosynthesis of fatty acid esters in *E. crassipes* might have followed the fatty acid pathway with the fatty alcohols as the precursors in the cytosol. The esterification of fatty alcohol and fatty acyl-CoA/ACP to form wax ester in other plants is catalysed by wax ester synthase enzyme (**Doan, 2011**) and the same enzyme might have taken part in the esterification in *E. crassipes* leading to the formation of oxo fatty acid ester.

4.4.2 Isolation of compounds from ethyl acetate extract of *E. crassipes*

4.4.2. 1 Characterization of E6

Open column chromatography of ethyl acetate extract (10% ethyl acetate) gave a dark brown liquid (8 g). A pale white compound (440 mg) settled on adding ethanol. The compound was recrystallized with ethanol giving a white amorphous powder.

Physical characteristics

(i) Melting point- 48 °C.

(ii) Appearance- White amorphous solid.

Chemical characteristics

(i) TLC - R_f - 0.6 (100% Chloroform).

Spectral data

^{1}H NMR (500 MHz, $CDCl_3$, δ): 3.66 (t, 2 H), 2.36 (q, 2 H), 1.64 (q, 2H), 1.59 (p, 2 H), 1.27 (s, H), 0.90 (t, 6 H).

^{13}C NMR (500 MHz, $CDCl_3$, δ): 178.0, 63.10, 33.77, 32.79, 31.93, 29.70, 29.66, 29.61, 29.43, 29.367, 29.25, 29.08, 25.74, 24.73, 22.69, 14.11.

Spectral interpretation

The UV spectrum of E6 in chloroform showed an absorption maximum at 242 nm. The IR spectrum contained absorption bands of a carbonyl group at 1712 cm^{-1}. The band at 1261 cm^{-1} and 1174 cm^{-1} indicated the presence of C–O–C group and –C–O group of ester.

NMR analysis

The ^{1}H NMR spectrum (Figure 24) of E6 displayed signals for terminal methyl protons at δ_H 0.903. The broad singlet at δ_H 1.27 corresponds to the methylene protons in the same environment. The pentet at δ_H 1.64 and δ_H 1.59 was indicative of the deshielding of the methylene protons. A well defined triplet at δ_H 2.36 was attributed to the methylene protons. The triplet at δ_H 3.66 corresponds to the oxymethylene proton.

A combination of ^{13}C NMR spectrum (Figure 25), DEPT 45 and DEPT 135 (Table 16) permitted the assignment of the carbon multiplicities. The δ_C 178.00 corresponded to carbonyl group of the ester. The deshielded carbon resonance in the region δ_C 63.10 was attributed to the carbon attached to the oxymethylene proton. The carbon resonances in the region δ_C 32 to 22 were attributed to the methylene group. The carbon resonance at δ_C 14.11 was that of the methyl group.

^{1}H-^{1}H cosy spectrum (Figure 26) showed the coupling between the proton at δ_H 3.66 and δ_H 1.59. Cross peaks between the resonances at δ_H 1.59 and δ_H 1.27 and δ_H 1.27 and δ_H 0.90 indicated the correlation between these protons. 2D HSQC spectrum (Figure 27) revealed the ^{1}H-^{13}C correlations in the molecule. The HMBC spectrum (Figure 28) showed long range coupling between δ_C 63.10 and δ_H 1.59. HMBC correlations between the carbon resonance at δ_C 31.93 and δ_H 1.27, δ_C 22.69 and δ_H 0.90 were noted.

The combination of these data suggested the compound to be a higher fatty ester. **This is the first reported isolation of saturated fatty acid ester from *E. crassipes.***

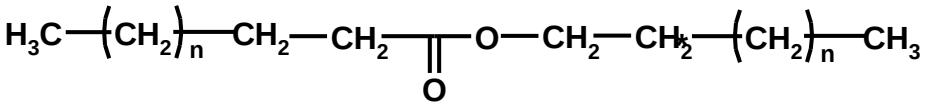

Table 16. ^{1}H NMR, ^{13}C NMR, DEPT 45, DEPT 135 values, ^{1}H-^{1}H COSY and HMBC correlation of E6

^{1}H (ppm)	^{13}C (ppm)	DEPT 45	DEPT 135	^{1}H-^{1}H COSY	HMBC
-	178.00	-			3.66;1.56
3.66	63.10	63.10	63.10*		1.56;1.27
1.56	32.79	32.79	32.79*	1.27	
1.27	29.70	29.70	29.70*		
1.27	29.66	29.66	29.66*		
1.27	29.61	29.61	29.61*		
1.27	29.43	29.43	29.43*	0.89	
0.89	14.12	14.12	14.12		2.36;1.27
2.36	33.79	33.79	33.79*	1.64	
1.64	32.79	32.79	32.79*		
1.27	29.36	29.36	29.36*		
1.27	29.25	29.25	29.25*		
1.27	29.08	29.08	29.08*		
1.27	25.74	25.74	25.74*		
1.27	24.73	24.73	24.73*		
1.27	22.69	22.69	22.69*		
0.89	14.11	14.11	14.11		

*Downward peak

A mixture of mono-alkyl fatty acid esters together can function as a biodiesel. The fatty acyl chain length and the number of double bonds, play a critical role in the utility of such oils (**http://lipidlibrary.aocs.org**). Biofuels made up of fatty acid methyl esters (**Laurens *et al*, 2012**) are advantageous as they are renewable and have lower pollutant emissions (**Sarathy *et al,* 2007**). Fatty acid methyl esters can be transformed

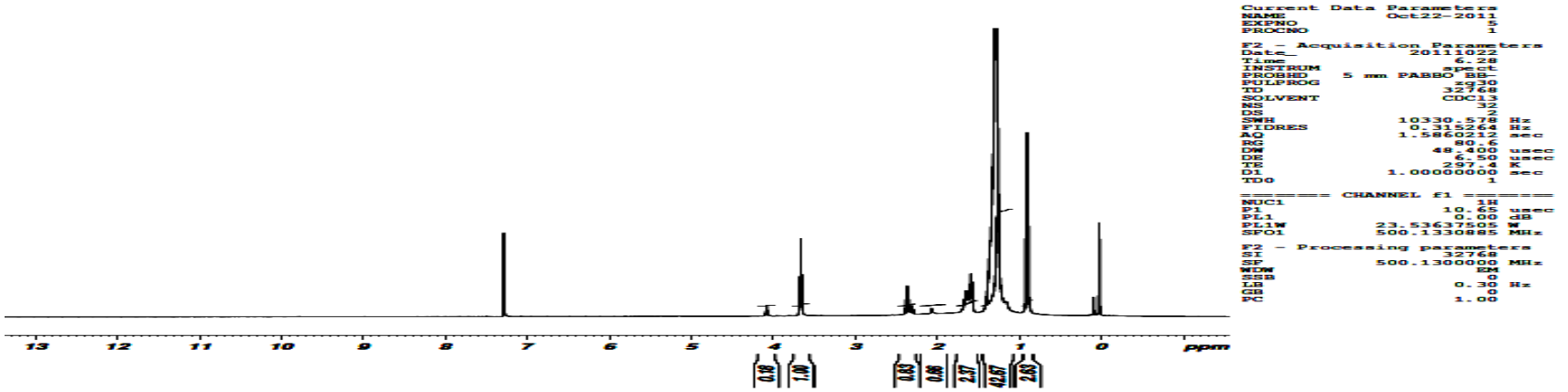

Figure 24. ^{1}H NMR spectrum of E6

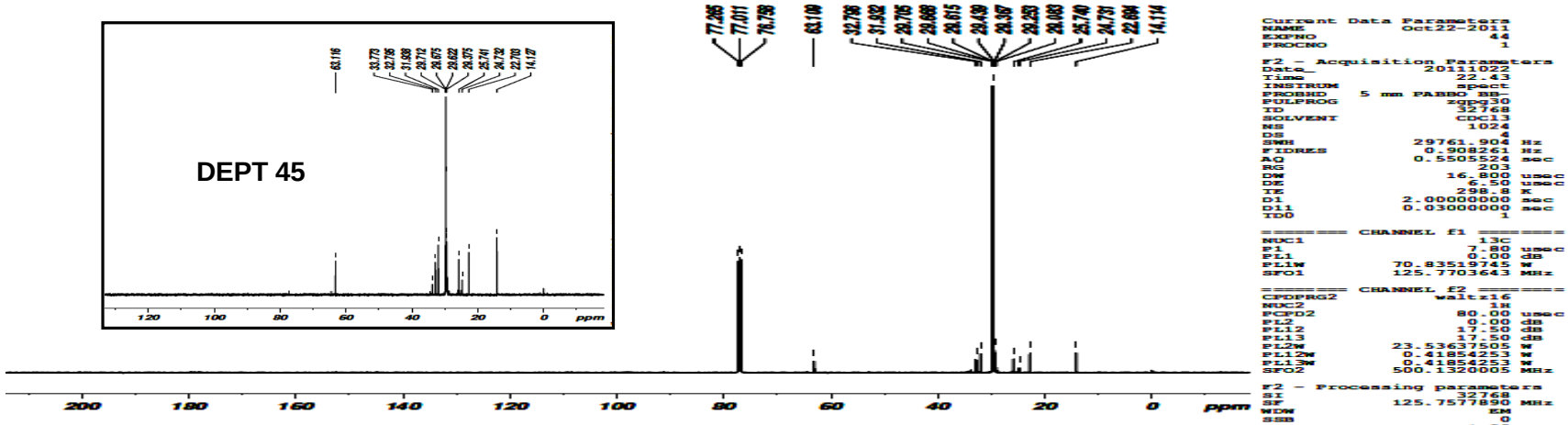

Figure 25. ^{13}C NMR spectrum of E6

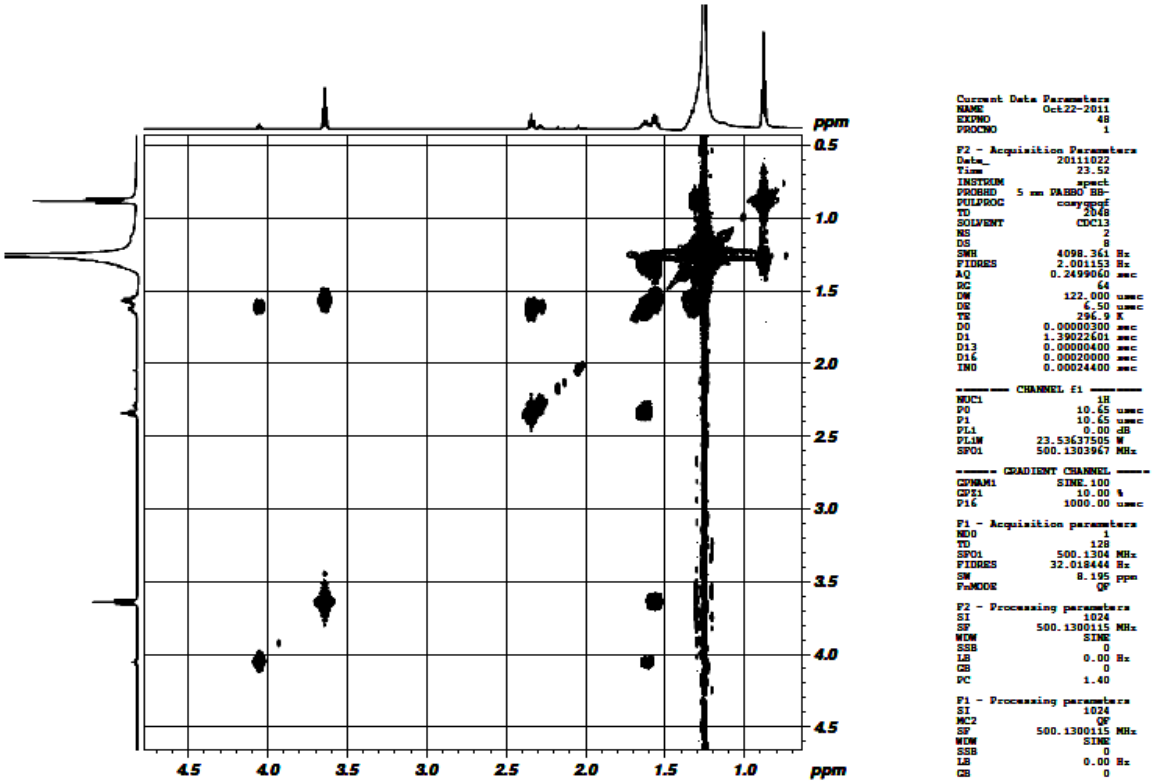

Figure 26. ^{1}H-^{1}H COSY spectrum of E6

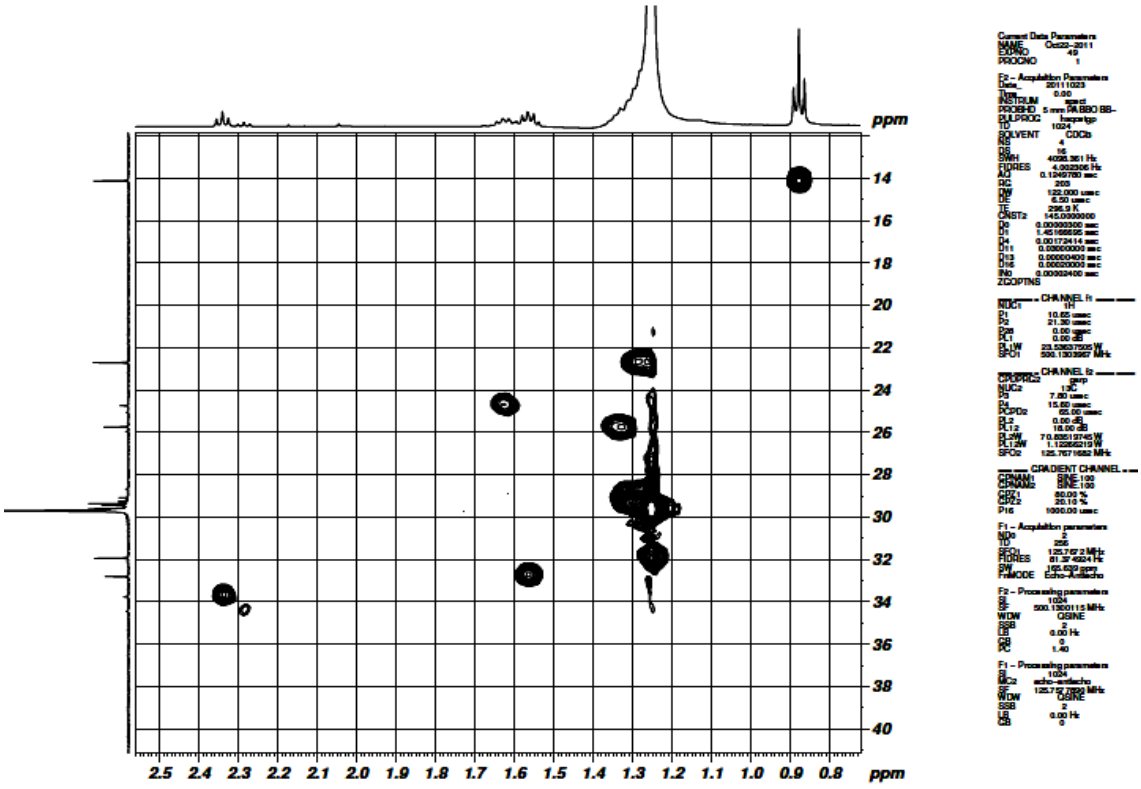

Figure 27. HSQC spectrum of E6

into useful chemicals and raw materials for further synthesis. Alkanolamides, fatty alcohols, and sucrose polyesters are few products that can be generated from fatty acid methyl esters (**Zappi *et al,* 2003**). Fatty acid esters are also used in metal working fluids. These esters are widely used in skin creams and other cosmeceutics and have an excellent health and safety profile (**www.inolex.com**).

Aliphatic long chain fatty esters are the major constituents of plant leaf waxes (**http://lipidlibrary.aocs.org**). Such fatty esters show antibacterial and antifungal activity (**Agoramoorthy *et al,* 2007; Chandrasekaran *et al,* 2011**).

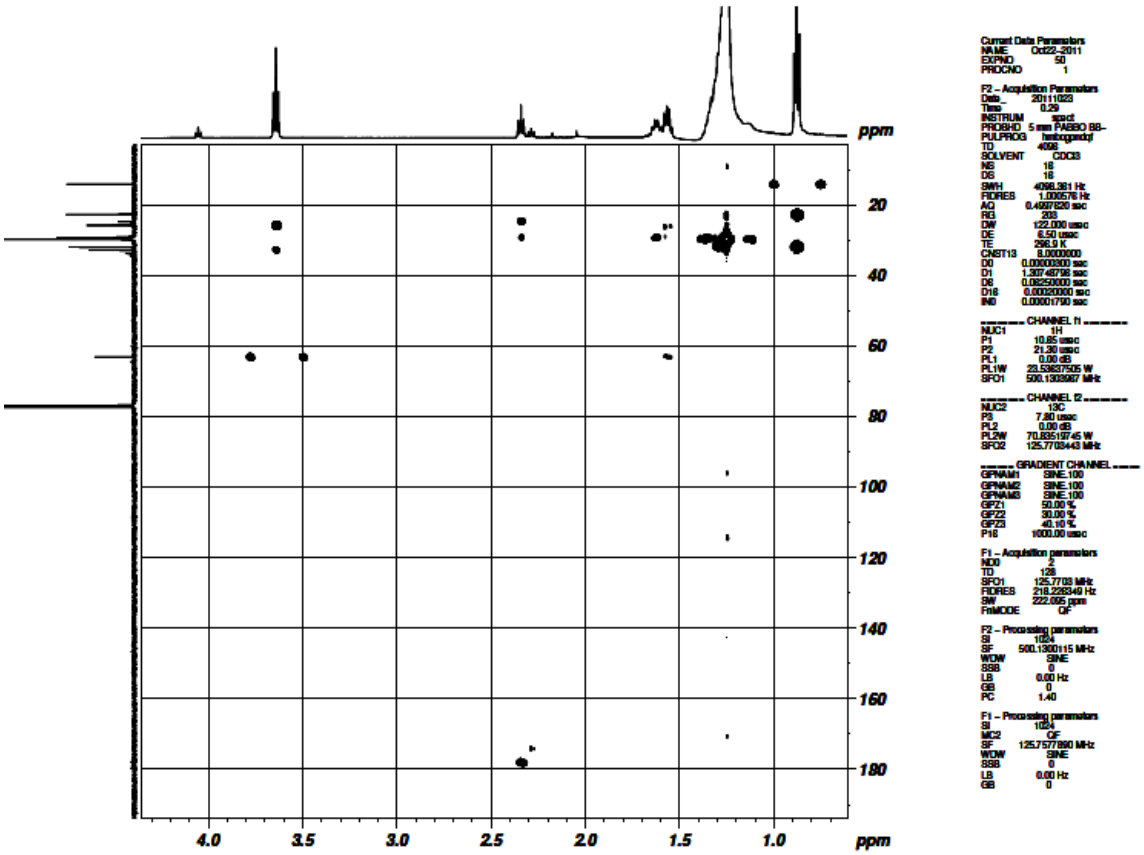

Figure 28. HMBC spectrum of E6

The importance of saturated fatty acid esters in biodiesel industry calls for the exploitation of the plant in the production of biodiesel. This plant has mostly been exploited as a source of biofuel and a large number of papers have been devoted to the efficient production of bioethanol from *E. crassipes* (**Bhattacharya and Kumar, 2010; Bergier *et al,* 2012; Ganguly *et al,* 2012**). The presence of higher fatty acid esters in *E. crassipes* can be a leading line for the production of biodiesel from this plant and hence the significance of *E. crassipes*.

4.4.2.2 Characterization of E8

A dark brown liquid (2 g) was obtained by the open column chromatography of the ethyl acetate extract with 10% ethyl acetate. On purification, a reddish brown liquid (E8) was obtained.

Physical characteristics

(i) Appearance- Reddish brown liquid.

Chemical characteristics

(i) TLC - R_f - 0.57 (100% chloroform).

Spectral interpretation

The UV spectra of E8 in chloroform showed an absorption maximum at 243 nm that indicated the presence of conjugation in the molecule. The IR spectrum showed an absorption band at 2925 cm^{-1} and 2854 cm^{-1} (C–H stretching) and 1710 cm^{-1} (carbonyl group).

^{1}H NMR and ^{13}C NMR interpretation

The ^{1}H NMR, ^{13}C NMR spectral values, ^{1}H-^{1}H COSY, HMBC correlations are given in Table 17. The proton NMR spectrum (Figure 29) of E8 showed a multiplet at δ_H 5.36 that was attributed to the olefinic protons. The presence of methylic hydrogen of ester centered at δ_H 3.68 and a triplet at δ_H 2.86 corresponding to that of methylene proton were observed. The triplet at δ_H 2.36 and a multiplet at δ_H 2.03 corresponds to the deshielded methylene proton in α position to the carbonyl group of the ester and deshielded methylene group on both sides of olefinic proton respectively. The proton resonances at δ_H 1.65 and δ_H 1.27 were that of the methylene proton in β position to that of the carbonyl group and the methylene protons of the long chain respectively. The well defined triplet at δ_H 0.90 were attributed to the terminal methyl protons.

The ^{13}C NMR spectrum (Figure 30) showed a signal at δ_C 180.16, characteristic of the carbonyl group. All the carbon asignments were established using DEPT 45, 90, 135 (Table 17), HSQC, HMBC and further confirmed by comparison with literature (**Diaz and Gavin, 2007**). The carbon NMR spectrum showed the presence of four olefinic carbons at δ_C 130.19, δ_C 130.0, δ_C 128.0 and δ_C 127.90. The carbon resonance in the region δ_C 31- δ_C 22 was that of the methylene carbon attached to proton at δ_H 1.27. The terminal methyl carbon exhibited a resonance at δ_C 14.09. The ^{1}H-^{1}H COSY spectrum showed correlation between δ_H 5.37 and δ_H 2.03; δ_H 5.37 and δ_H 2.80; δ_H 2.03 and δ_H 1.27; δ_H 2.36 and δ_H 1.65; δ_H 1.27 and δ_H 0.90. HMBC correlations were

observed between carbonyl carbon and δ_H 2.36 and δ_H 1.65. On the basis of the foregoing evidence and comparison with literature, the structure of the compound was deduced as **methyl linoleate**.

Methyl linoleate

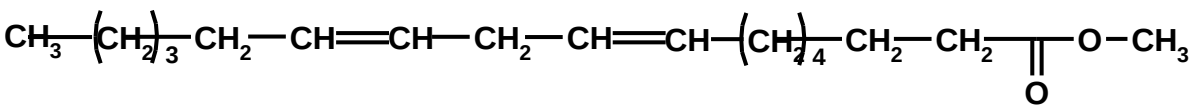

Methyl linoleate is an unsaturated fatty ester and is a constituent of many plants (**Kordali *et al,* 2009; Badoni *et al,* 2010; Joseph *et al,* 2011**). It has been isolated from plants like *Garnoderma lucidum* (**Lee *et al,* 2003**) and was shown to possess antimicrobial activity (**Lee *et al,* 2003; Badoni *et al,* 2010**).

The cost of 1 g methyl linoleate is 3,090 INR approximately. Methyl linoleate (2 g) that costs around 6000 INR approximately was obtained from 300 g ethyl acetate extract of *E. crassipes*.

Table 17. ^{1}H NMR, ^{13}C NMR, DEPT 45, DEPT 90, DEPT 135 values, ^{1}H-^{1}H COSY and HMBC correlation of E8

C no	^{1}H (ppm)	^{13}C (ppm)	DEPT 45	DEPT 90	DEPT 135	^{1}H-^{1}H COSY	HMBC
1	-	180.16	-				H-2; H-3
2	2.36 (t, 2 H)	34.09	34.09		34.09*		H-3; H-4
3	1.65 (m, 2 H)	24.68	24.68		24.68*		H-2; H-4
4	1.27 (s, 14 H)	29.64	29.64		29.64*		
5	1.27	29.67	29.67		29.67*		
6	1.27	29.69	29.69		29.69*		
7	1.27	29.74	29.74		29.74*	H-8	
8	2.03 (m, 4 H)	27.20	27.20		27.20*		
9	5.37 (m, 4 H)	130.0	130.0	130.0	130.0		H-8; H-11
10	5.37	127.9	127.9	127.9	127.9		H-10
11	2.86 (m, 2 H)	24.95	24.95	-	24.95*	H-12	
12	5.37	128.0	128.0	128.0	128.0		H-11
13	5.37	130.1	130.1	130.1	130.1		H-11; H-14
14	2.03	27.20	27.20		27.20*	H-13	
15	1.27	29.43	29.43		29.43*		
16	1.27	31.90	31.90		31.90*		H-17
17	1.27	22.68	22.68		22.68*		H-16 ;H-18
18	0.90 (t, 3 H)	14.09	14.09		14.09		H-16 ;H-17
19	3.68 (s, 3 H)	51.44	51.44		51.44		

*Downward peak

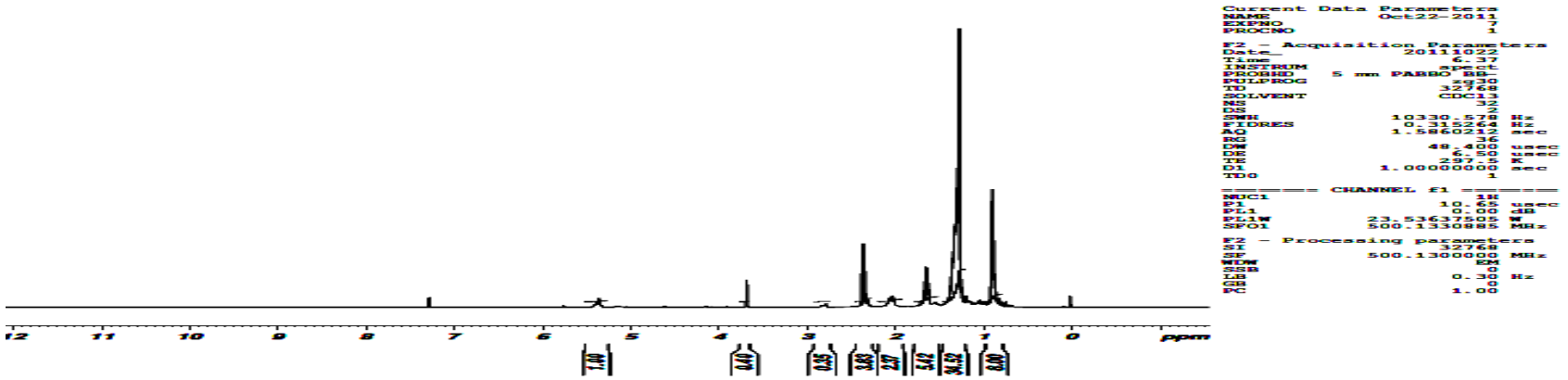

Figure 29. ^{1}H NMR spectrum of E8

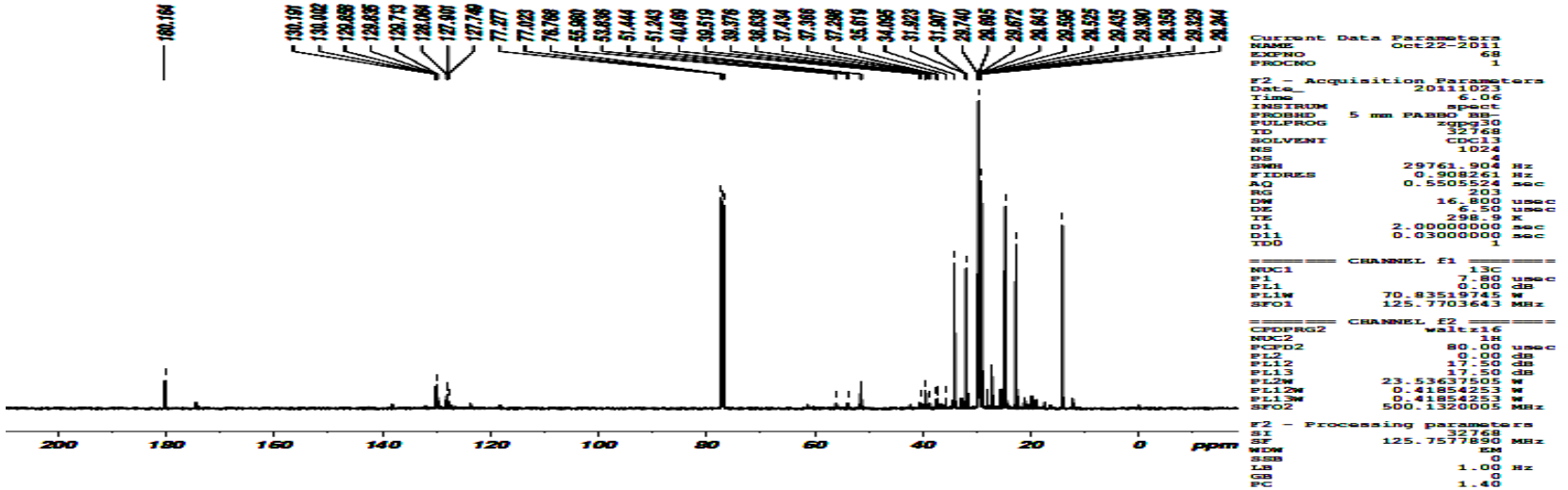

Figure 30. ^{13}C NMR spectrum of E8

4.4.2.3 Structure elucidation of E10

A dark brown liquid (3.95 g) by the open column chromatography of the ethyl acetate extract with10% ethyl acetate. A pale green compound precipitated on addition of petroleum ether. Purification of the compound was done by recrystallization with ethyl acetate when a white amorphous solid was obtained (180 mg).

Physical characteristics

(i) Melting point- 74 °C.

(ii) Appearance- White amorphous solid.

Chemical characteristics

(i) Hydroxamate test- Wine red colour indicating the presence of an ester group.

(ii) TLC- R_f - 0.57 (100% Chloroform).

(iii) It decolourised bromine water indicating its unsaturated nature.

Spectral interpretation

The UV spectrum (Figure 31) of E10 in chloroform showed an absorption maximum at 280 and 311 nm. The molecular formula of the compound was established as $C_{26}H_{42}O_4$ on the basis of its ESI-MS at m/z 418.

The IR spectrum (Figure 32) showed an absorption band at 3552 cm^{-1} characteristic of phenolic O–H stretching. The absorption peaks at 3014 cm^{-1}, 2952 cm^{-1} (=CH–stretching), 2952 (–CH_3 stretching) 2916 cm^{-1} (asymmetric –CH_2– stretching) were also noted. The presence of a sharp peak at 2848 cm^{-1} corresponded to symmetric –CH_2 stretching. Absorption at 1711 cm^{-1} showed the existence of a feruloyl  group. The presence of the vinyl group of cinnamate was apparent from the absorption at 1682 cm^{-1}. Aromatic C=C stretch was confirmed by the presence of peak at 1599, 1518 and 1472 cm^{-1}. The presence of a band at 1430 cm^{-1} due to the cyclic –$(CH_2)_n$–bonding frequency and 1399 cm^{-1}, the bending frequency for –$CH_2(CH_3)_2$ were also noted. Absorption at 1277 and 1251 cm^{-1} indicated the presence of C-O-C ester. An -OCH-CHO group was specified by the presence of an absorption band at 1185 cm^{-1}. The -C-CH_2O stretching was observed at 1042 cm^{-1}.

^{1}H NMR Study

The ^{1}H, ^{13}C NMR values, ^{1}H-^{1}H COSY and HMBC correration are given in Table 18. The proton NMR spectrum (Figure 33) of E10 showed proton resonances at δ_H 7.08, δ_H 7.05 and δ_H 6.92, δ_H 5.94 and was attributed to hydroxyl cinnamic ester.

Peaks at δ_H 7.61, δ_H 6.92, δ_C 167.44 were the characteristic of trans α,β - unsaturated carboxyl functional group. The 1, 2, 4 trisubstitution of the aromatic ring was noted from the resonances at δ_H 7.08, δ_H 7.05 and δ_H 6.92. The triplet at δ_H 4.20 was attributed to H-1''. A signal at δ_H 3.94 corresponded to the methoxyl group attached to the aromatic ring. A quintet at δ_H 1.71 was attributed to the proton at H-2'' in the side chain. H-3'' to H-15'' resonances was seen as a broad signal at δ_H 1.27. The methyl proton H-16'' resonated as a triplet at 0.88.

Table 18. ^{1}H NMR, ^{13}C NMR, DEPT 90, DEPT 135, ^{1}H-^{1}H COSY and HMBC data of E10

C no	^{1}H (ppm)	^{13}C (ppm)	DEPT 90	DEPT 135	^{1}H-^{1}H COSY	HMBC
1	-	127.06	127.06	127.06		H-2'
2	-	147.91	147.91	147.91		H-3; H-4
3	7.05 (dd, *J* = 2 Hz, 1 H) 5.94 (br, s, 1 H)	109.34		109.34		H-2; H-5; H-3'
4	-	146.77	146.77	146.77		H-5; H-17
5	7.09 (dd, *J* = 6, 2 Hz, 1 H)	123.04		123.04		H-6; H-3'
6	6.93 (d, *J* = 8.5 Hz, 1 H)	114.72		114.72	H-3'	
1'	-	167.44		167.44		H-2'; H-1''
2'	6.31 (d, *J* = 16 Hz, 2 H)	115.66	115.66	115.66		
3'	7.63 (d, *J* = 16 Hz, 2 H)	144.66	144.66	144.66		H-1'
1''	4.20 (t, *J* = 6.5 Hz, 2 H)	64.64		64.64*	H-2''	
2''	1.71 (q, *J* = 7.5 Hz, 2 H)	28.78		28.78*	H-3''	
3''	1.27 (br, s, 26 H)	29.70		29.70*		
4''	1.27 (br, s)	29.70		29.70*		
5''	1.27 (br, s)	29.70		29.70*		
6''	1.27 (br, s)	29.70		29.70*		
7''	1.27 (br, s)	29.70		29.70*		
8''	1.27 (br, s)	29.70		29.70*		
9''	1.27 (br, s)	29.70		29.70*		
10''	1.27 (br, s)	29.66		29.66*		
11''	1.27 (br, s)	29.60		29.60*		
12''	1.27 (br, s)	29.55		29.55*		
13''	1.27 (br, s)	29.36		29.36*		
14''	1.27 (br, s)	29.31		29.31*		
15''	1.27 (br, s)	26.00		26.00*		
16''	0.88 (t, 3 H)	14.11		14.11		
17	3.94 (s, 3 H)	55.93		55.93		

* Downward Peak

^{13}C NMR Study

The assignments of individual carbons were made by the assistance of ^{1}H-^{1}H COSY, HSQC and HMBC spectra. The carbon resonance at δ_C167.442 was attributable to the cinnamoyl group (C-1'). The carbon NMR spectrum (Figure 34) showed the presence of twenty six carbon resonances of which six were olefinic δ_C 147.91, δ_C 146.77, δ_C 127.06, δ_C 123.04, δ_C 109.34 and δ_C 114.72. Proton decoupled ^{13}C NMR together with DEPT 45 (Figure 35), DEPT 90 (Table 17) and DEPT 135 (Table 18) indicated the presence of three quaternary, two methyl, eighteen aliphatic methylene, three aromatic methine and two aliphatic methine carbons. The carbon resonances at δ_C 14.11 and δ_C 55.93 corresponded to the C-16'' and –OMe carbon owing to the oxygenation at this carbon. In addition to this methoxy carbon, another carbon resonance at δ_C 64.64 indicated the presence of a carbon at the ester group. The presence of a hydroxyl substituent on C-2 was indicated by the carbon resonance at δ_C 147.9. The resonance at δ_C 144.6 was attributed to C-3' attached to the aromatic ring at C-1. The carbon atom near the ester moiety showed resonance at δ_C 115.6 due to the presence of an oxygenated carbon nearby. The carbon resonances δ_C 29-31 corresponded to the $-(CH_2)_n-$ of the side chain.

2D NMR Analysis

The resonances at δ_H 4.20 and δ_H 1.71 were coupled as seen in ^{1}H-^{1}H COSY (Figure 36). The hydrogen at δ_H 7.61 and δ_H 6.92 were identified to be the coupling partners as notable from the cross peaks between these two resonances. The ^{1}H-^{1}H COSY showed the coupling betwen δ_H 1.72 and δ_H 1.27. The ^{1}H -^{13}C HSQC spectrum (Figure 37) revealed all ^{1}H - ^{13}C direct (^{1}J) correlations and thus established the ^{1}H and ^{13}C assignments of all methyl, methylene and methine groups. Coupling between the proton H-1'' and C-1'' was affirmed by the correlation between these two in HSQC spectra. The long range correlations in the HMBC spectra (Figure 38) was observed between C-1' (δ_C167.44) and H-1'' (δ_H 4.20) (^{2}J) , H-2' (δ_H 6.298) (^{2}J) and H-3' (δ_H 7.61) (^{3}J). Additionally, HMBC together with HSQC gave information about the other deprotonated carbons C-1, C-2 and C-4. The methoxy carbon δ_C 55.93 did not show correlation to any proton indicating the absence of hydrogen in the vicinity of this carbon. The key HMBC spectra which aided in the assignment of the carbon and proton signals are given in Figure 39.

A combination of 1D and 2D NMR spectra together with other spectral details permitted the identification of the compound to be a **hexadecanyl 2-hydroxy**

4-methoxy cinnamate. This chemical structure is primarily consistent with the literature (**Rosas *et al*, 2011**). **This is the first reported isolation of this compound from the family Pontederiaceae**. **This compound has so far been isolated only from the plant *Raputia praetermissa* belonging to the family Rutaceae** (**Rosas *et al*, 2011**). Hence, the isolation of cinnamate ester from the widely available plant *E. crassipes* promises be a suitable alternative in cosmeceutical industries.

Cinnamic esters obtained from plant sources are used in perfumery, cosmeceuticals and pharmaceutical industries. Substituted methoxy cinnamates, a long chain cinnamic ester are used in cosmeceutical industry as sunblock, and they are preferred in this industry as these esters are non-irritant to skin and provide lubricity to prevent drying effect of wind (**Sharma, 2011**). 2-ethylhexyl-p-methoxycinnamate is one of the widely used sunscreen agents in suncare products (**Cheng *et al,* 1997**). It is also used in cleansers/washers, cosmeceutics like moisturizers, creams or lotions for UV protection, hair care products like hair spray, shampoo and conditioners, hair colour, inset repellants, lipstick and nail colour (**http://allergeaze.com**). 2-ethylhexyl-p-methoxycinnamate aids in the protection from UV radiation- induced erythema and oedema (**Reeve *et al*, 1991**). Octyl methoxy cinnamate is widely used as sunscreen in various cosmetic formulations (**Pattanaargson and Limphong, 2001**).

Hexadecanyl p-hydroxycinnamate isolated from *Argyreia speciosa* roots tested against *Fusarium fusiformis* (IMI-211848), *Fusarium semitectum* (IMI-211833) and *Alternaria alternata* (IMI-305675) was highly potent against the test organisms (**Shukla *et al*, 1999**). Ethyl-*p*-methoxycinnamate has been isolated from *Kaempferia galanga* L. extracts and this compound exerts anti-inflammatory activity (**Umar *et al*, 2012**).

Cinnamate esters have long been synthesized because of its use in various industries. **Suzana *et al* (2010)** have synthesised octyl p-methoxycinnamate, a sunblock by transesterification reaction with the starting material p-methoxycinnamate. **Vora and Prajabati** (**2001**) have synthesised a series of α-methyl cinnamates by condensing different 4-*n*-alkoxybenzoyl chloride with methoxyethyl *trans*-4-hydroxy- α -methylcinnamate. There are no reports on the synthesis of this compound. Ethyl acetate extract (300 g) on column chromatography with 90:10 petroleum ether:ethyl acetate yielded (180 mg) of the compound hexadecanyl 2-hydroxy 4-methoxy cinnamate.

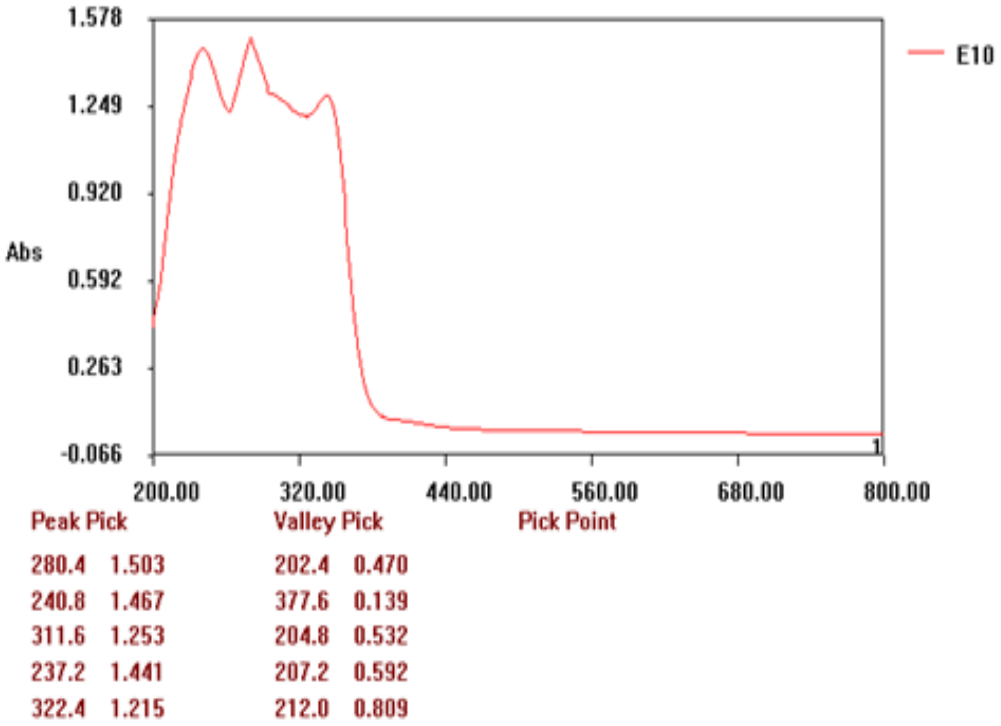

Figure 31. UV spectrum of E10

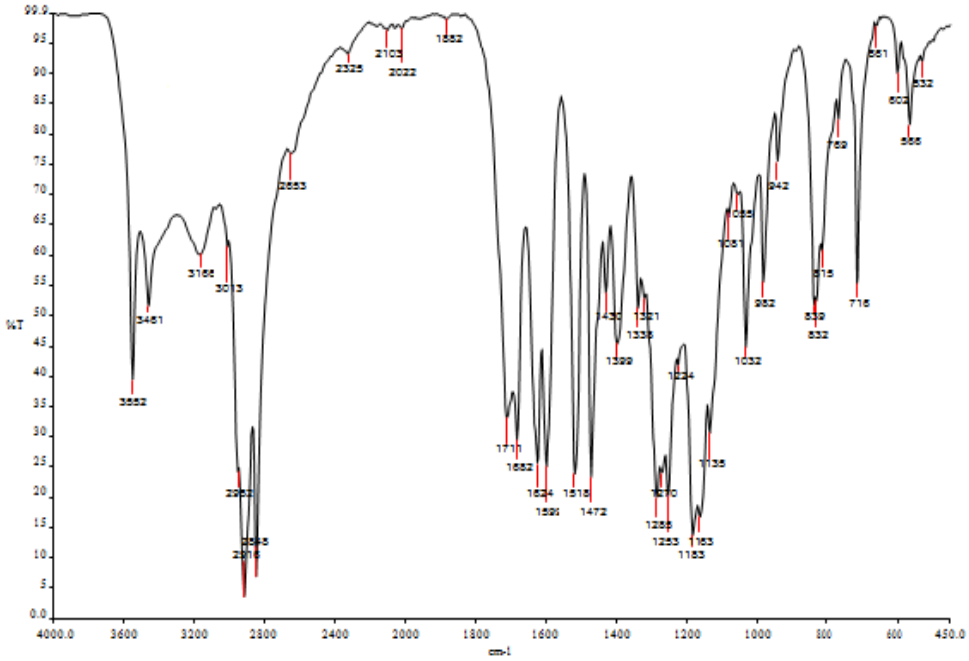

Figure 32. IR spectrum of E10

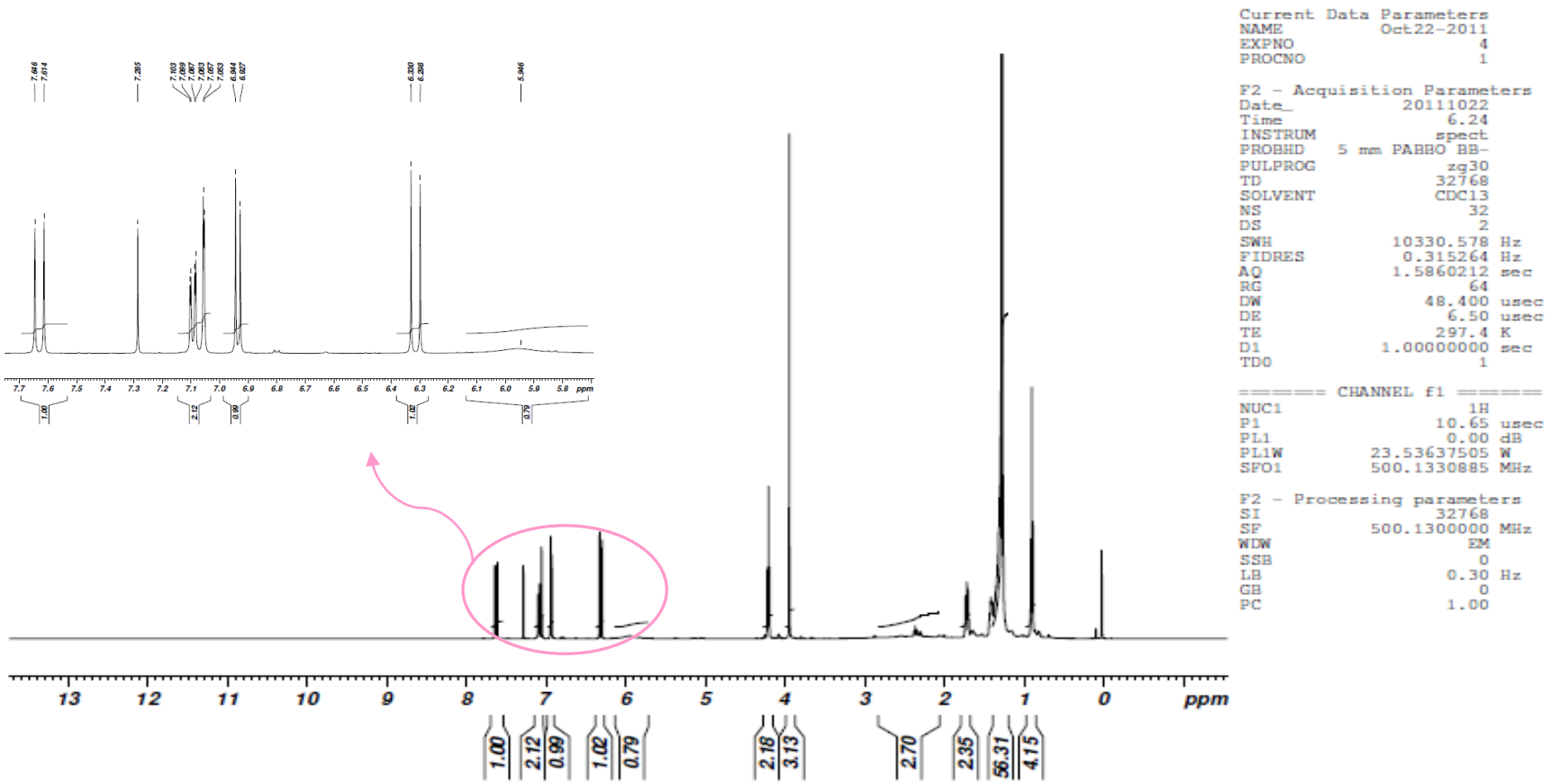


```
Current Data Parameters
NAME                  Oct22-2011
EXPNO                          4
PROCNO                         1

F2 - Acquisition Parameters
Date_                   20111022
Time                        6.24
INSTRUM                    spect
PROBHD     5 mm PABBO BB-
PULPROG                    zg30
TD                        32768
SOLVENT                   CDC13
NS                           32
DS                            2
SWH                  10330.578 Hz
FIDRES                0.315264 Hz
AQ                    1.5860212 sec
RG                           64
DW                       48.400 usec
DE                        6.50 usec
TE                       297.4 K
D1                    1.00000000 sec
TD0                           1

====== CHANNEL f1 ======
NUC1                         1H
P1                       10.65 usec
PL1                       0.00 dB
PL1W                23.53637505 W
SFO1                500.1330885 MHz

F2 - Processing parameters
SI                        32768
SF                  500.1300000 MHz
WDW                          EM
SSB                           0
LB                        0.30 Hz
GB                            0
PC                         1.00
```

Figure 33. ^{1}H NMR spectrum of E10

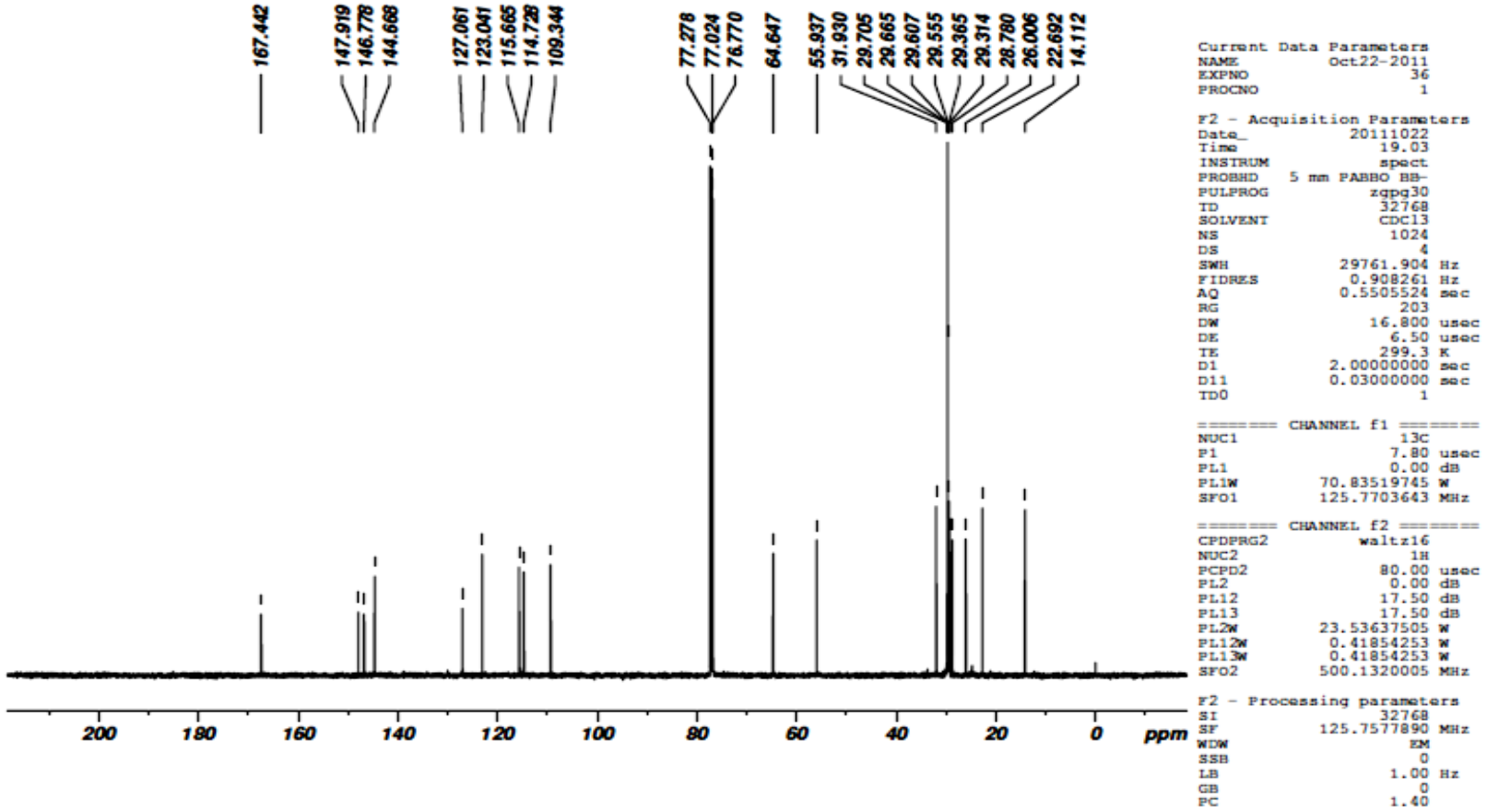

Figure 34. ^{13}C NMR spectrum of E10

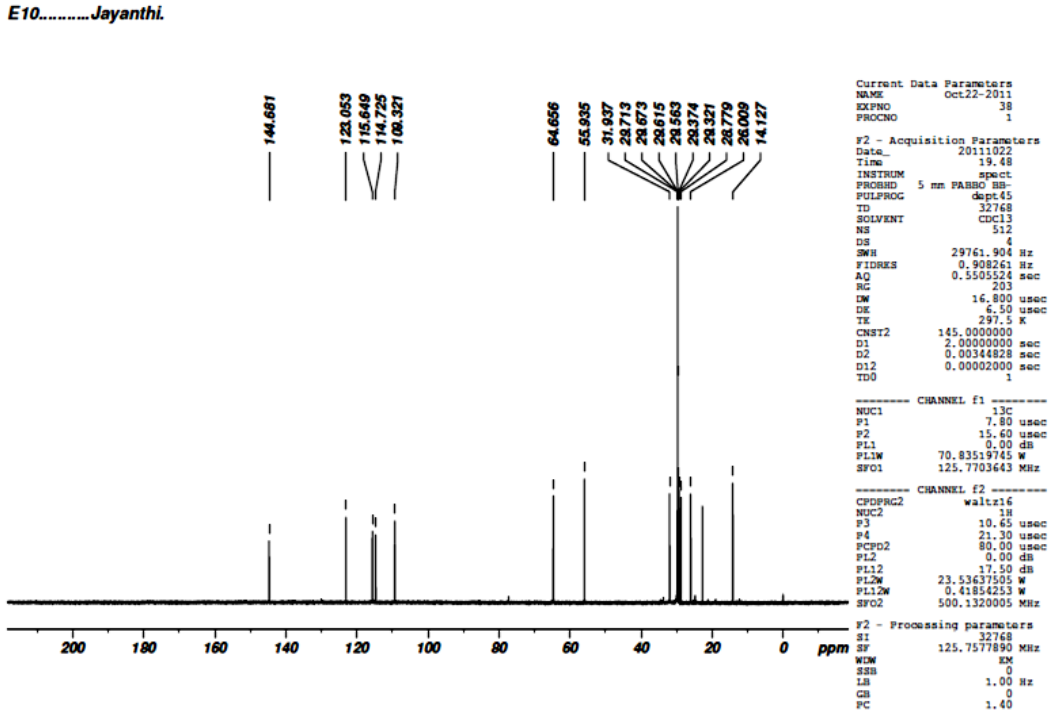

Figure 35. DEPT 45 NMR spectrum of E10

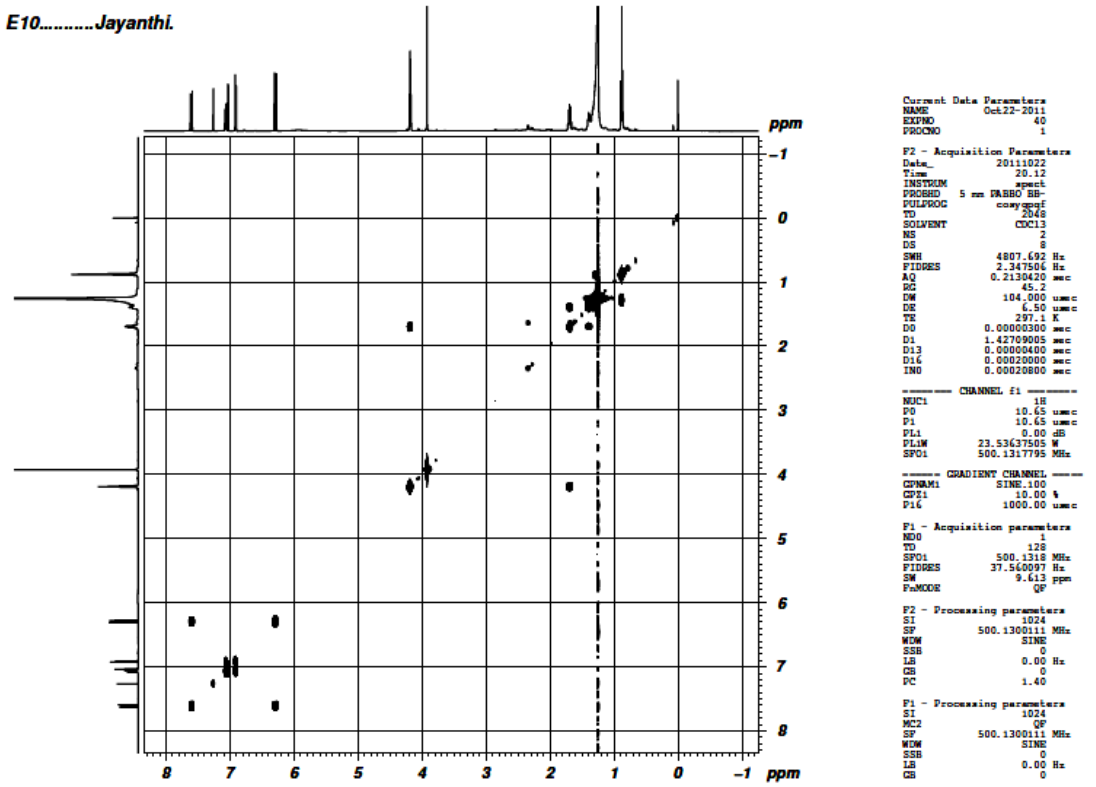

Figure 36. ^{1}H-^{1}H COSY spectrum of E10

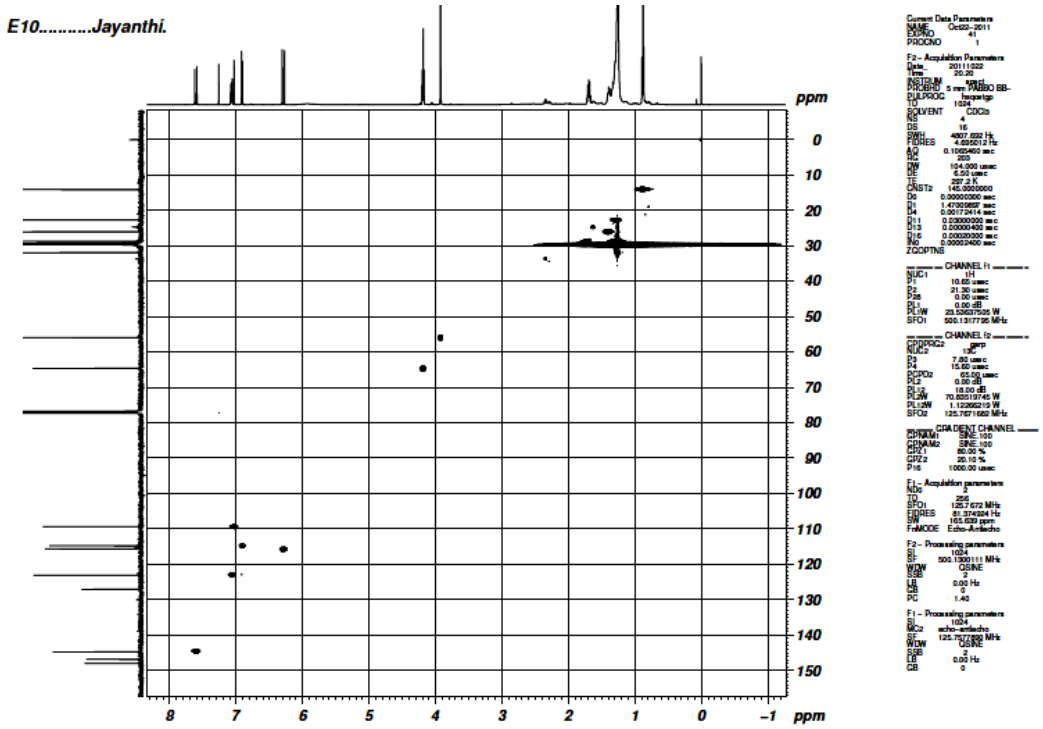

Figure 37. ^{1}H -^{3}C HSQC spectrum of E10

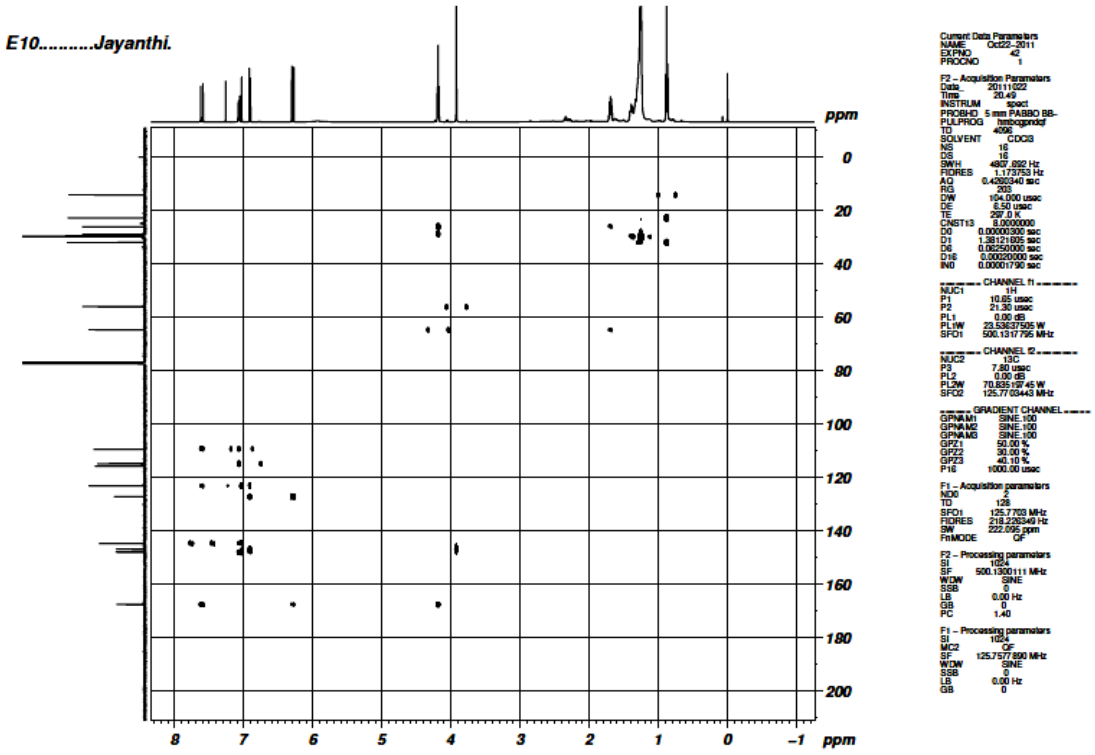

Figure 38. ^{1}H -^{3}C HMBC spectrum of E10

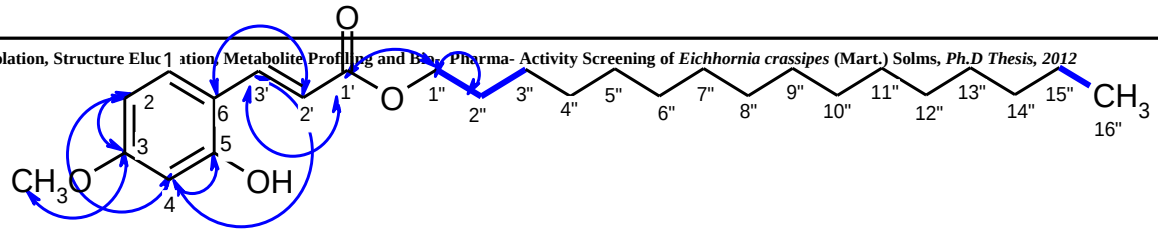

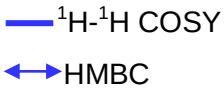

Figure 39. ^{1}H-^{1}H and HMBC correlations of Hexadecanyl 2-hydroxy 4-methoxy cinnamate

Biosynthesis of hydroxycinnamate in *E. crassipes*

New secondary metabolites are crucial in this era of diverse diseases which are resistant to the existing drugs. Biosynthetic aspects are important in functional investigations and a profound understanding of the biosynthetic pathway is essential for synthesis of these metabolites in large quantities.

The biosynthesis of hydroxycinnamate in *E. crassipes* might have followed a combination of phenylpropanoid and fatty acid pathway. **Kosma *et al*** (**2012**) demonstrated that the biosynthesis of alkyl hydroxylcinnamates in Arabidopsis root waxes represents the junction of two distinct metabolisms *viz* phenylpropanoid biosynthesis and very-long-chain fatty acid and fatty alcohol biosynthesis.

The fatty acid pathway might have contributed to the long chain alkane (C_{16}) in the compound. The formation of fatty acid takes place in cytosol and plastid which requires acetyl CoA as the precursor. The simplest description of the plastidial pathway of fatty acid biosynthesis consists of two enzyme systems: acetyl-CoA carboxylase (ACCase) and fatty acid synthase (FAS) (**Ohlrogge and Jaworski, 1997**). The formation of hexadecanoic acid involves four enzyme-catalysed steps involving condensation, reduction, dehydration and reduction (**Beisson *et al*, 2010**). The hexadecanoic acid thus formed in the fatty acid pathway might enter into the cytoplasm where the phenylpropanoid pathway occurs. Phenylpropanoid pathway is the major pathway for the synthesis of phenolic compounds and lignins in plants (**Boudet, 2007**). In this pathway, phenylalanine is lysated to cinnamic acid which is hydroxylated to 2,4-hydroxycinnamic acid by cinnamate monooxygenases. O-methyl transferase (**Hakkinen, 2000**) converts 2,4-hydroxycinnamic acid to 2-hydroxy 4- methoxy cinnamic acid. This might combine with the hexadecanoic acid from the fatty acid pathway catalysed by acyltransferases (**Kosma *et al*, 2012**) that might have probably lead to the formation of the compound hexadecanyl 2-hydroxy 4-methoxy cinnamate in *E. crassipes*.

4.4.2.1.4 Characterisation of E11

E11 was obtained as a green solid (450 mg) by the open column chromatography of the ethyl acetate extract (10% ethyl acetate). Purification of the compound was done by recrystallization with chloroform giving white amorphous solid.

Physical characteristics

(i) Melting point- 138-140 °C.

(ii) Appearance- White needle crystals.

Chemical characteristics

i) Liebermann - Burchard test: Green colour indicating the presence of sterol moiety.

ii) Salkowski test: Formation of red colour in upper layer indicates the presence of sterol moiety.

iii) TLC -R_f -0.5 (100% chloroform), an intense brown spot in iodine vapour that remains for a longer period.

iv) Forms sharp needles in ethyl acetate and floats in ethanol at room temperature.

Spectral interpretation

UV spectrum of compound E11 showed an absorption band at 257 nm indicating a conjugation in the compound. The IR spectrum showed a peak at 3432 cm^{-1} characteristic of OH. The peaks due to C-H stretching and cyclic $-(CH_2)_n-$ bonding frequency were observed at 2955, 2917 cm^{-1} and 1463 cm^{-1}. The presence of cyclohexane ring can be inferred from the peak at 1050 cm^{-1}. Mass spectral fragment ions were noted at *m/z* 429, 399, 385, 355, 283, 256, 237, 209, 168 (100), 138 and 107.

1D and 2D NMR study

^{1}H NMR spectrum showed the presence of signals as that of a sterol compound with characteristic doublet doublet at δ_H 5.17 and δ_H 5.03 corresponding to the exocyclic double bond and a unresolved singlet at δ_H 5.37 corresponding to the steroidal skeleton double bond. All the signals between δ_H 0.7 and 2.4 were noted as multiplets and were unresolved in the ^{1}H NMR spectra. Table 19 indicates the ^{1}H and ^{13}C NMR values of E11. In ^{13}C NMR, 50 peaks were noted indicating the compound to be a mixture of three sterols. The DEPT 45, 90 and 135 spectra together with HSQC helped in identifying the multiplicity of the carbon atoms. The presence of additional signals at δ_C 14.11, δ_C 29.70, δ_C 33.96 correlating with the proton at δ_H 0.85, δ_H 1.27, δ_H 1.02 corresponds to H-29, H-23 and H-22 and indicated the presence of sterol mixture as there were other signals that as well correlated with the same protons. The structural interpretation was made

based on the literature values (HMDB). HSQC and HMBC plots showed the short and the long range coupling between the proton and the carbons. In HMBC plot, long range coupling between δ_C 33.96 and δ_H 0.94 indicated the correlation between C-22 and H-21. Also the signal at δ_C 39.78 (C-24) correlated with δ_H 1.27 (H-23). This may indicate the presence of campesterol together with other sterols. The presence of signals at δ_C 138.31 and δ_C129.29 indicated the presence of stigmasterol in the mixture. Presence of an additional signal at δ_C 45.85 indicated the presence of sitosterol in the mixture. Distinguishable ^{1}H-^{1}H COSY and HMBC correlations for campesterol are given in Figure 40.

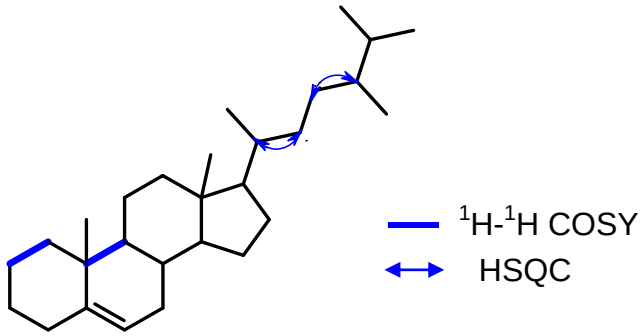

Figure 40. Distinguishable ^{1}H-^{1}H COSY and HMBC correlations of Campesterol

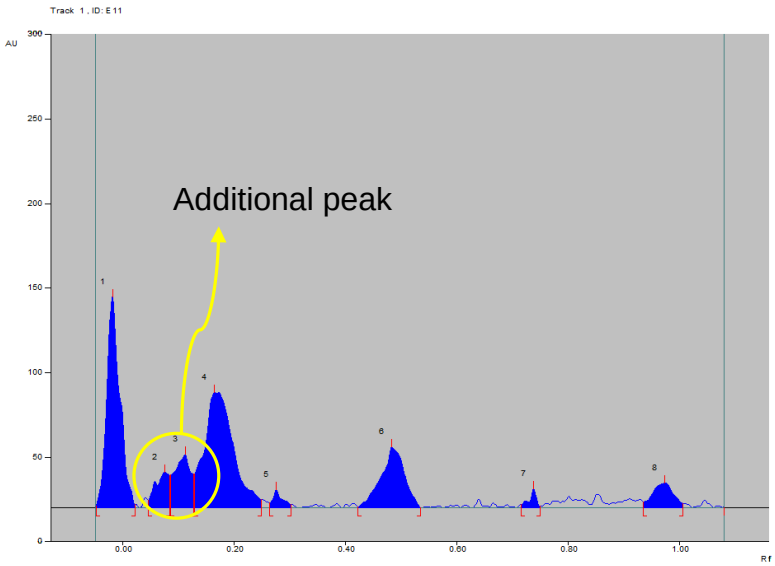

Figure 41. HPTLC chromatogram of E11

The presence of sterol mixture was further confirmed by GC-MS of E11 which showed a peak at *m/z* 399 corresponding to campesterol and a lowering of the melting point to 138-140 °C corroborated it. All these information led to the identification of the sterol mixture to be composed of campesterol together with β-sitosterol and

stigmasterol. In HPTLC chromatogram (Figure 41), the presence of an additional peak apart from that corresponding to β-sitosterol and stigmasterol suggested the presence of a mixture of sterols which was confirmed with the standard β-sitosterol and stigmasterol.

Table 19. ^{1}H NMR and ^{13}C NMR values of E11

C no	^{1}H (ppm)	^{13}C (ppm)
1	1.84	37.26
	1.09	
2	1.86	31.66
	1.55	
3	3.54	71.80
4	2.29	42.33
5	-	140.76
6	5.37	121.71
7	1.97	31.91
	1.55	
8	1.466	31.96
9	0.94	50.17
10	-	36.52
11	1.55	21.08
12	2.01	39.69
	1.19	
13	-	42.30
14	1.01	56.87
15	1.55	24.30
	1.06	
16	1.70	28.25
	1.27	
17	1.19	56.07
18	1.03	19.39
19	0.71	11.98
20	1.35	36.15
21	0.94	18.98
22	1.35	33.96
23	1.27	29.70
24	1.19	39.78
25	1.55	31.91
26	0.85	21.08
27	0.84	18.78
28	0.85	14.11

Sterol mixture consisting of campesterol, β-sitosterol and stigmasterol has been previously isolated from various plants (**Neto *et al*, 1998; Chang *et al*, 2001; do Nascimento and de Oliveira, 2001; Huang *et al*, 2004; Juang *et al*, 2005; Georges *et al*, 2006; Velozo *et al*, 2006; Backhouse *et al*, 2008; De Carvalho *et al*, 2010; Goncalves *et al*, 2011; Tamokou *et al*, 2011**). Campesterol has also been isolated as a mixture with sitosterol (**Gangwal *et al*, 2010),** stigmasterol and cholesterol (**Waller *et al*, 1978; Riyanto, 2007**). Isolation of pure sterols from a sterol mixture is difficult due to the structural similarities of the sterols (**Chuang *et al*, 2006**). The sterol is an important constituent (**Yokota *et al*, 1997; Singariya *et al*, 2012; Araujo *et al*, 2012**) isolated from

many plants (**Hammami *et al*, 2009; Jain and Bari, 2010; Parhoodeh *et al*, 2012**). Sterol mixture isolated from acetone extract of *E. crassipes* has also been reported to contain campesterol, sitosterol and stigmasterol by GLC analysis (**Goswami *et al*, 1983**). However, this is the first reported isolation and characterisation of campesterol mixture from *E. crassipes*.

Campesterol, a C_{28} sterol is known to have cholesterol lowering (**Smahelova *et al*, 2004**) and anticarcinogenic and antiangiogenic effects (**Choi *et al*, 2007**). It also possesses antioxidant effects (**Yoshida and Niki, 2004**). The cost of 1 mg campesterol is INR 6,600 whereas the same from *E. crassipes* will be comparatively very low. This suggests that *E. crassipes*, an aquatic weed can be a useful source for the isolation of sterols.

Reaction with anisaldehyde

Anisaldehyde-sulphuric acid reagent (0.5% Anisaldehyde in solution of methanol:acetic acid:sulfuric acid (85:10:5) was used to identify sterols and differentiate the types of sterols in the mixture. The sterol mixture was spotted on a precoated TLC plate and eluted with 7:3 petroleum ether:ethyl acetate. The plate was sprayed, and then heated at 100 ºC for 2-5 minutes. The spots developed were examined both in visible and UV light. There is no specific reaction of Anisaldehyde-Sulfuric acid Reagent with various compounds. Heating the TLC plate produced colour changes. This might be due to the condensation reaction of anisaldehyde with functional groups of the sterols. Colour changes were observed after the TLC plate was heated possibly due to condensation of anisaldehyde with certain functional groups of compounds. β-sitosterol gives pinkish grey colour, stigmasterol gives greyish violet (**Archana *et al*, 2011**).

E11 spots on visualization with Anisaldehyde-sulphuric acid reagent separately gave a pinkish green colour confirming the presence of campesterol together with other sterols.

4.4.2.1.5 Structure elucidation of E12

Column chromatography of ethyl acetate extract yielded a green solid (1.5 g) on elution 10% ethyl acetate. Purification of the compound was done by recrystallization with chloroform when a white amorphous solid was obtained .

Physical characteristics

(i) Melting point- 148 °C.

(ii) Appearance- White needle crystals

Chemical characteristics

(i) Liebermann - Burchard test-Green colour indicating the presence of sterol moiety.

(ii) Salkowski test: Formation of red colour in upper layer indicates the presence of sterol moiety.

(iii) TLC - R_f -0.5 (100% chloroform), an intense brown spot in iodine vapour that remains for a longer period.

Spectral interpretation

UV spectrum of compound E12 showed absorption maxima at 257 nm indicating the presence of a conjugation in the molecule. The IR spectrum resembled that of E11 ascertaining the compound to be a sterol.

1D and 2D NMR study

The ^{1}H NMR and ^{13}C NMR spectral values of the compound (Table 20) were similar to those that of E11, the difference being the lack of few carbon signals in E12 at δ_C 29.70, δ_C 29.66, δ_C 29.36, δ_C 22.69, δ_C 14.11. This suggested the compound to be mixture of sterols. Careful examination of the ^{13}C NMR spectra together with DEPT and HSQC suggested the compound to be a mixture of two sterols. The presence of signals at δ_C 138.31 and δ_C 129.29 indicated the presence of stigmasterol in the mixture. Presence of an additional signal at δ_C 45.85 correlating with δ_H 0.92 indicated the presence of sitosterol in the mixture. The only difference between the structure of two compounds is the presence of olefinic bond in the side chain (C-22 and C-23) in stigmasterol which is absent in β-sitosterol. The R_f of the compounds is also the same in most of the solvent systems and hence the difficulty in the separation of the two mentioned sterols (**Pateh *et al*, 2009; Kamboj and Saluja, 2010**). HMBC correlations of β-sitosterol are given in Figure 42.

The presence of sterol mixture was further confirmed by the lowering in melting point to 148 °C. The HPTLC chromatogram on comparison with standard β-sitosterol and stigmasterol confirmed the presence of a mixture of sterols. In the ^{1}H NMR spectrum of E12, integration of proton signals at δ_H 5.36 (H-6), δ_H 5.15 (H-22), δ_H 5.02 (H-23) and δ_H 3.53 (H-3) were approximately in the ratio 2:1:1:2. Thus, the ratio of β-sitosterol and stigmasterol in E12 might be 1:1. The same ratio of mixture of sterols has been previously isolated from the chloroform extract of *Mammea siamensis* flowers

(**Subhadhirasakul and Pechpongs, 2005**) and hexane extract of aerial parts of *Acacia cochliacantha* (**Torres *et al*, 2007**).

Table 20. ^{1}H NMR and ^{13}C NMR values of E12

C no	^{1}H (ppm)	^{13}C (ppm)
1	1.84	37.26
	1.09	
2	1.86	31.66
	1.55	
3	3.52	71.81
4	2.29	42.33
5	-	140.76
6	5.35	121.71
7	1.97	31.88
	1.55	
8	1.466	31.91
9	0.92	50.17
10	-	36.52
11	1.49	21.08
12	2.01	39.69
	1.16	
13	-	42.30
14	1.01	56.77
15	1.55	24.30
	1.06	
16	1.70	28.25
	1.27	
17	1.16	56.07
18	1.03	19.39
19	0.71	11.86
20	1.35	36.15
21	0.94	18.98
22	1.35	33.96
23	1.27	29.70
24	0.92	45.85
25	1.66	29.17
26	0.85	21.08
27	0.84	18.98
28	1.25	23.08
29	0.85	19.81

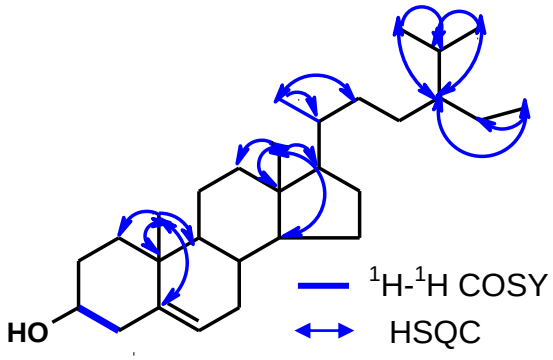

Figure 42. Key HMBC correlation of β-sitosterol

Sterol mixture of β-sitosterol and stigmasterol in various ratios has been previously isolated from various plants (**Burdi *et al*, 1991; Castellanos *et al*, 2002; Araujoa *et al*, 2005; Prachayasittikul *et al*, 2009; Hussain *et al*, 2010; Dendougui *et al*, 2011; Kamboj and Saluja, 2011; Mezhoud *et al*, 2012; Phung *et al*, 2012; Rodriguez *et al*, 2012; Veloso *et al*, 2012**). The sterol mixtures show many pharmacological activities including anti-inflammatory effect (**Rodriguez *et al*, 2012**), antihyperglycemic activity (**Phung *et al*, 2012**), antibacterial activity (**Prachayasittikul *et al*, 2009**).

β-sitosterol is the major phytosterol in higher plants. Animal studies revealed that β-sitosterol reduces carcinogen-induced cancer of the colon, as well as exhibits anti inflammatory, antipyretic, antineoplastic, and insulin-releasing effects (**Bouic and Lamprecht, 1999; Gallova *et al*, 2011**) and immune-modulating properties. In other *in vitro*, animal, and human studies, a proprietary mixture of these two has shown promise in normalizing T-cell function, dampening overactive antibody responses, and normalizing DHEA:cortisol ratios (**Anonymous, 2001**). β-sitosterol isolated from the methanol root extract of *Pluchea indica* has shown viper and cobra venom neutralisation (**Gomes *et al*, 2010**).

This is the first report of isolation and characterisation of this sterol from *E. crassipes*. Giving consideration to the pharmacological importance of β-sitosterol, this plant can be regarded as a good and easily available source of this sterol. The cost of β-sitosterol (10 mg) is INR 11,528 approximately and hence the isolation of β-sitosterol from *E. crassipes* is a much economical option.

4.4.2. 6 Structural characterization of compound E13

E13 was obtained as pale white powder (1.5 g) by the column chromatography of the ethyl acetate extract (10% ethyl acetate). Purification of the compound was done by recrystallization with chloroform giving white needle crystals.

Physical characteristics

(i) Melting point - 161 °C.

(ii) Appearance - White needle crystals

Chemical characteristics

The chemical characteristics of E13 were similar to that of E12.

Spectral data

The UV spectrum of E13 in chloroform showed an absorption maximum at 257 nm. The molecular formula of the compound was established as $C_{29}H_{48}O$ on the basis of its ESI-MS at m/z 412 and this was confirmed by NC-MS which showed a peak at 379 due to the loss of water and a methyl group. The other major fragments in the spectrum appeared at 412 [$C_{29}H_{48}O$, M+1] (15), 394 [M-H_2O]$^+$, 366 [M- H_2O-CH_2= CH_2]$^+$, 351 [M-C_3H_7-H_2O]$^+$, 330 [M-$H_2OC_5H_7$]$^+$, 300 [M-C_8H_{16}], 273 [M-H_2O-C_7H_{13}]$^+$.

The IR spectrum showed an absorption band at 3446 cm^{-1} characteristic of OH stretching. Absorption at 3030 cm^{-1} might be attributed to =CH stretching and 2968 and 2937 cm^{-1} may be attributed to C–H stretching. The presence of a band at 1458 cm^{-1} due to the cyclic −$(CH_2)_n$− bonding frequency and 1383 cm^{-1} (bending frequency for –$CH_2(CH_3)_2$) were noted. Absorption at 1332 cm^{-1} was attributed to OH (def.) and absorption at 1051 cm^{-1} indicated the presence of cyclohexyl moiety. The IR absorption frequencies corresponded with that of the frequencies of stigmasterol reported in literature (**Pateh *et al*, 2009**).

The ^{1}H NMR and ^{13}C NMR values of E13 are given in Table 21. In the ^{1}H NMR spectrum, most important signals which aided in the structure elucidation of sterol compounds were those present in the region above δ_H 5. The ^{1}H NMR showed a doublet at δ_H 5.37, a characteristic of the olefinic proton of the steroidal skeleton which is quaternary and endocyclic. The doublet doublet signals at δ_H 5.03and δ_H 5.17 was attributed to the trans disubstituted double bond which are exocyclic. A pentet at δ_H 3.54 was assigned for the carbinolic hydrogen. The six methyl groups resonated at δ_H 0.94 and δ_H 0.54 as two singlets and were assigned to H-18 and H-19 of the tertiary methyl groups. Doublets in the proton spectrum at δ_H 1.01, δ_H 0.87 and δ_H 0.82 corresponded to H-21, 26 and 27 of the secondary methyl group respectively. The one primary methyl group was noted as a triplet at δ_H 0.72 in the ^{1}H NMR spectrum.

The broadband decoupled ^{13}C NMR showed 29 signals which indicated that the compound might possess a steroidal skeleton with side chain. The DEPT 45 spectrum revealed the presence of 26 carbons that have attached protons. Thus, the signal at δ_C 140.75, δ_C 36.52, δ_C 42.22 was attributed to quaternary carbon at 5, 10 and 13 positions respectively. DEPT 90 revealed that the compound contains 11 methine carbon at δ_C 71.81, 121.71, 31.88, 50.97, 56.87, 55.96, 40.9, 138.31, 129.38, 51.24, 31.90 were attributed to the C-3, 6, 8, 9, 14, 17, 20, 22, 23, 24 and 25 respectively.

DEPT 135 showed the number of methyl, methylene and methine carbons and it was found that the compound contains six methyl carbons. The methylene carbons were seen at δ_C 19.40, 12.05, 21.22, 21.08 and 12.25 that corresponding to C-18, 19, 21, 26, 27 and 29. The signals at δ_C 12.05 and 19.40 corresponded to angular carbon atom (C-19 and C-18 respectively). The value for C-18 was found to be lower than C-19 due to γ-gauche interaction that increased the screening of the C-18 and hence the lower chemical shift. However, the loss of H in C-6 resulted in decrease in screening of the C-19 leading to increase in ^{13}C chemicals shift to higher frequency. This was found to be tenable as in chemical shift of 12.05 and 19.40 ppm (for C-19 and C-18 respectively) (**Pateh *et al*, 2009**).

Table 21. ^{1}H NMR and ^{13}C NMR values of E13

C no	^{1}H (ppm)	^{13}C (ppm)
1	1.86 (m, 1 H); 1.08 (m, 1 H)	37.26
2	1.86 (m, 1 H) 1.49 (m, 1 H)	31.66
3	3.54 (m, 1 H)	71.81
4	2.27 (m, 2 H)	42.30
5	-	140.75
6	5.37 (d, 1 H)	121.71
7	1.99 (m, 1 H) 1.49 (m, 1 H)	31.90
8	1.49 (m, 1 H)	31.88
9	0.94 (m, 1 H)	50.17
10	-	36.52
11	1.49 (m, 2 H)	21.10
12	2.00 (m, 1 H) 1.18 (m, 1 H)	39.69
13	-	42.22
14	1.03 (m, 1 H)	56.87
15	1.49 (m, 1 H) 1.08 (m, 1 H)	24.37
16	1.71 (m, 1 H) 1.28 (m, 1 H)	28.25
17	1.18 (m, 1 H)	55.96
18	0.94 (s, 3 H)	19.40
19	0.57 (s, 3 H)	12.05
20	1.99 (d, 3 H)	40.49
21	1.01 (d, 3 H)	21.22
22	5.03 (dd, 1 H)	138.31
23	5.17 (dd, 1 H)	129.28
24	1.49 (m, 1 H)	51.24
25	1.99 (m, 1 H)	31.90
26	0.87 (d, 3 H)	21.08
27	0.87 (d, 3 H)	18.98
28	1.49 (m, 1 H)	25. 40
29	0.72 (t, 3 H)	12.25

The assignment of the NMR data was confirmed using a combination of 1D DEPT and 2D ^{1}H-^{1}H COSY and HSQC. The assigned values were also confirmed with the literature (**Forgo and Kover, 2004**). ^{1}H-^{1}H COSY showed that δ_H 3.5 and δ_H 2.3 are coupled to each other since they have cross peaks. There were cross peaks between the protons at position δ_H 3.5 and δ_H 1.5 indicating the correlation between the two protons. HSQC correlations assisted in distinguishing the position of the hydroxyl group with δ_C 71.81 showing a correlation to the methine proton resonance at δ_H 3.54. Key HMBC correlations are shown in Figure 43. In the HMBC spectrum, C-4 showed correlations to the methine proton resonance at δ_H 3.54. H-18 showed HMBC correlations with three carbon resonances at δ_C 12.05, δ_C 21.22 and δ_C 55.96. On the basis of the above assignments and comparison with the literature, the structure of the compound was deduced as stigmasterol, the most common sterol found in plants.

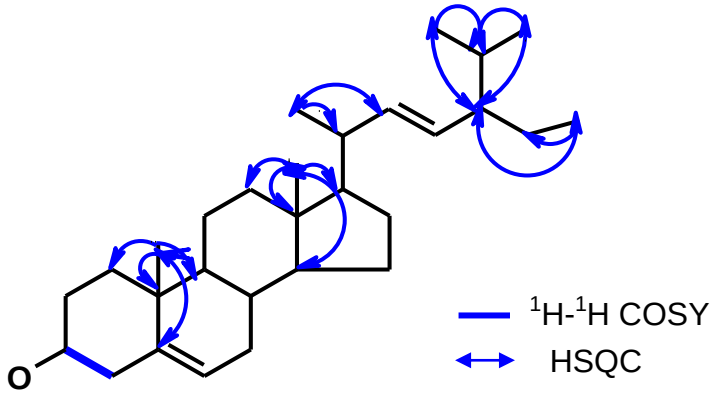

Figure 43. Key HMBC and ^{1}H-^{1}H COSY of Stigmasterol

Further confirmation was made by visualizing the TLC spot of E13 in Anisaldehyde- sulphuric acid reagent after elution of the TLC plate in the solvent system 7:3 petroleum ether:ethyl acetate. The compound gave a greyish violet colour with this reagent confirming it to be stigmasterol (**Archana *et al*, 2011**).

Stigmasterol has been shown to be the starting compound of many plant hormones. A large number of papers have been dedicated to the synthesis of many stigmasterol derivatives, other steroids and compounds of pharmacological importance from stigmasterol (**Kaur *et al*, 2011**). Stigmasterol has been isolated from several plants but there are no reports on its quantitative isolation from waterhyacinth. **Goswami *et al*** (**1983**) have identified stigmasterol, campesterol, β-sitosterol in the acetone extract by gas-liquid chromatography and suggested water hyacinth to be a prospective source of sterols. Apart from this identification there are no other studies on the isolation of

stigmasterol from this plant and from such aquatic weeds which are considered to be futile. This is the first report of the isolation of stigmasterol from the ethyl acetate extract in quantitative yields.

E. crassipes is available in plenty in all water bodies and is being thrown out in bulk as a waste and hence isolation of valuable compounds from this plant would be equally welcomed by everyone. In consideration of the high cost of standard stigmasterol, *E. crassipes* will be a cheap source for its isolation in good yields. Isolation of stigmasterol from *E. crassipes* in quantitative yields makes the plant a rich source of this particular metabolite and the present work thus proves to be much significance. Stigmasterol has been isolated from many plants. Table 22 shows the yield of stigmasterol obtained from various plants and it is obvious that the yield of stigmasterol obtained from *E. crassipes* is comparatively high when compared with other plants thus making it an imperative source of stigmasterol. Rather than exploiting the rare and endemic medicinal plants for the commonly available stigmasterol, *E. crassipes* may be a welcome source of this dietary supplement.

Table 22. Yield of stigmasterol isolated from various plants

S. No	Plant	Plant part	Extract	Quantity of the extract (g)	Yield of Stigmasterol (mg)	Reference
1	***Eichhornia crassipes***	**Leaves and shoot**	**Ethyl acetate**	**300**	**1500**	**Present work**
2	*Micromelum minutum*	Leaves	Chloroform	2.0	5.2	Susidarti *et al*, 2007
3	*Euphorbia heterophylla* Linn		Chloroform	16.22	25	Falodun *et al*, 2008
4	*Phyllanthus reticulates*	leaves	Methanol	4	2.5	Jamal *et al*, 2008
5	*Spilanthes acmella* Murr	-	Hexane	55	14.9	Prachayasitti kul *et al*, 2009
			Chloroform	50	60	
6	*Dillenia indica* Linn	Leaves	Hexane	0.820	4.3	Muhit *et al*, 2010
7	*Etlingera sphaerocephala* var. *grandiflora*	Rhizome	Hexane	1.5	6.6	Yahya *et al*, 2011
8	*Dioclea reflexa*	Hook seed	Methanol	9.49	40	Faleye, 2012
9	*Saraca thaipingensis*	Flower	Dicholorom ethane	2.5	18	Prachayasitti kul *et al*, 2012

Stigmasterol (1.5 g) has been obtained from 300 g of the ethyl acetate extract of *E. crassipes*. 1 g of commercially available stigmasterol costs around 3,683 INR (Ref:Sigma-Aldrich-S2424). The stigmasterol amounting approximately 10,000 INR is obtained from 300 g of the ethyl acetate extract, thus making the isolation of stigmasterol from *E. crassipes* a cost effective procedure.

Biosynthesis of sterols in *E. crassipes*

The biosynthetic route to campesterol, sitosterol and stigmasterol in *E. crassipes* as in the case of most plants may perhaps follow either of the two independent pathways *viz* the cytosolic mevalonic acid (MVA) pathway and the plastidial methyerythritol phosphate (MEP) pathway. The two pathways differ in the mode of formation of (isopentenyl pyrophosphate) (IPP) and dimethylallyl diphosphate (DMAPP) where in MVA pathway the precursors are acetyl CoA whereas for MEP pathway the precursors are pyruvate and glycerinaldehyde-3-Phosphate both forming isoprene units (**Dubey *et al*, 2003; Rohmer *et al*, 2005; Liao *et al*, 2006; Christie, 2012**). IPP is utilised in a sequence of elongation reactions which serves as the immediate precursors of different classes of terpenoids.

The squalene formed in one of the step in the pathways is oxidised to form 2,3-epoxide, oxidosqualene, and then cyclised in a protonation reaction to produce the common sterol cycloartenol (**Croteau *et al*, 2007**) and lanosterol (**Suzuki *et al*, 2006**). The biosynthesis is essentially linear until reaching 24-methylene lophenol, with a bifurcation downstream of this compound that result in two main pathways leading to 24-methyl- (Campesterol) and 24-ethyl-sterols (Sitosterol). Cycloartenol or lanosterol is metabolized into sitosterol via obusifoliol (4α,14α-dimethyl- ergosta-8,24(28)-dien-3β-ol), which is biosynthesized from cycloartenol after C-24 methylation, C-4 demethylation, and cyclopropyl isomerisation (**Ohyamaa *et al*, 2009**). Stigmasterol is formed from sitosterol by a C-22 desaturation in the side chain by sterol desaturase (CYP710A1) (**Morikawa *et al*, 2006; He *et al*, 2008; Griebel and Zeier, 2010; Bawankar *et al*, 2012**). There are more than thirty enzyme-catalysed steps in the overall process, each associated with membranes. The 4,4-dimethyl- and 4α-methylsterols are part of the biosynthetic pathway, but are only minor if ubiquitous sterol components of plants (**Christie, 2012**). The simplicity of this pathway is essentially due to i) the relatively high substrate specificity of most enzymes from the postsqualene segment of the biosynthetic chain and ii) to the channeling of substrates/products through microdomains of the endoplasmic reticulum (**Benveniste, 2004**).

Phytosterol composition in plants is known for its high complexity compared with sterols of other eukaryotes. Sitosterol, stigmasterol, isofucosterol, campesterol and 24-methylcholestrol are some of the end sterols common in most plants. In vascular plants, sitosterol and stigmasterol are the major sterols (**Bawankar *et al*, 2012**). Inspite of their similarity in structure, β-sitosterol has been shown to be a membrane reinforcer whereas stigmasterol is not (**Eknamkul and Potduang, 2003**). The nearly planar aliphatic core and 3-hydroxyl head group of the phytosterols enable them to be incorporated into phospholipid membranes in cells, where they play a critical role in controlling the membrane fluidity or rigidity. The chemical structures of phytosterols are finely tuned to their physiological function; the flexible aliphatic side chains of sitosterol and campesterol, can stack in an ordered fashion in the membranes, increasing their rigidity, but the *trans*-double bond in the side chain of stigmasterol interferes with membrane ordering and promotes greater fluidity (**Crozier *et al*, 2006**).

4.4.2.1.7 Structure elucidation of E16

Silica gel column chromatography of ethyl acetate extract furnished a brown powder (1.8 g) from 90:10 petroleum ether:ethyl acetate eluates. The molecular formula was inferred as $C_{29}H_{46}O_2$ on the basis of 1D and 2D NMR. The compound was recrystallized using ethyl acetate giving a white powder (40 mg).

Physical characteristics

(i) Melting point- 192 °C.

(ii) Appearance- White amorphous solid

Chemical characteristics

(i) TLC - R_f - 0.75 (100% chloroform), intense brown spot.

(ii) Solubility- Completely soluble in ethyl acetate and chloroform; partially soluble in ethanol at room temperature.

Spectral data

The UV spectrum (Figure 44) of E16 in chloroform showed an absorption maximum at 236 nm and 310 nm which indicated the presence of n→π* transitions. FTIR absorption bands (Figure 45) were found at 3436 cm^{-1} and 1710 cm^{-1} (α,β- unsaturated carbonyl group), 2954 and 2869 cm^{-1} (C-H stretch), 1463 cm^{-1} (cyclic $(CH_2)_n$), 1383 cm^{-1} ($–CH_2(CH_3)_2$ bending), 1240 cm^{-1} (C-O) group

The ^{1}H NMR (Figure 46) of E16 showed deshielded methine resonances as a doublet doublet at δ_H 5.17 (H-22) and δ_H 5.06 (H-23) which are exocyclic and a methine

resonance of the steroidal skeleton at δ_H 2.61 (H-8). One of the protons of the methyl group resonated at δ_H 0.98 (H-27), the other resonated as a singlet at δ_H 0.73 (H-29) and the third proton resonated at δ_H 0.84 (H-19). Four other methyl groups found in the ^{1}H NMR spectrum resonated as doublets at δ_H 1.04 (H-19), δ_H 0.87 and δ_H 0.82. The methylene groups present in the region δ_H 1.19 to δ_H 2.42 were seen as multiplets.

The ^{13}C NMR spectrum (Figure 47) of the compound indicated the presence of twenty nine carbon resonances of which two were attributed to the carbonyl groups (C-3 and C-7), and two to quarternary carbon resonances (C-10 and C-13), ten to methine (C-5, 8, 9, 14,17, 20, 22-25), nine to methylene (C-1, 2, 4, 6, 11, 12, 15, 16, 28) and six to methyl carbon atoms (C-18, 19, 21, 26,27, 29). The DEPT 45 (Figure 48), DEPT 90 (Figure 49) and DEPT 135 spectra (Figure 50) aided in the assignment of methine, methylene and methyl resonances. The absence of the peaks around δ_H 9 in the proton NMR spectrum confirmed the absence of aldehydic group and suggested the carbonyl carbon at δ_C 211.315 and δ_C 209.153 to be a ketonic group.

The connectivities within the molecule were interpreted using the 2D ^{1}H-^{1}H COSY (Figure 51), HSQC (Figure 52) and HMBC spectra (Figure 53). In the ^{1}H-^{1}H COSY spectrum (Table 23) of E16, correlations were seen between δ_H 5.17 (H-22) and δ_H 2.04 (H-20) which further correlated with δ_H 1.05 (H-21) and δ_H 1.21 (H-17). The proton resonance at δ_H 5.06 (H-23) showed coupling correlation with δ_H 1.53 (H-23). The HMBC plot revealed a long distance coupling between the carbonyl carbon at δ_C 209.153 and δ_H 2.61, δ_H 2.38, δ_H 2.06. The carbon at δ_C 137.875 coupled with δ_H 5.06, δ_H 2.02, δ_H 1.12 and δ_H 1.05. The latter was coupled to the carbon at δ_C 40.415 and δ_C 55.903. The carbon at δ_C 129.705 coupled to δ_H 5.17, δ_H 2.02, δ_H 1.45, δ_H 0.87 and δ_H 0.82. The carbon at δ_C 57.537 was coupled to the proton resonances at δ_H 2.61, δ_H 2.39 and δ_H 2.06. HMBC spectrum also revealed the correlation of the carbon resonance δ_C 56.732 with δ_H 2.60 and δ_H 0.72. Other HMBC correlations are given in Table 23 and Figure 54. From this data it was concluded that the compound had a steroidal skeleton with two keto group at C-3 and C-7. Based on the spectroscopic interpretation, the compound E16 is characterized as **17-(4-Ethyl-1,5-dimethyl-hex-2-enyl)-10, 13-dimethyl-tetradecahydro cyclopenta [a] phenanth rene -3,7-dione** (Stigmast-22-ene-3,7-dione). **This is the first reported isolation of this compound from *E. crassipes*.**

22*E*,24*R*-stigmast-22-ene-3,7-dione and 24*R*-stigmasta-5,22-diene-3,7-dione is naturally occurring compounds and has been isolated from the methanol extract of dried fruits of *Odyendyea gabonensis* (**Donkwe *et al*, 2012**). There are no other reports on the isolation of this compound.

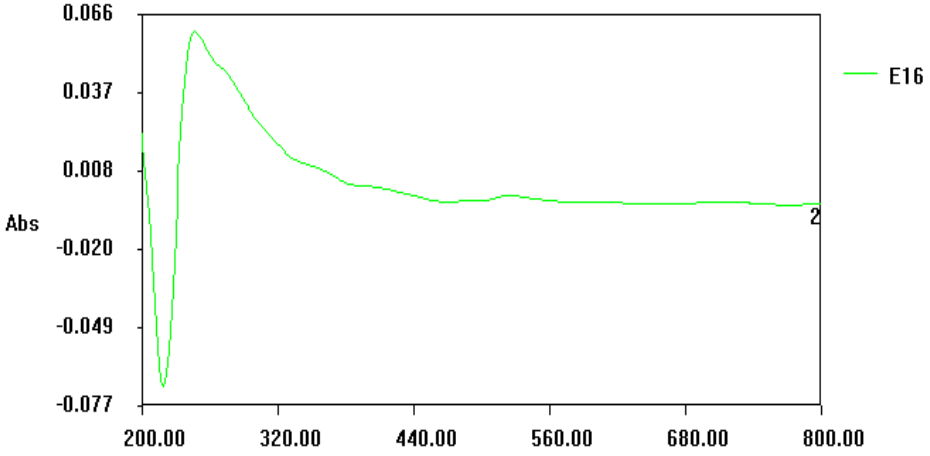

Figure 44. UV spectrum of E16

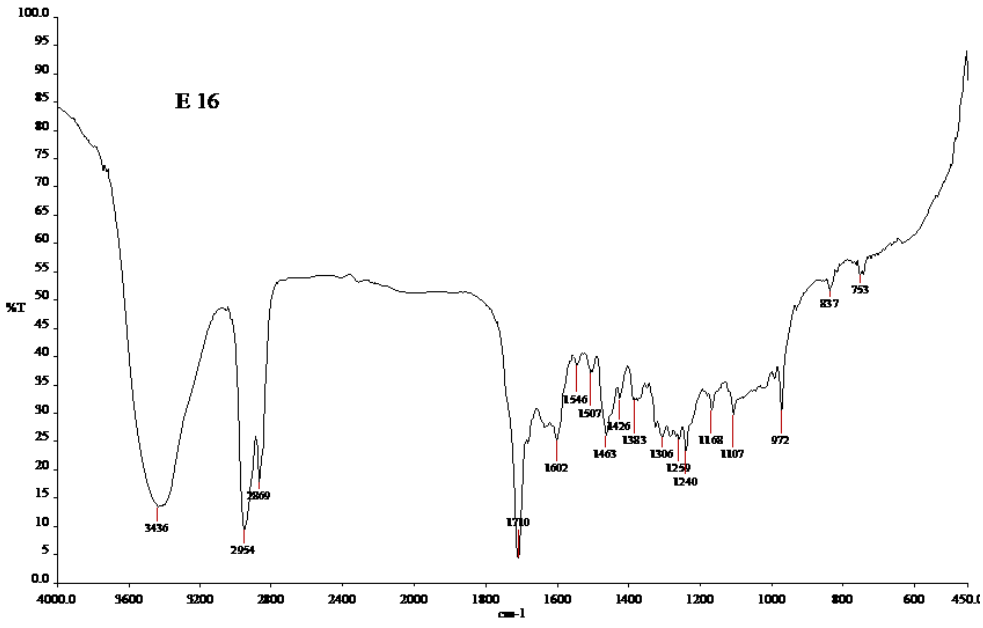

Figure 45. IR spectrum of E16

Stigmast-4-ene-3,6-dione possess anti-inflammatory and anti-allergic activities whereas Stigmasta-4,22-diene-3,6-dione inhibits the growth of inhibit the growth of some microalgae (**Radulovic and Dordevic, 2011**). Stigmast-4-ene-3,6-dione has been demonstrated to show moderate antitumour promoting activity (**Khan *et al*, 2005**).

Table 23. ^{1}H NMR, ^{13}C NMR values, ^{1}H -^{1}H COSY and HMBC correlation of E16

C no	^{1}H (ppm)	^{13}C (ppm)	COSY	HMBC
1	1.66 (m, 1 H) 2.04 (m, 1 H)	38.11	2.32	
2	2.32 (m, 1 H)	37.39	2.0	
3		211.31		
4	2.32 (m, 1 H) 1.99 (m, 1 H)	46.62		
5	1.21 (m, 1 H)	55.89		
6	2.04 (m, 1 H) 1.88 (m, 1 H)	38.11		
7		209.13		H-6; H-8; H-9
8	2.6 (m, 1 H)	57.5		
9	2.09 (m, 1 H)	38.03		
10		41.27		
11	1.6 (m, 1 H)	21.67		
12	1.6 (m, 1 H) 1.6 (m, 1 H)	37.00		
13		42.89		H-18
14	1.35 (m, 1 H)	53.50		
15	1.66 (m, 1 H) 1.19 (m, 1 H)	24.07		
16	1.19 (m, 1 H) 1.66 (m, 1 H)	28.73		
17	1.21 (m, 1 H)	56.73		
18	0.982(s, 1 H)	12.57		
19	2.04 (m, 1 H) 1.66 (m, 1 H)	18.98		
20	2.04 (d, 3 H)	40.42	1.05; 5.16	H-21
21	1.05 (d, 3 H)	21.16	2.04	
22	5.16 (dd, 1 H)	137.8		H-17; H-20; H-23
23	5.05(dd, 1 H)	129.7	5.16	
24	1.53 (m, 1 H)	51.24		H-26; H-27
25	1.66 (m, 1 H)	31.86		
26	0.82 (d, 3 H)	12.25		
27	0.87(d, 3 H)	21.10		
28	1.49 (m, 1 H)	25.39		
29	0.73 (t, 3 H)	12.21		

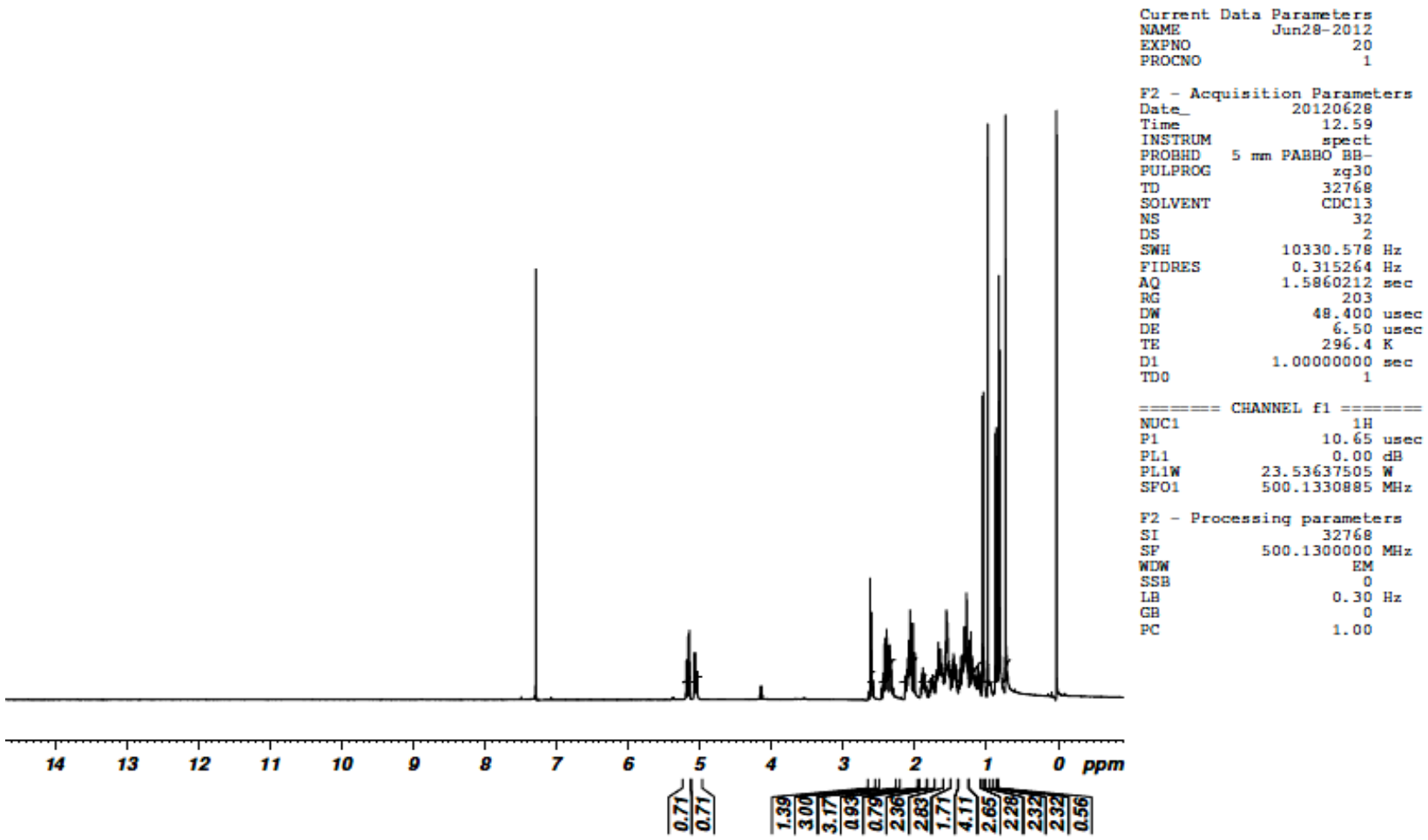

Figure 46. ^{1}H NMR spectrum of E16

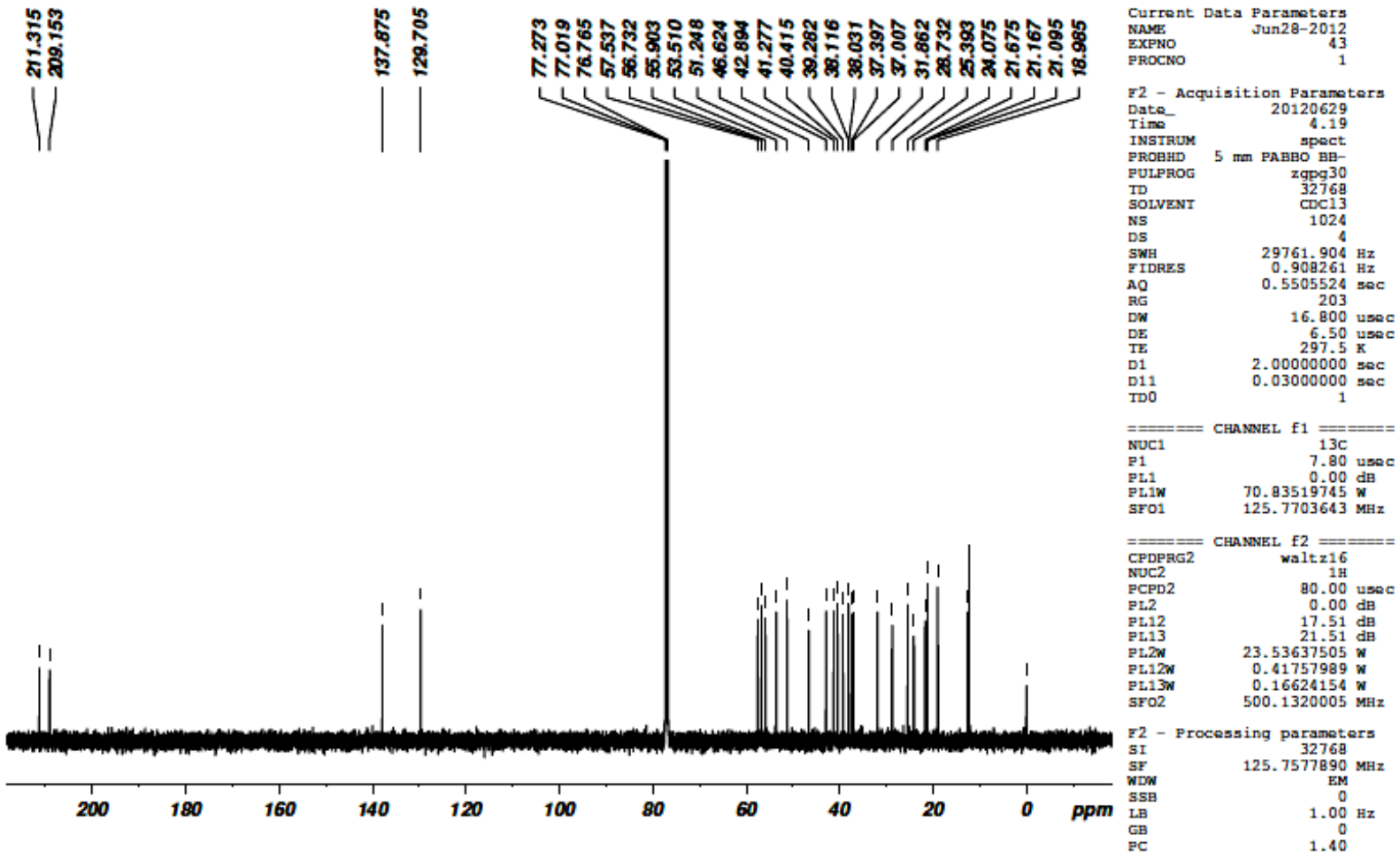

Figure 47. ^{13}C NMR spectrum of E16

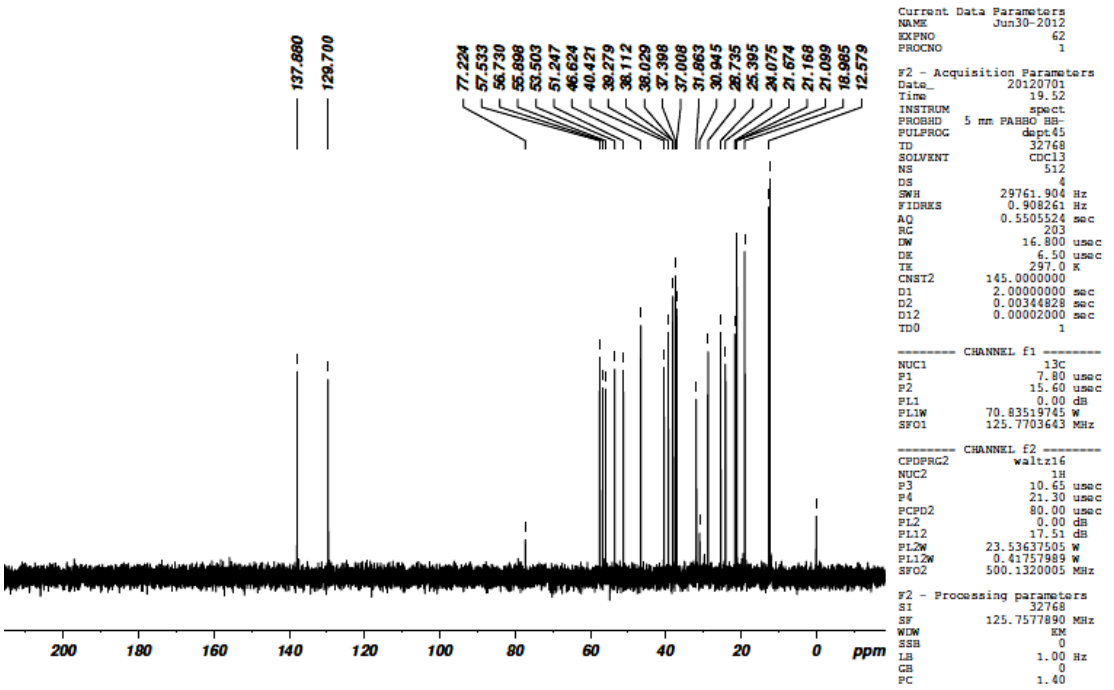

Figure 48. DEPT 45 spectrum of E16

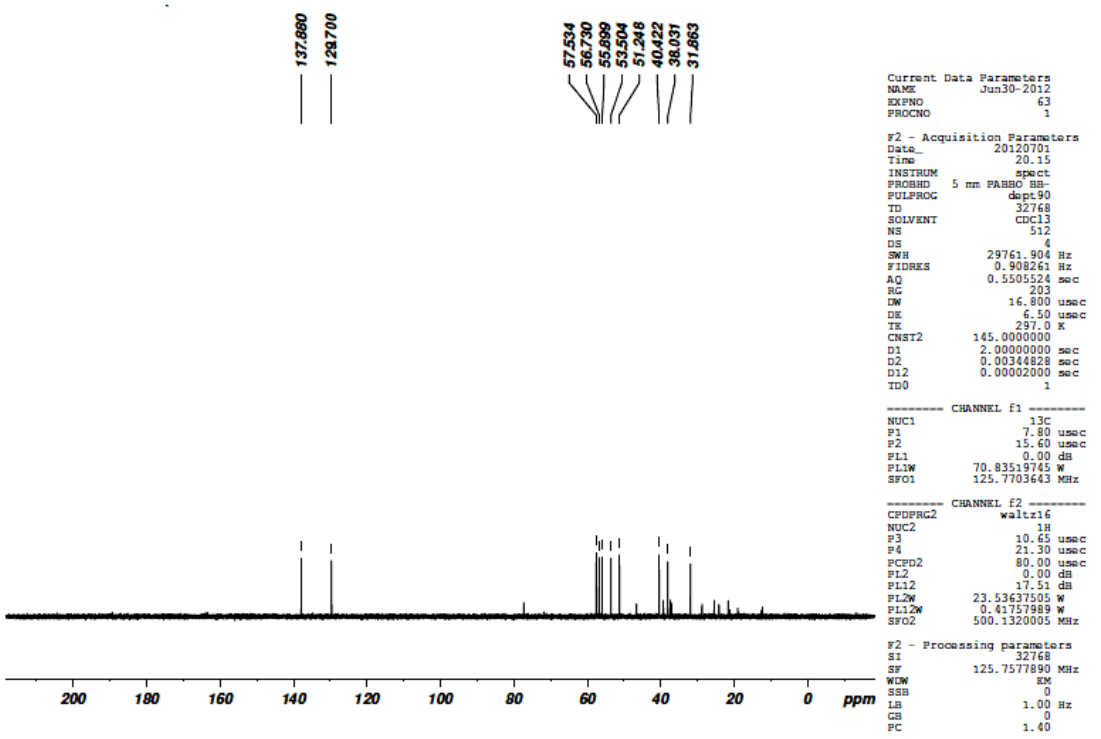

Figure 49. DEPT spectrum 90 of E16

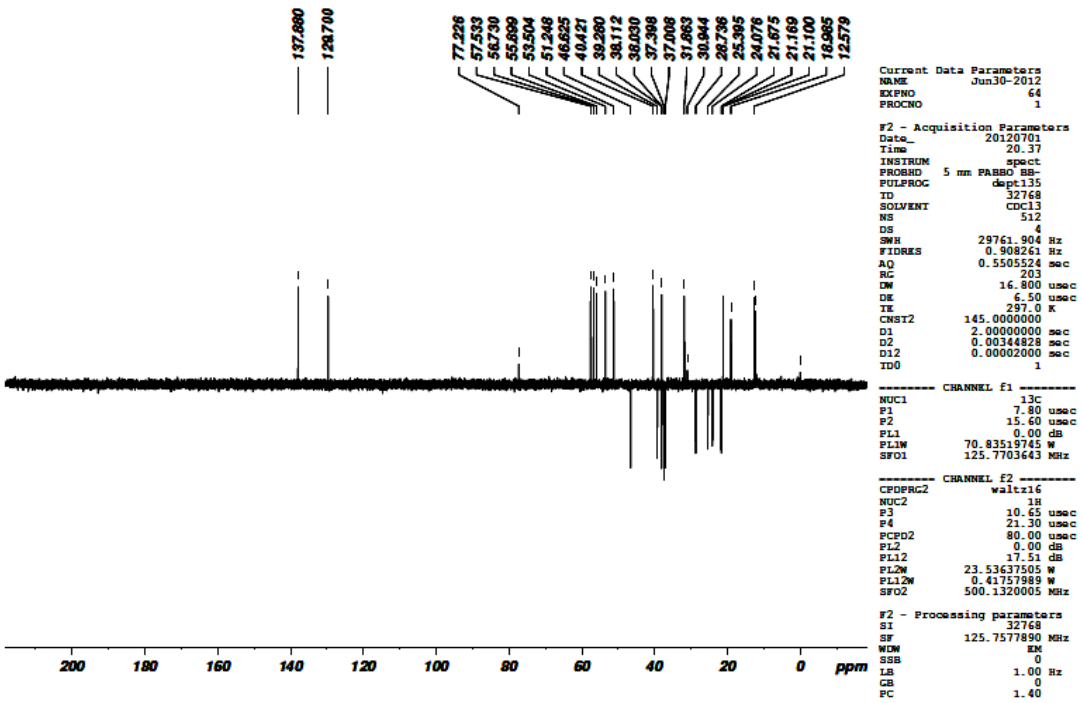

Figure 50. DEPT 135 spectrum of E16

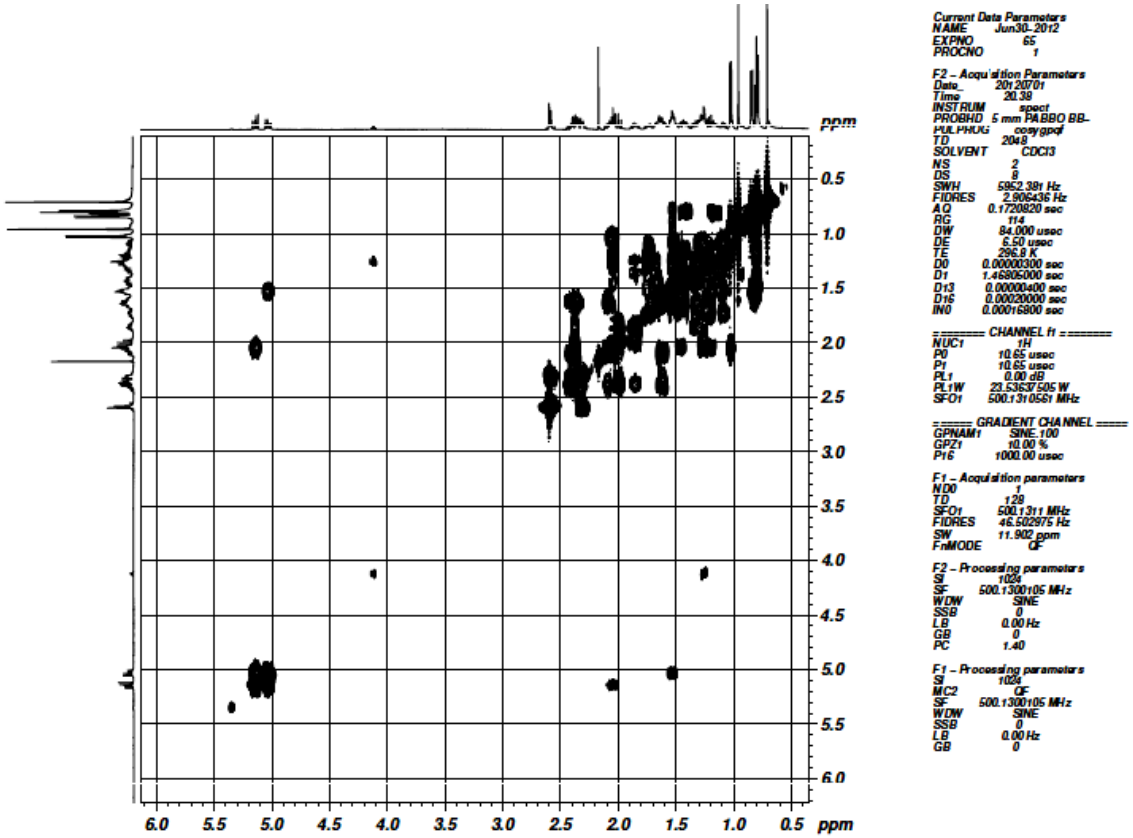

Figure 51. ^{1}H-^{1}H COSY spectrum of E16

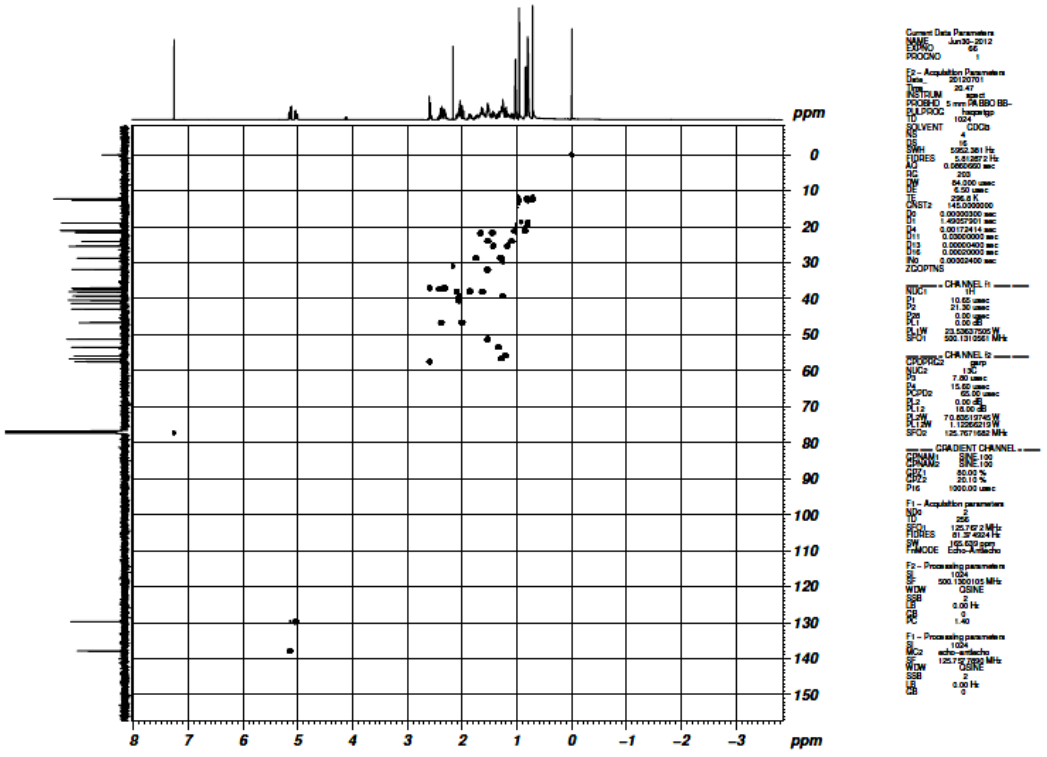

Figure 52. HSQC spectrum of E16

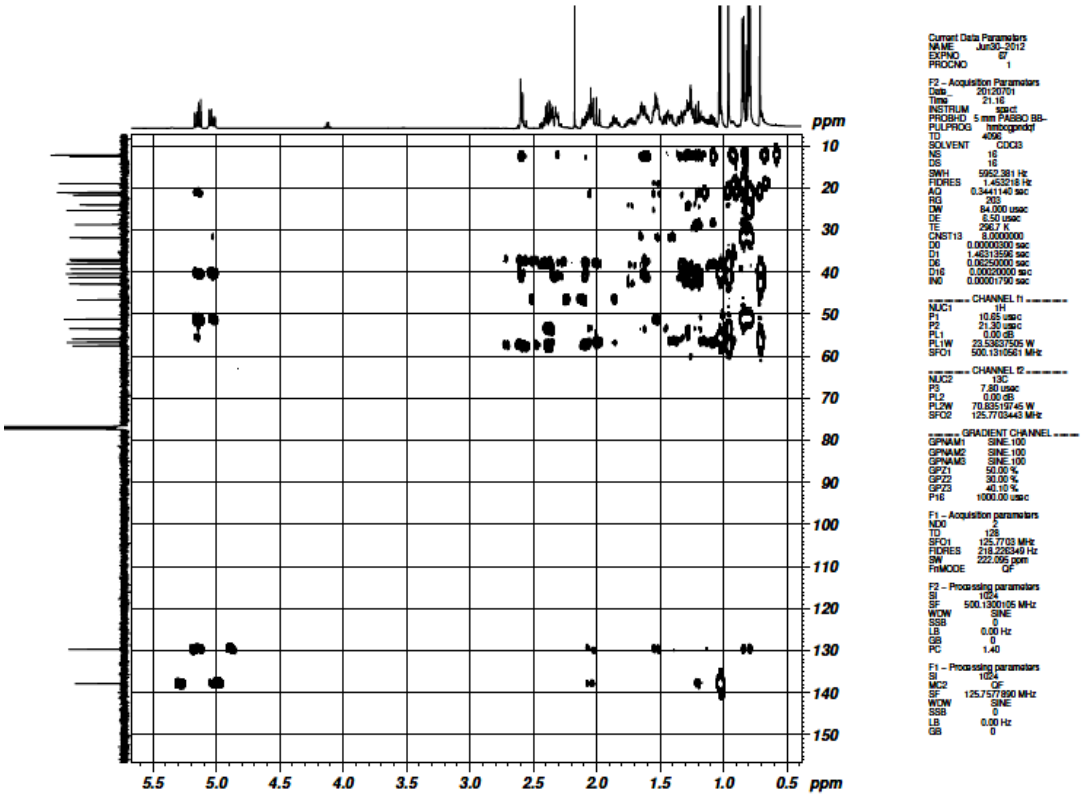

Figure 53. HMBC spectrum of E16

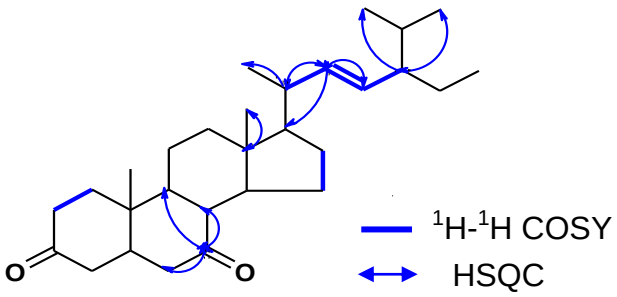

Figure 54. HMBC and ^{1}H-^{1}H COSY correlations of E16

4.4.2.8 Structure elucidation of E21

Silica gel column chromatography of ethyl acetate extract furnished a solid (black) (5.5 g) from 80% and 100% ethyl acetate eluates. The solid was dissolved in chloroform and extracted with 1:1 ethanol/water. The aqueous portion was distilled under vacuum when an orange liquid was obtained which was designated as E21 (Yield-2 mL).

Physical characteristics

(i) Appearance- Reddish orange liquid.

Chemical characteristics

(i) TLC- R_f - 0.5 (9:1 ethyl acetate: ethanol).

(ii) Flame test- Compound charred.

(iii) Element test- The compound gave a blue solution indicating the presence of nitrogen in Lassaigne's test and absence of sulphur was noted in sodium prusside test.

Spectral analysis

The UV spectrum (Methanol) of E21 showed an absorption maximum at 231 nm. FTIR absorption bands were found at 3363 cm^{-1}(C–N stretching), 2503 cm^{-1} (C-H stretch), 1045 cm^{-1} (C–O stretching) and 1240 cm^{-1} (C–N stretching). The molecular formula of the compound was established as $C_9H_{19}O_3N$ on the basis of its mass spectrum (GC-MS). The mass spectrum showed fragment ions at 175 $[M\text{-}CH_2NH_2]^+$, 147 $[M\text{-}CH_2NH_2\text{-}C_2H_4]^+$, 133 $[M\text{-}CH_2NH_2\text{-}C_2H_4\text{-}CH_2]^+$, 117 $[M\text{-}CH_2NH_2\text{-}C_2H_4\text{-}O]^+$ (100), 101 $[M\text{-}CH_2NH_2\text{-}C_2H_4\text{-}O\text{-}O]^+$, 75, 59 and 45.

The ^{1}H, ^{13}C NMR spectral values and HMBC correlations are given in Table 24. The ^{1}H NMR spectrum (Figure 55) of E21 showed deshielded methylene resonances as a pentet at δ_H 3.68. The doublet doublets at δ_H 3.61 and δ_H 3.54 showed that these protons are in the vicinity of heteroatom. The methyl proton resonances were observed

at δ_H 2.09. The ^{13}C NMR spectrum (Figure 56) of E21 indicated the presence of three carbon resonances at δ_C 72.45, δ_C 63.00 and δ_C 19.51. The multiplicities of the carbon were established with the aid of DEPT 45, 90, 135 (Table 24) and HSQC spectra. DEPT 45 indicated all three carbons (δ_C 72.45, δ_C 63.00 and δ_C 19.51) to be attached with protons. DEPT 90 showed no signals indicating the absence of two methine carbon. DEPT 135 spectra suggested the presence of one methyl group at δ_C 19.51. In the 2D ^1H-^1H COSY spectrum (Figure 57), the cross peaks between the doublet doublets at δ_H 3.61 and δ_H 3.54 indicated the coupling between these protons. HSQC spectrum (Figure 58) indicated ^1J coupling between δ_C 63.53 and δ_H 3.61, δ_C 72.45 and δ_H 3.54 and δ_C 19.51 and δ_H 2.09. HMBC spectrum (Figure 59) showed that the carbon resonance at δ_C 63.00 is correlated to δ_H 3.68, δ_H 3.61 and δ_H 3.54. The latter two protons showed long range coupling with δ_H 3.60 and δ_H 3.54.

Table 24. ^1H NMR, ^{13}C NMR values and HMBC correlation of E21

C no	^1H (ppm)	^{13}C (ppm)	DEPT 45	DEPT 135	HMBC correlated to proton
1	-	-			
2	3.68	72.45	72.45	72.45*	3.61; 3.54
3	-	-	-	-	
4	3.68	72.45	72.45	72.45*	
5	-	-	-	-	
6	3.61	63.00	63.00	63.00*	3.68; 3.61; 3.54
7	3.54	63.00	63.00	63.00*	3.68; 3.61; 3.54
8	-	-	-	-	
9	3.61	63.00	63.00	63.00*	3.68; 3.61; 3.54
10	3.54	63.00	63.00	63.00*	3.68; 3.61; 3.54
11	-	-	-	-	
12	3.61	63.00	63.00	63.00*	3.68; 3.61; 3.54
13	3.54	63.00	63.00	63.00*	3.68; 3.61; 3.54

* Downward peak

The presence of nitrogen in the compound was identified from Lassaigne's test. The peaks in the region δ_H 3.68, δ_H 3.61 and δ_H 3.54 indicated the presence of deshielded protons attached to nitrogen. The spectral interpretation together with the literature aided in the structure elucidation of the compound E21and the structure of the compound was deduced as an oxoazacrown,-methyl-1,5,8,11-tetraoxa-3-aza-cyclotridecane.

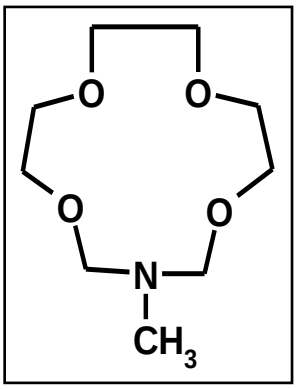

The GC-MS spectrum of the compound revealed the presence of nitrogen in E21 which further supported the proposed structure.

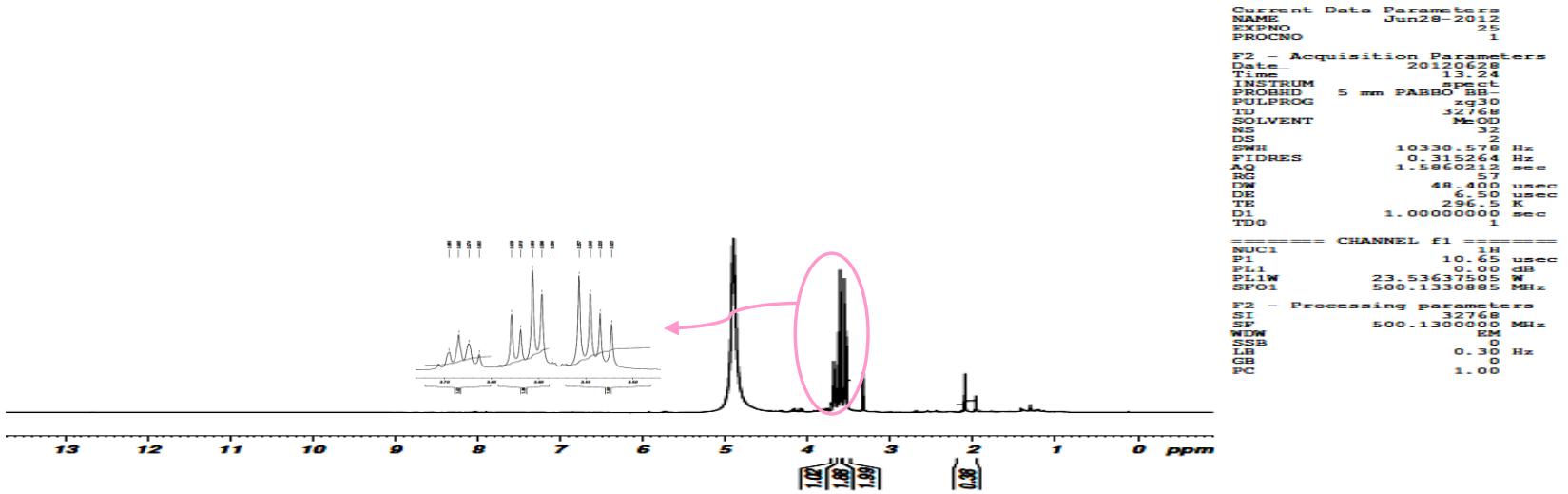

Figure 55. ^{1}H NMR spectrum of E21

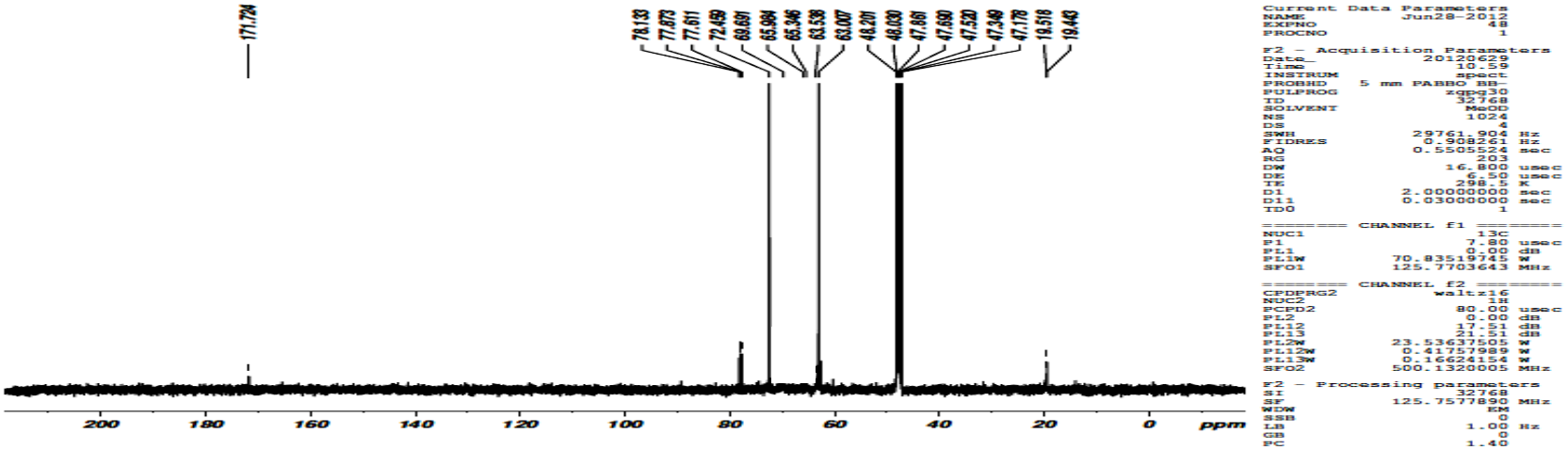

Figure 56. ^{13}C NMR spectrum of E21

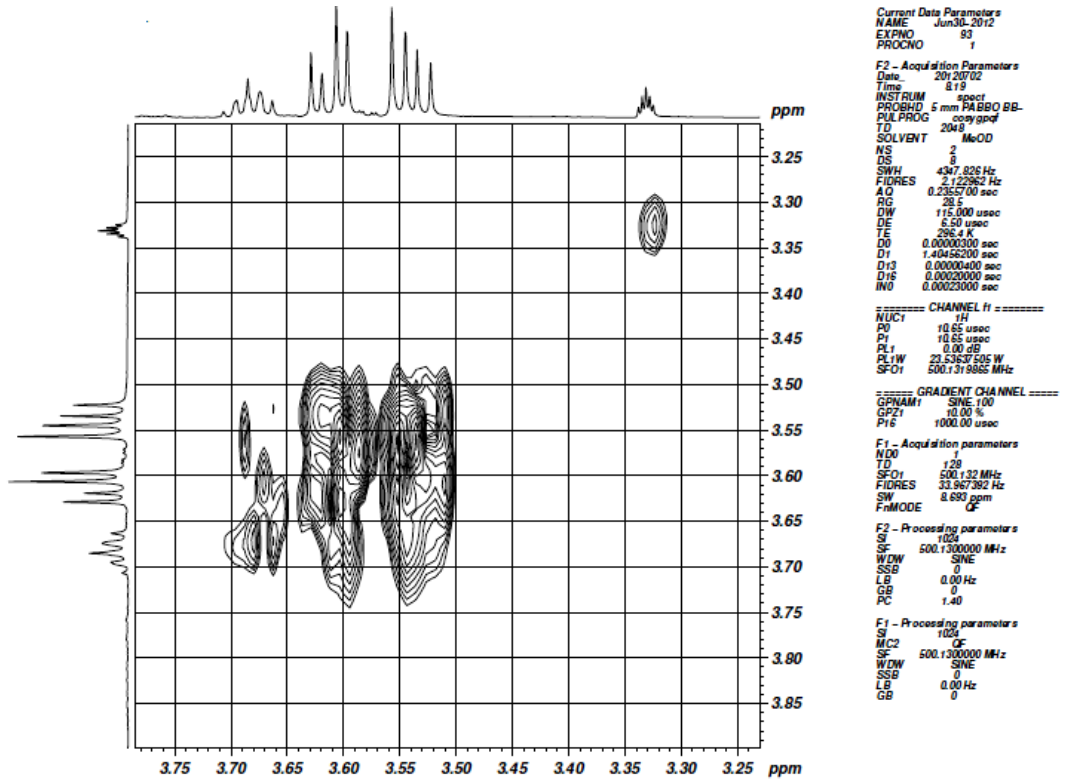

Figure 57. ^{1}H-^{1}H COSY spectrum of E21

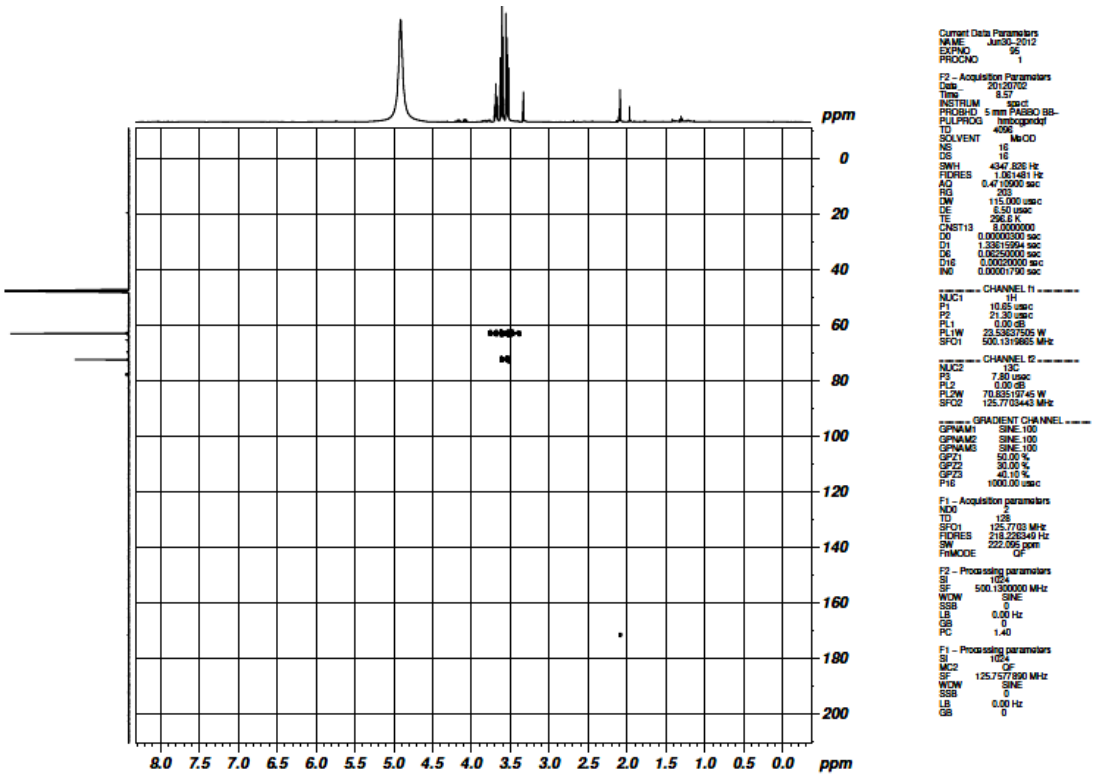

Figure 58. HSQC spectrum of E21

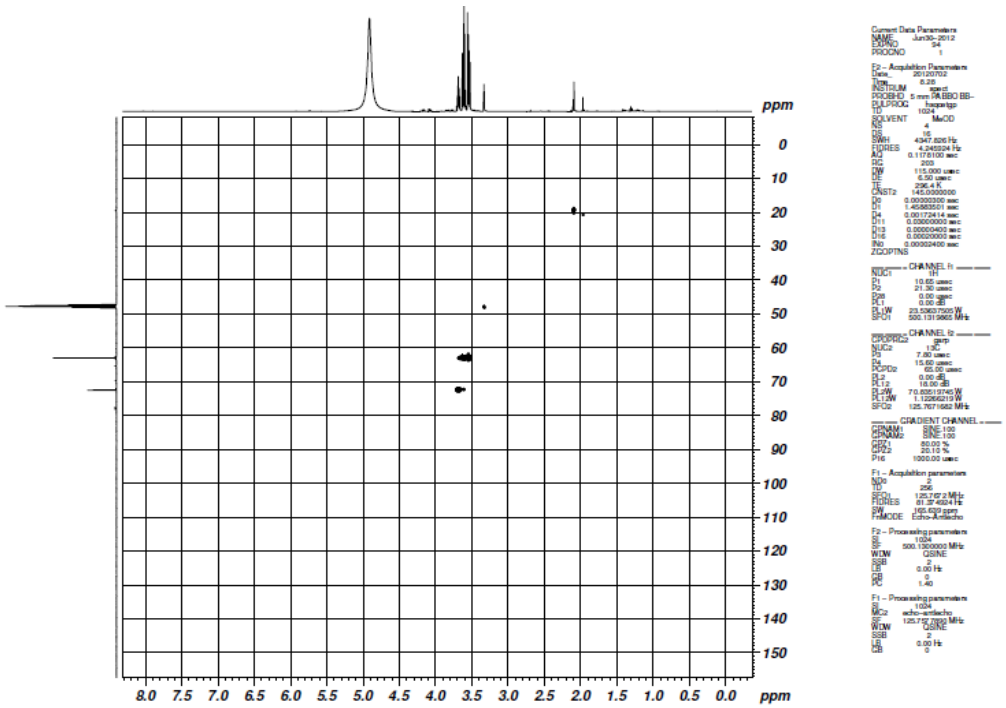

Figure 59. HMBC spectrum of E21

Isolation of such type of azacrowns from *E. crassipes* has not been reported. *E. crassipes* has been used in the removal of heavy metals, toxic organic compounds, dyes from contaminated water. Crown ethers have the capabaility to capture and transport cations with sizes comparable to the size of the crown cavity (**Suzuki *et al,* 2001**). This property of such compounds present in the plants might have rendered the capability to adsorb cations from the water making this plant an efficient adsorbent. Crown ethers also associate covalently with various dyes (**Forgues and Ali, 2004**). The presence of crown ethers in *E.crassipes* thus justifies the adsorption efficiency of this plant.

4.4.3 Isolation of compounds from the aqueous extract of *E. crassipes*

4.4.3.1 Characterisation of W5

Silica gel column chromatography of aqueous extract furnished W5 as a solid (6 .5 g) from 75% ethyl acetate:ethanol and 50% ethyl acetate:ethanol eluates.

Physical characteristics

(i) Appearance- White powder.

Chemical characteristics

(i) TLC- R_f - 0.5 (9:1 ethanol:ethyl acetate) - white spot in iodine vapours.

(ii) Element test- Absence of nitrogen and sulphur.

Spectral interpretation

The UV spectrum of W5 showed an absorption maximum at 232 nm. FTIR absorption bands were observed at 3448 cm^{-1}(–O–H stretch), 2924 cm^{-1} (C–H stretch), 1636 cm^{-1} (–C=C stretching), 1454 cm^{-1} (–CH_3 antisymmetric deformation), 875 (–C–H stretch) and 466 (–C=C–C bend).

The ^{1}H NMR spectrum (Figure 60) of W5 showed unresolved signals at δ_H 1.17 and δ_H 3.65. 2D ^{1}H-^{1}H COSY spectrum (Figure 61) revealed the coupling between the two protons. The signals at δ_H 3.65 and δ_H 1.17 suggested the presence of anomeric protons. Similar pattern of signals was noted in sugars like galactose, xylitol etc., The diagnostic signals for carbohydrates are those of the anomeric proton in the region around δ_H 3-4 and that of the methyl protons around δ_H 1.2. In carbohydrates, nearly all of the protons attached to the carbons are in the similar environment and resonate in the range δ_H 3.3- 4.1. Due to lower solubility of the compound in organic solvents, the spectrum was recorded in deuterated water. This might have caused deuterium exchange and hence, the absence of signals corresponding to the oxygenated protons.

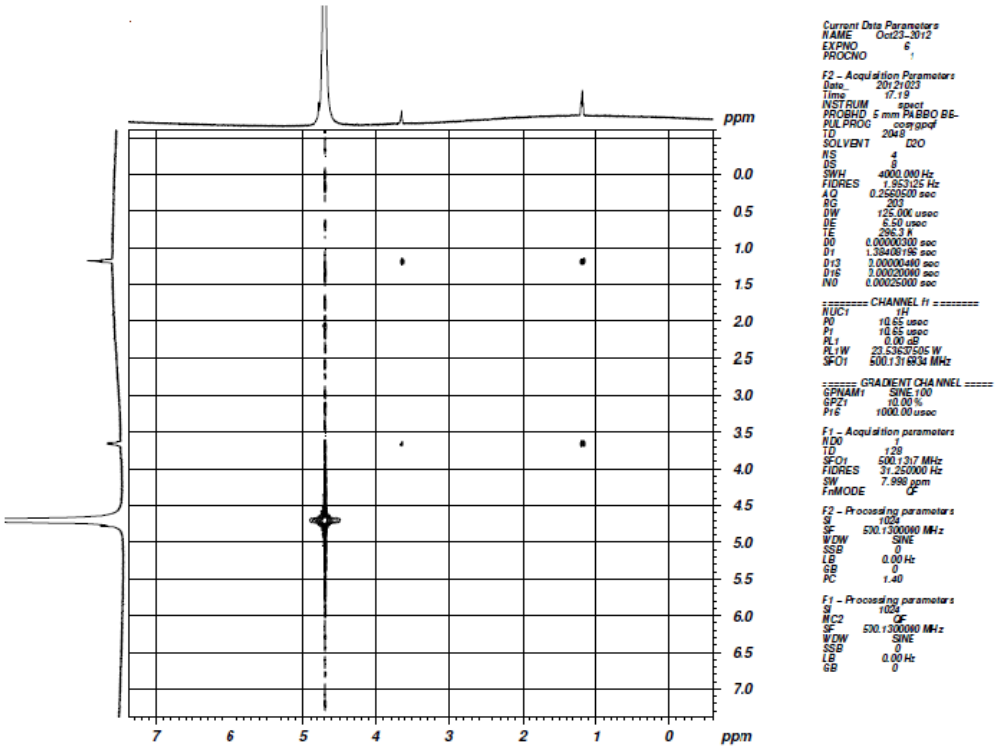

Figure 61. ^{1}H-^{1}H COSY spectrum of W5

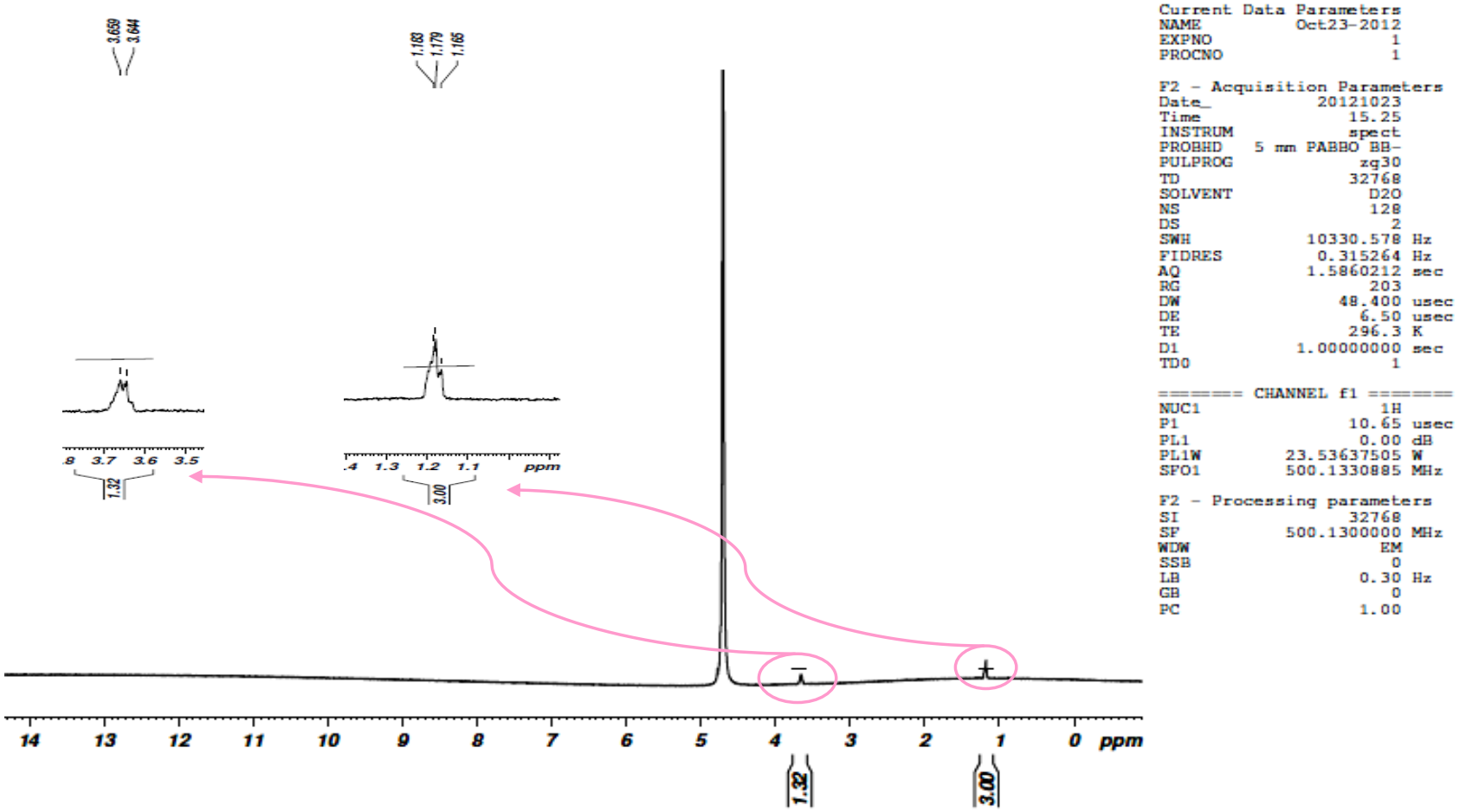


```
Current Data Parameters
NAME                  Oct23-2012
EXPNO                          1
PROCNO                         1

F2 - Acquisition Parameters
Date_                   20121023
Time                       15.25
INSTRUM                    spect
PROBHD    5 mm PABBO BB-
PULPROG                     zg30
TD                         32768
SOLVENT                      D2O
NS                           128
DS                             2
SWH                  10330.578 Hz
FIDRES                0.315264 Hz
AQ                   1.5860212 sec
RG                           203
DW                      48.400 usec
DE                       6.50 usec
TE                      296.3 K
D1                   1.00000000 sec
TD0                            1

======= CHANNEL f1 =======
NUC1                         1H
P1                      10.65 usec
PL1                      0.00 dB
PL1W                23.53637505 W
SFO1                500.1330885 MHz

F2 - Processing parameters
SI                         32768
SF                  500.1300000 MHz
WDW                           EM
SSB                            0
LB                       0.30 Hz
GB                             0
PC                          1.00
```

Figure 60. ^{1}H NMR spectra of W5

The compound W5 tested positive in Benedicts' test and osazone test. Hence the compound W5 is characterized as a carbohydrate.

The isolation of carbohydrate in good yield (6.5 g) from the aqueous extract of *E. crassipes* suggests the presence of higher amount of carbohydrate in the plant.

4.4.4 Isolation of compounds from ethyl acetate extract of *E. crassipes* using activated charcoal as adsorbent

4.4.4.1 Characterisation of EAC1

Column chromatography of ethyl acetate extract over activated charcoal furnished a pale white compound designated as EAC1 (100 mg) from 90:10 petroleum ether: ethyl acetate. The compound was purified using methanol giving a white waxy compound (100 mg).

Physical characteristics

(i) Low melting white waxy solid.

Chemical characteristics

(i) TLC- R_f - 0.3 (petroleum ether: ethyl acetate- 9.5:1.5), strong iodine absorption.

Spectral data

The UV spectra of EAC1 in chloroform showed an absorption maximum at 214 nm indicating the absence of chromophoric groups. FTIR absorption bands were noted at 1746 cm^{-1} and 1731 cm^{-1} (carbonyl group), 1235 cm^{-1} (–C–O–), 1162 and 1113 cm^{-1} (–C–O–C–) group.

The ^{1}H NMR, ^{13}C NMR values and ^{1}H -^{1}H COSY correlation of EAC1 are represented in Table 25. The ^{1}H NMR spectrum (Figure 62) of EAC1 showed the presence of tertiary methyl group at δ_H 0.92. The methylene protons resonated as a broad singlet at δ_H 1.31. The signal at δ_H 1.62 was attributed to the deshielded methylene protons. The triplet at δ_H 2.29 corresponds to the highly deshielded methylene proton resonance. The signals attributable to oxygenated methylene protons were observed at δ_H 4.18. The proton resonance at δ_H 4.16 and δ_H 4.38 corresponds to the methylene proton in β-position to the carbonyl group. The signals at δ_H 5.36 and δ_H 5.29 suggested the presence of a highly deshielded methylene group. The signal at δ_H 2.05 revealed the presence of a deshielded proton attached to a heteroatom, supported by HSQC spectrum (Figure 64) where the proton did not show correlation with any carbon.

Table 25. ^{1}H NMR, ^{13}C NMR values and ^{1}H -^{1}H COSY correlation of EAC1

C no	^{1}H (ppm)	^{13}C (ppm)	DEPT 135	COSY
1	4.18	64.55	64.55*	4.38
2	4.16	61.91	61.91*	
	4.38			4.16
3	5.29	69.26	69.26*	
	5.36			
1'	-	173.42	173.4*	
2'	2.29	33.49	33.49*	
3'	1.62	24.70	24.70*	
4'	1.62	24.62	24.62*	1.31
5'	1.31	28.77	28.77*	
6'	1.31	28.83	28.83*	
7'	1.31	29.33	29.33*	
8'	1.31	29.19	29.19*	
9'	1.31	29.05	29.05*	
10'	1.31	29.01	29.01*	
11'	1.31	31.66	31.66*	
12'	1.31	22.32	22.32*	0.90
13'	1.31	13.03	13.03	
-	2.05	-		

* Downward peak

The ^{13}C NMR spectrum (Figure 63) of the compound together with DEPT 45, 90 and 135 spectra (Table 25) indicated the presence of sixteen carbon resonances including one carbonyl carbon (δ_C 173.42), fourteen methylene, one methyl and one methine carbon. The short range coupling HSQC spectrum also confirmed the assignment for the carbons. In the ^{1}H-^{1}H COSY (Table 24) of EAC1, off-diagonal peaks were observed between the methylene protons at δ_H 2.29 and δ_H 1.62. The proton at δ_H 1.62 showed correlation with methylene group at δ_H 1.31 which coupled to δ_H 0.92. Furthermore, the protons at δ_H 4.16 showed coupling correlations with δ_H 4.38. On the basis of the spectral characterization, strucuture of EAC1 was elucidated as **1,3-propanediol tridecanoate** (**$C_{16}H_{32}O_3$**). **This is the first reported isolation of this compound from *E. crassipes*.** This compound is a fatty acid ester which finds application in many areas. The isolation of such fatty acid esters from *E. crassipes* by column chromatography over activated charcoal as adsorbent paves an easy and convenient way of isolating such compounds from a universally available plant.

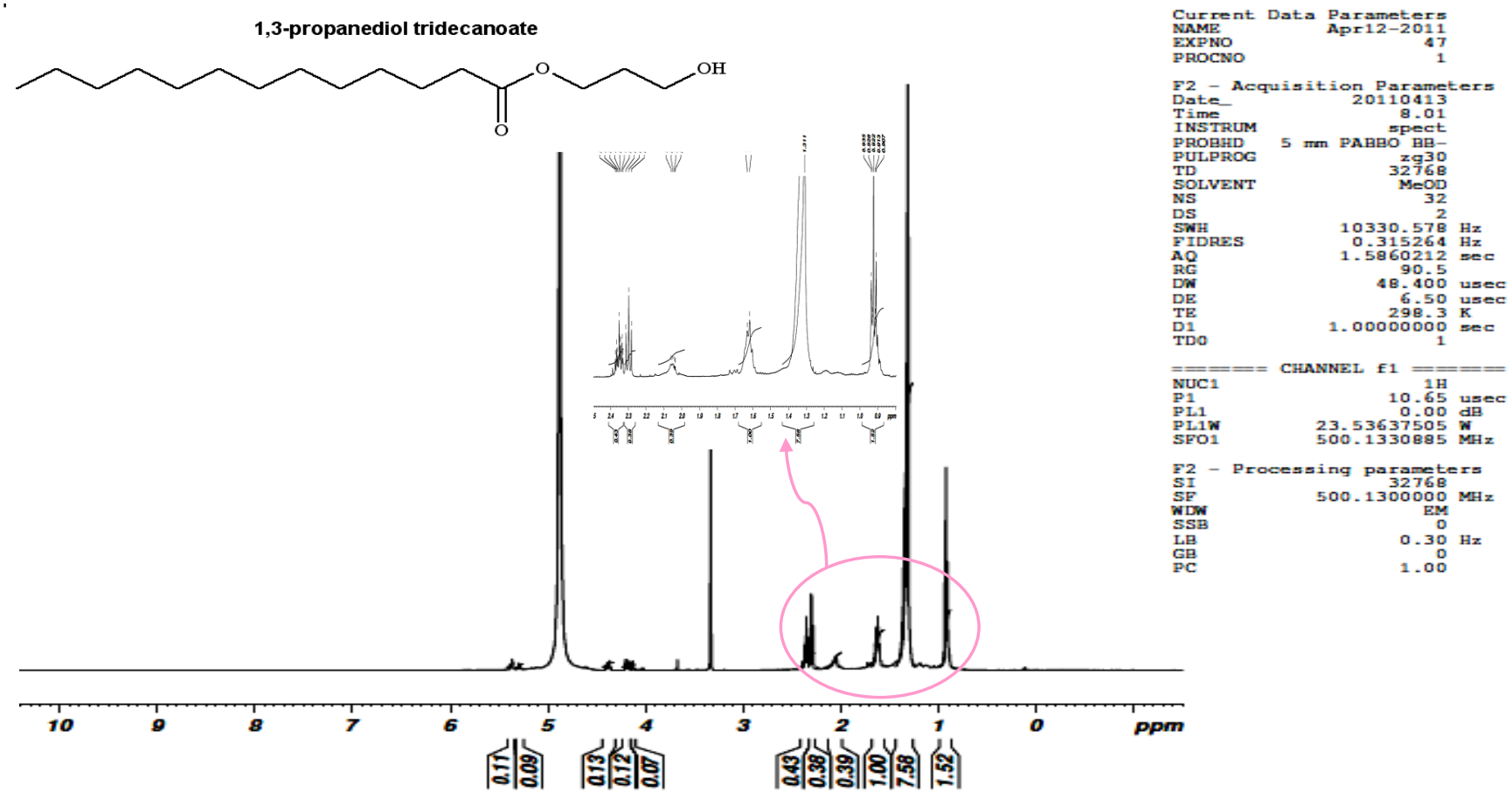


```
Current Data Parameters
NAME                  Apr12-2011
EXPNO                         47
PROCNO                         1

F2 - Acquisition Parameters
Date_                   20110413
Time                        8.01
INSTRUM                    spect
PROBHD     5 mm PABBO BB-
PULPROG                    zg30
TD                        32768
SOLVENT                    MeOD
NS                           32
DS                            2
SWH                   10330.578 Hz
FIDRES                0.315264 Hz
AQ                    1.5860212 sec
RG                         90.5
DW                       48.400 usec
DE                        6.50 usec
TE                       298.3 K
D1                    1.00000000 sec
TD0                            1

======== CHANNEL f1 =======
NUC1                          1H
P1                         10.65 usec
PL1                         0.00 dB
PL1W                 23.53637505 W
SFO1                 500.1330885 MHz

F2 - Processing parameters
SI                        32768
SF                   500.1300000 MHz
WDW                          EM
SSB                           0
LB                         0.30 Hz
GB                            0
PC                         1.00
```

Figure 62. ^{1}H NMR spectrum of EAC1

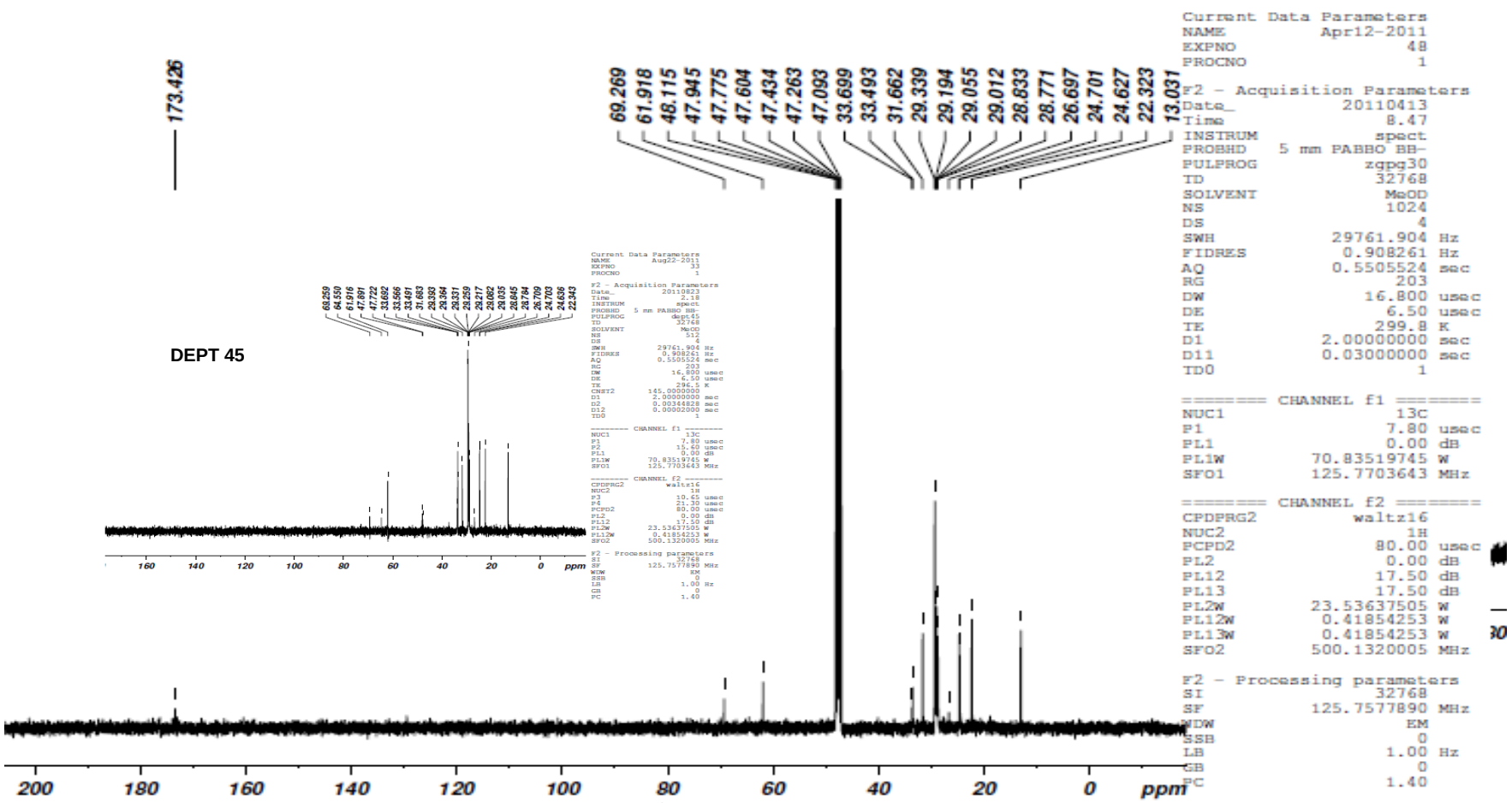

Figure 63. ^{13}C NMR spectrum of EAC1

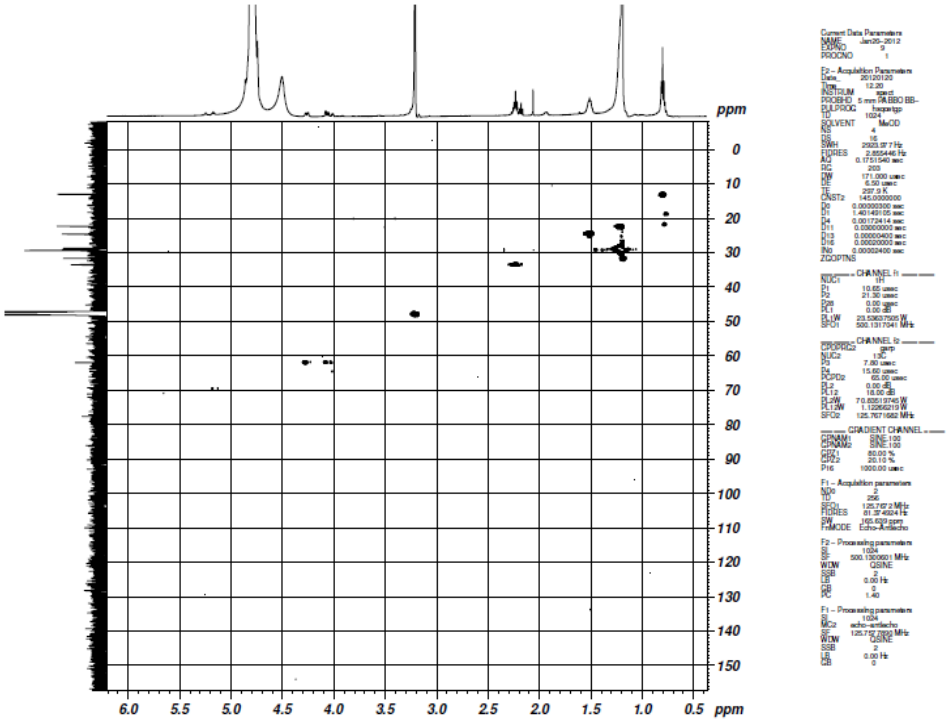

Figure 64. HSQC spectrum of EAC1

4.4.4.2 Characterisation of EAC2

The ethyl acetate extract of *E. crassipes* column chromatographed over activated charcoal furnished a pale white compound (30 mg) from 90:10 petroleum ether:ethyl acetate. The compound designated as EAC2 was purified using methanol giving a white waxy compound.

Physical characteristics

(i) Melting point- 117 °C.

(ii) Appearance-White powder.

Chemical characteristics

(i) TLC - R_f 0.6 (petroleum ether: ethyl acetate - 8.5: 1.5)

Spectral data

The UV spectra (Chloroform λ_{max}) of EAC2 in showed an absorption maximum at 263 nm. FTIR absorption bands were noted at 1746 cm^{-1} and 1731 cm^{-1} (carbonyl group), 1235 cm^{-1} (–C–O–), 1162 and 1113 cm^{-1} (–C–O–C–) group.

The ^{1}H NMR, ^{13}C NMR, DEPT 45, 90, 135, ^{1}H-^{1}H COSY and HMBC data are given in Table 26. The ^{1}H NMR spectrum (Figure 65) of EAC2 showed the presence of tertiary methyl group at δ_H 0.90. The broad signal at δ_H 1.27 corresponds to the

methylene protons $(CH_2)_n$. The oxymethylene protons resonated at δ_H 1.64 and δ_H 2.33. The ^{13}C NMR spectrum (Figure 66) of the compound together with DEPT 45, 90, 135 and HSQC spectra (Table 26) showed the presence of eleven signals corresponding to twenty five carbon atoms. The peak at δ_C 179.8 was attributed to the carbonyl carbon. The methylene carbons resonated at δ_C 33.87, δ_C 31.93, δ_C 29.71, δ_C 29.45, δ_C 29.37, δ_C 29.25, δ_C 29.07, δ_C 24.71, δ_C 22.70 and the carbon resonance at δ_C 14.12 corresponds to terminal methyl carbon.

2D NMR interpretation

2D spectra were used in conjunction with the literature data to establish the structure of the compound. Inspection of ^1H-^1H COSY spectrum (Table 26) of EAC2 revealed the presence of off-diagonal peaks between the methylene proton at δ_H 2.35 and δ_H 1.64, δ_H 1.64 and δ_H 1.27 and between δ_H 1.27 and δ_H 0.90. These high field methylene signals indicated the presence of a long chain chain alkane connected to the carbonyl group. In the HMBC spectrum (Table 26), several important correlations were seen that substantiated the structural evidences observed in ^1H-^1H COSY spectrum. The correlation between the carbonyl carbon δ_C 179.8 and the deshielded methylene proton at δ_H 2.33 was observed in HMBC plot. The latter correlated to δ_C 24.71 and this carbon correlated to δ_H 1.27. The carbon resonance at δ_C 31.93 was found to correlate with δ_H 1.27 and δ_H 0.90 and the latter coupled with δ_C 22.90 (Table 26). The compound EAC2 was thus characterised to be **pentacosan-13-one ($C_{25}H_{50}O$)**.

Table 26. ^1H NMR, ^{13}C NMR values, COSY and HMBC correlation of EAC2

C no	^1H (ppm)	^{13}C (ppm)	DEPT 45	DEPT90	DEPT 135	COSY	HMBC
1		178.8					2.33
1' & 1''	2.35 (t, 4 H)	33.87	33.87	-	33.87*	1.64	1.64
2' & 2''	1.64 (p, 4 H)	24.71	24.71	-	24.71*	2.35, 1.27	1.27
3' & 3''	1.27 (s, 32 H)	29.37	29.37	-	29.37*	1.66	
4' & 4''	1.27	29.45	29.45	-	29.45*		
5' & 5''	1.27	29.71	29.71	-	29.71*		
6' & 6''	127	29.71	29.71	-	29.71*		
7' & 7''	1.27	29.71	29.71	-	29.71*		
8' & 8''	1.27	29.25	29.25	-	29.25*		
9' & 9''	1.27	29.07	29.07	-	29.07*		
10' & 10''	1.27	31.93	31.93	-	31.93*		0.90
11' & 11''	1.27	22.69	22.69	-	22.69*	0.90	1.27
12' & 12''	0.90 (t, 6 H)	14.15	14.15	-	14.15	1.27	

* Downward peak

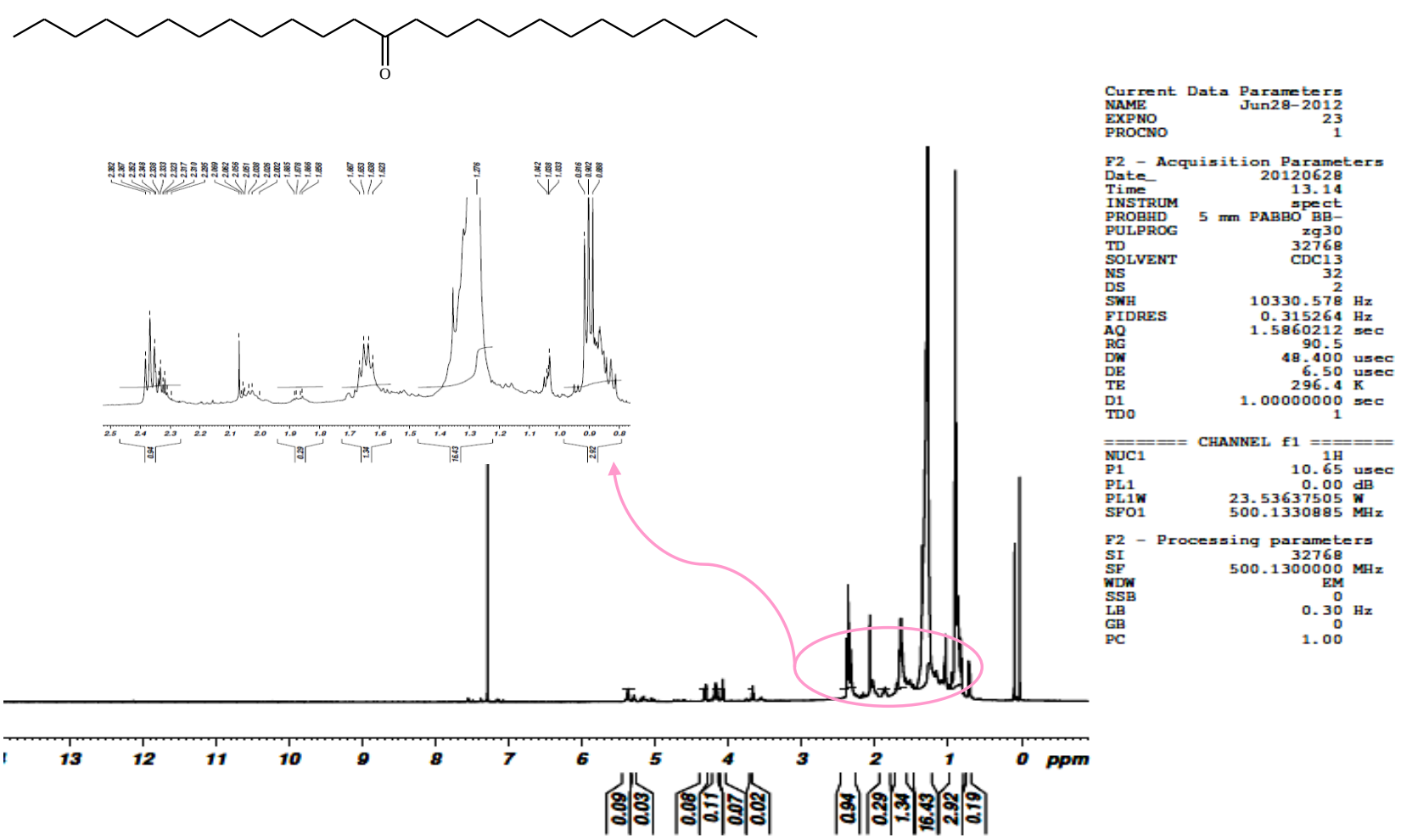

Figure 65. ^{1}H NMR spectra of EAC2

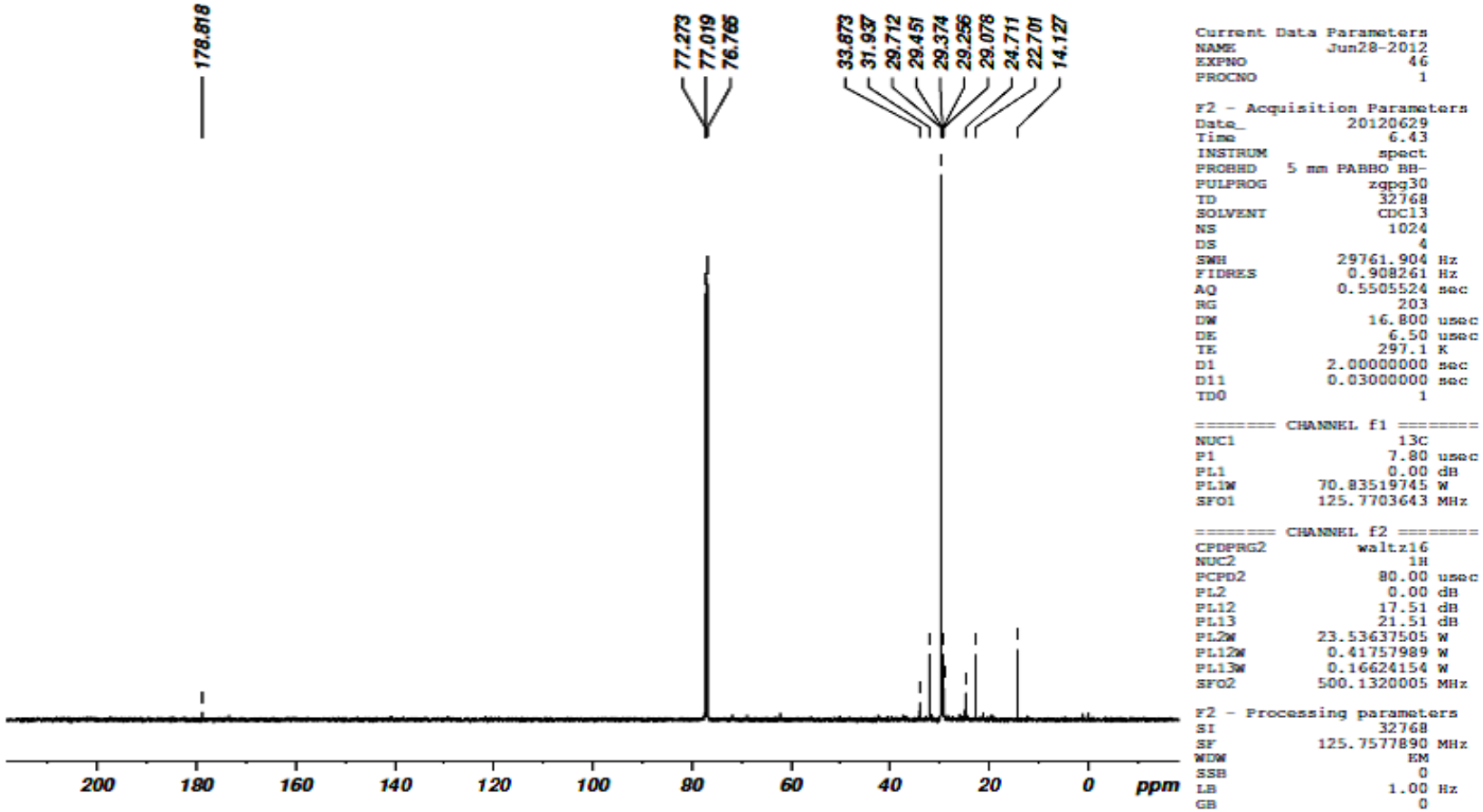

Figure 66. ^{13}C NMR spectra of EAC2

The compound pentacosan-13-one was isolated from *E. crassipes* for the first time. The compound is present in *Arabidopsis thaliana* (**http://pmn.plantcyc.org**)**.** There are no other reports on the isolation of this compound in plants.

Activated charcoal was used as the adsorbent for the isolation of the compounds from the ethyl acetate extract of *E. crassipes* to compare its effeciency with silica. The compound was obtained in high purity when activated charcoal was used as the solid phase. Purification of the compounds isolated from the ethyl acetate extract chromatographed over charcoal column was easy compared to those obtained from the silica column.

The use of activated charcoal as the solid phase in column chromatography has many advantages.

- Charcoal can be reused.
- After extraction of the plant, the marc thrown as a waste can be converted into activated charcoal.
- The cost of activated is less making the isolatin of compounds economical. Conversion of the marc into activated charcoal also makes the process much more economical.

In the present study, ethyl acetate extract (3.61 g) has yielded two compounds in good yields.

4.4.5 Isolation of compounds from the petroleum ether fractionate of ethyl acetate extract of *E. crassipes*

4.4.5.1 Characterisation of HP1

HP1 was obtained as a pale white wax from the petroleum ether fractionate of ethyl acetate extract of *E. crassipes* column chromatographed over silica from 100% petroleum ether. The compound was purified using methanol giving a pale white waxy compound (Yield- 2 g).

Physical characteristics

(i) Melting point- Low melting.

(ii) Appearance- Pale white wax.

Chemical characteristics

(i) TLC- R_f- 0.98 (petroleum ether).

Spectral data

^{1}H NMR (500 MHz, $CDCl_3$ δ) : 0.88 (t), 0.91 (t), 1.28 (s).

^{13}C NMR (500 MHz, $CDCl_3$ δ) : 14.13, 19.74, 22.70, 27.10, 29.38, 29.67, 29.71, 30.049, 31.94.

Spectral interpretation

The UV spectra of HP1 in chloroform showed an absorption maximum at 214 nm and 240 nm indicating the absence of chromophoric groups. FTIR spectrum exhibited absorption bands at 2934 cm^{-1} and 2865 (–C–H stetching) and 1453 cm^{-1} 1327 cm^{-1} (–C–H bending), 755 and 464 cm^{-1} (–CH_2) group.

The ^{1}H NMR spectrum (Figure 67) of HP1 showed the presence of two tertiary methyl groups at δ_H 0.91 and δ_H 0.88. The methylene protons were found to resonante as a broad singlet at δ_H 1.28. The ^{13}C NMR spectrum (Figure 68) of HP1 together with DEPT 45, 90 and 135 spectra (Table 27) indicated the presence of only methyl (δ_C 14.13) and methylene carbon resonances (δ_C 22.70, δ_C 29.37, δ_C 29.67, δ_C 29.71, δ_C 30.04 and δ_C 31.93). HSQC spectra showed the correlation between the protons and the carbons that are directly bonded. In the ^{1}H-^{1}H COSY spectrum (Table 27) of HP1, couplings were observed between the methylene protons at δ_H 1.28 and methyl protons δ_H 0.92 and δ_H 0.88. The HMBC plot (Table 27) showed the coupling between δ_C 22.70 and 0.92 which in turn correlated with δ_C 31.93. The carbon resonances in the region δ_C 29 correlated with δ_H 1.28.

Investigation of the foresaid spectra of HP1 showed it to be a **hydrocarbon** with twenty two protons of which six are methyl and the remaining are methylene protons. Alkanes of surface waxes from *E. crassipes* have been isolated by column chromatography from the chloroform extract. The GLC identification of the alkanes showed the waxes to be composed of long chain alkanes (**Amaral *et al,* 1990**).

Table 27. ^{13}C, DEPT 45, DEPT 90, DEPT 135 values and HMBC correlations of HP1

^{1}H (ppm)	^{13}C (ppm)	DEPT 45	DEPT 135	^{1}H-^{1}H COSY	HMBC
0.92	14.13	14.13	14.13	1.28	
0.88	19.74	19.74	19.74*	1.28	0.92
1.28	22.70	22.70	22.70*		
1.28	27.10	27.10	27.10*		
1.28	29.67	29.67	29.67*		1.28
1.28	29.71	29.71	29.71*		
1.28	30.04	30.04	30.04*		
1.28	31.94	31.94	31.94*		

*Downward peak

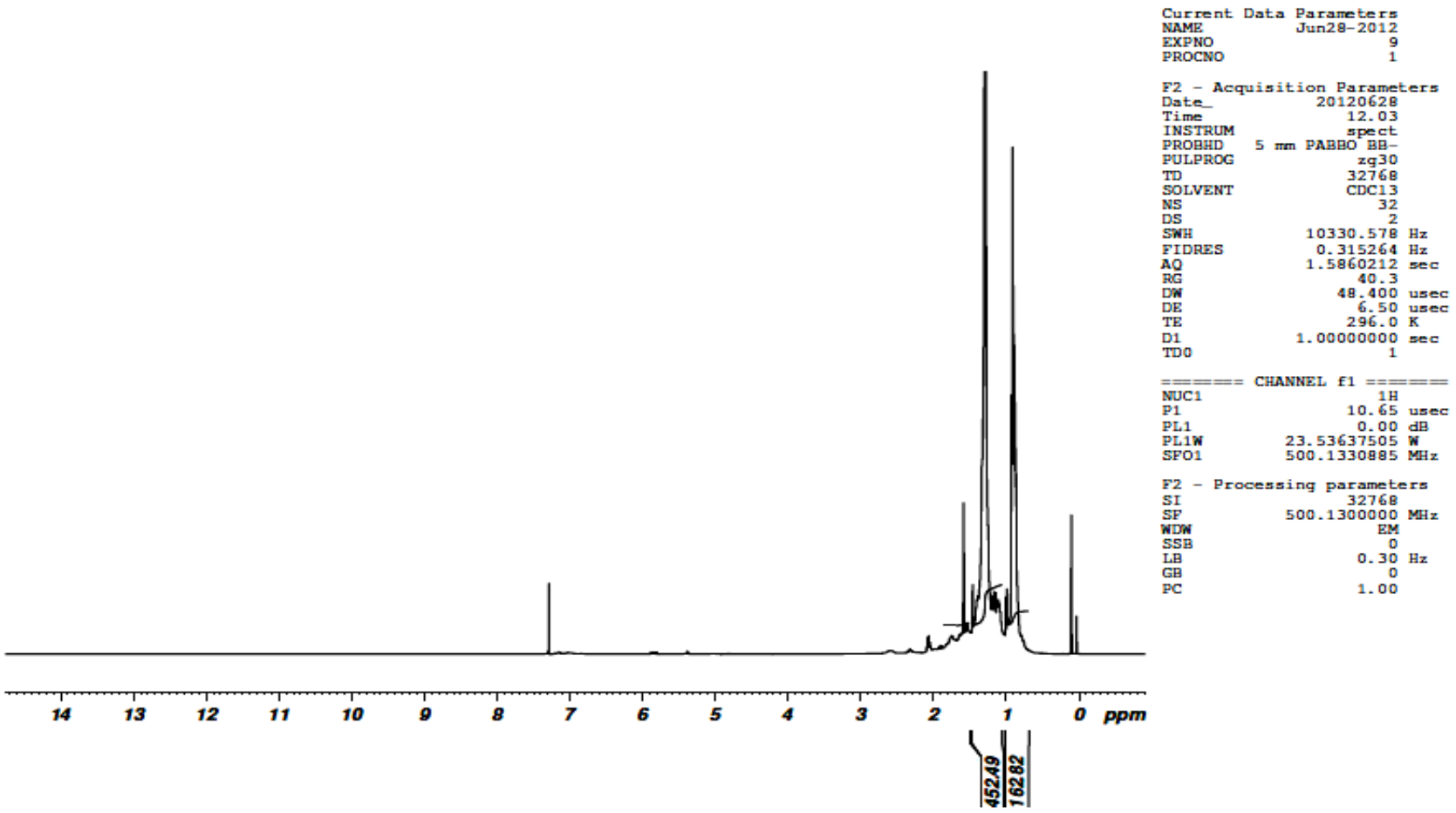

Figure 67. ^{1}H NMR spectrum of HP1

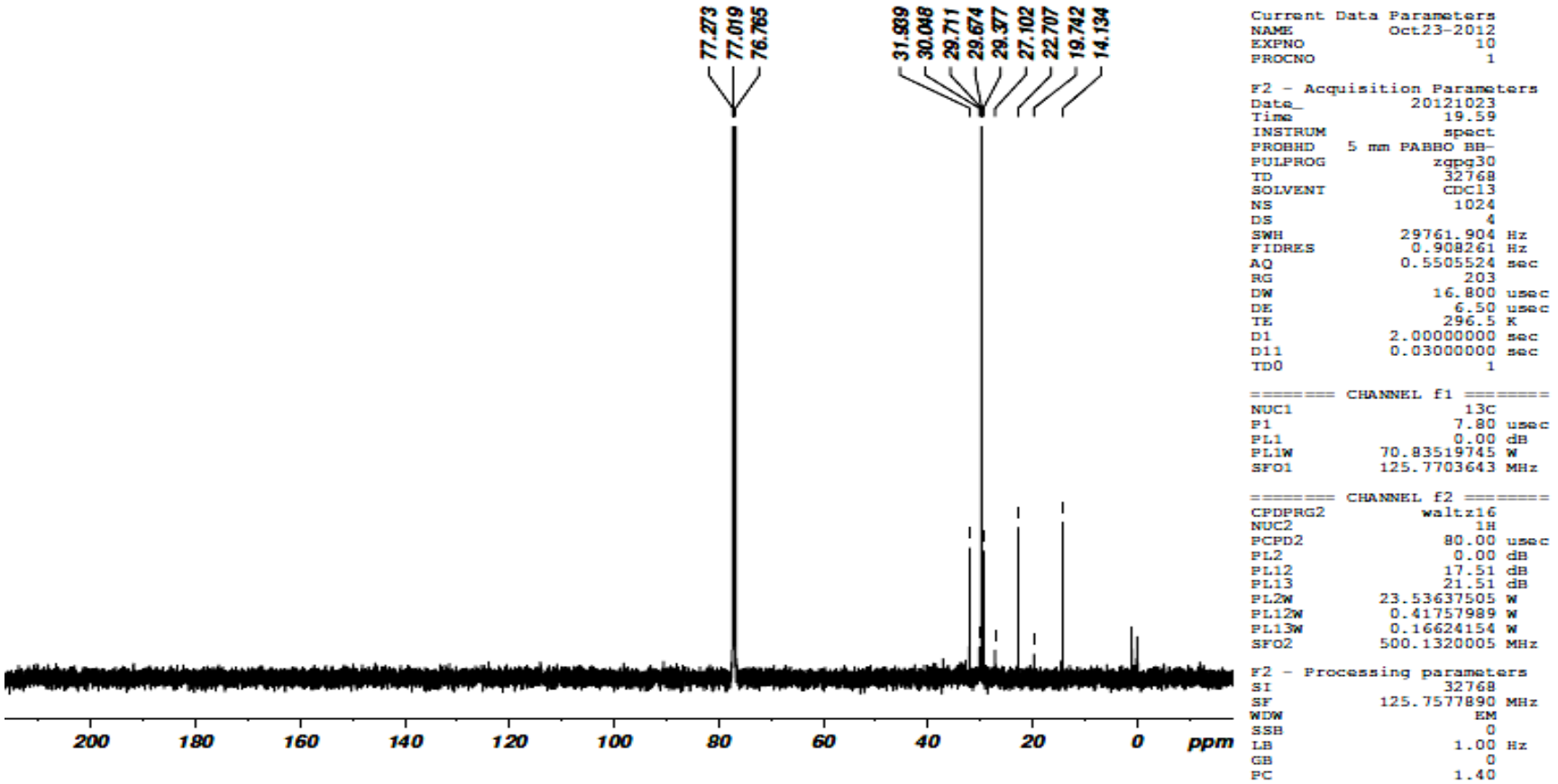

Figure 68. ^{13}C NMR spectrum of HP1

4.4.5.2 Characterisation of HP6

A white solid was obtained from the petroleum ether fractionate of ethyl acetate extract of *E. crassipes* column chromatographed over silica on elution with 99:1 petroleum ether: ethyl acetate. The compound was purified using ethanol giving a white compound (Yield- 240 mg).

Physical characteristics

(i) Melting point : 76-78 °C.

(ii) Appearance : White powder.

Chemical characteristics

(i) TLC- R_f - 0.57 (100% petroleum ether).

(ii) Solubility- chloroform.

Spectral interpretation

The UV spectrum (Chloroform) of HP6 showed an absorption maximum at 242 nm indicating the presence of a carbonyl group. Key FTIR absorption bands were noted at 1701 cm^{-1} (C=O group) and 1177 cm^{-1} (–C–O–C–) group.

1D NMR analysis

The ^{1}H NMR spectrum (Figure 69) of HP6 showed the presence of tertiary methyl group at δ_H 0.90. The broad signal at δ_H 1.27 corresponds to the methylene protons $(CH_2)_n$. The methylene protons at δ_H 1.66 and δ_H 2.33 were deshielded owing to the presence of a carbonyl group in α-position and β-position to the protons respectively. The ^{13}C NMR spectrum (Figure 70) of the compound together with DEPT 45 (Figure 71), 90, 135 (Table 28) spectra and HSQC showed the presence of twelve signals corresponding to twenty seven carbon atom. DEPT 90 spectrum revealed the absence of methine protons. Carbon resonance at δ_C 179.26 was indicative of the carbonyl carbon. Carbon resonances at δ_C 33.86, δ_C 31.93, δ_C 29.70, δ_C 29.59, δ_C 29.44, δ_C 29.36, δ_C 29.24, δ_C 29.07, δ_C 24.69, δ_C 22.69 corresponded to methylene carbon and the carbon resonance at δ_C 14.11 corresponded to terminal methyl carbon.

2D NMR analysis

Examination of ^{1}H-^{1}H COSY (Figure 72) of HP6 revealed the correlations between the methylene proton at δ_H 2.33 and δ_H 1.66, δ_H 1.66 and δ_H 1.27 and between δ_H 1.27 and δ_H 0.90 indicating the presence of a long chain chain alkane connected to the carbonyl group. HSQC spectrum (Figure 73) revealed the ^{1}J ^{1}H-^{13}C coupling in the

molecule. A diagnostic correlation between the carbonyl carbon δ_C 179.26 and the deshielded methylene proton at δ_H 2.33 in HMBC plot (Figure 74) was observed and this aided in confirming the connectivity within the compound. Other HMBC correlations substantiated the structural evidences noted from ^{1}H-^{1}H COSY.

Table 28. ^{1}H NMR, ^{13}C NMR values, ^{1}H -^{1}H COSY and HMBC correlation of HP6

C.no	^{1}H (ppm)	^{13}C (ppm)	DEPT 135	COSY	HMBC correlated to
1		179.26			2.33
1' & 1''	2.33	33.91	33.91*	1.66	1.66
2' & 2''	1.66	24.69	24.69*	2.33, 1.27	1.27
3' & 3''	1.27	29.36	29.36*	1.66	
4' & 4''	1.27	29.44	29.44*		
5' & 5''	1.27	29.59	29.59*		
6' & 6''	127	29.70	29.70*		
7' & 7''	1.27	29.70	29.70*		
8' & 8''	1.27	29.70	29.70*		
9' & 9''	1.27	29.24	29.24*		
10' & 10''	1.27	29.07	29.07*		
11' & 11''	1.27	31.93	31.93*		0.90
12' & 12''	1.27	22.69	22.69*	0.90	1.27
13' & 13''	0.90	14.15	14.15	1.27	

*Downward peak

The full structural assignment of HP6 was made by a combinational NMR spectroscopic interpretation together with UV and IR spectra. The compound was found to a mixture with stigmasterol. Also, the presence of carbonyl group in FTIR spectrum suggested the compound to contain a keto functionality rather than an ester moiety. Also the absence of deshielded prton resonance beyond δ_H 3 in 1H NMR spectrum further confirmed the absence of ester functional group. Based on the foresaid facts and the NMR investigation, the compound was deduced as **heptacosan-14-one** with the molecular formula $C_{27}H_{54}O$. The melting point of the compound HP6 matches with the literature (**www.chemicalbook.com**). Also the IR spectrum of the compound matches NIST FTIR of heptacosan-14-one further supporting the structure of the compound.

Asparagus officinalis leaf wax has been found to contain the C27 ketone heptacosan-14-one, a symmetric ketone with relatively short chain length (**Riederer and Muller, 2006**).

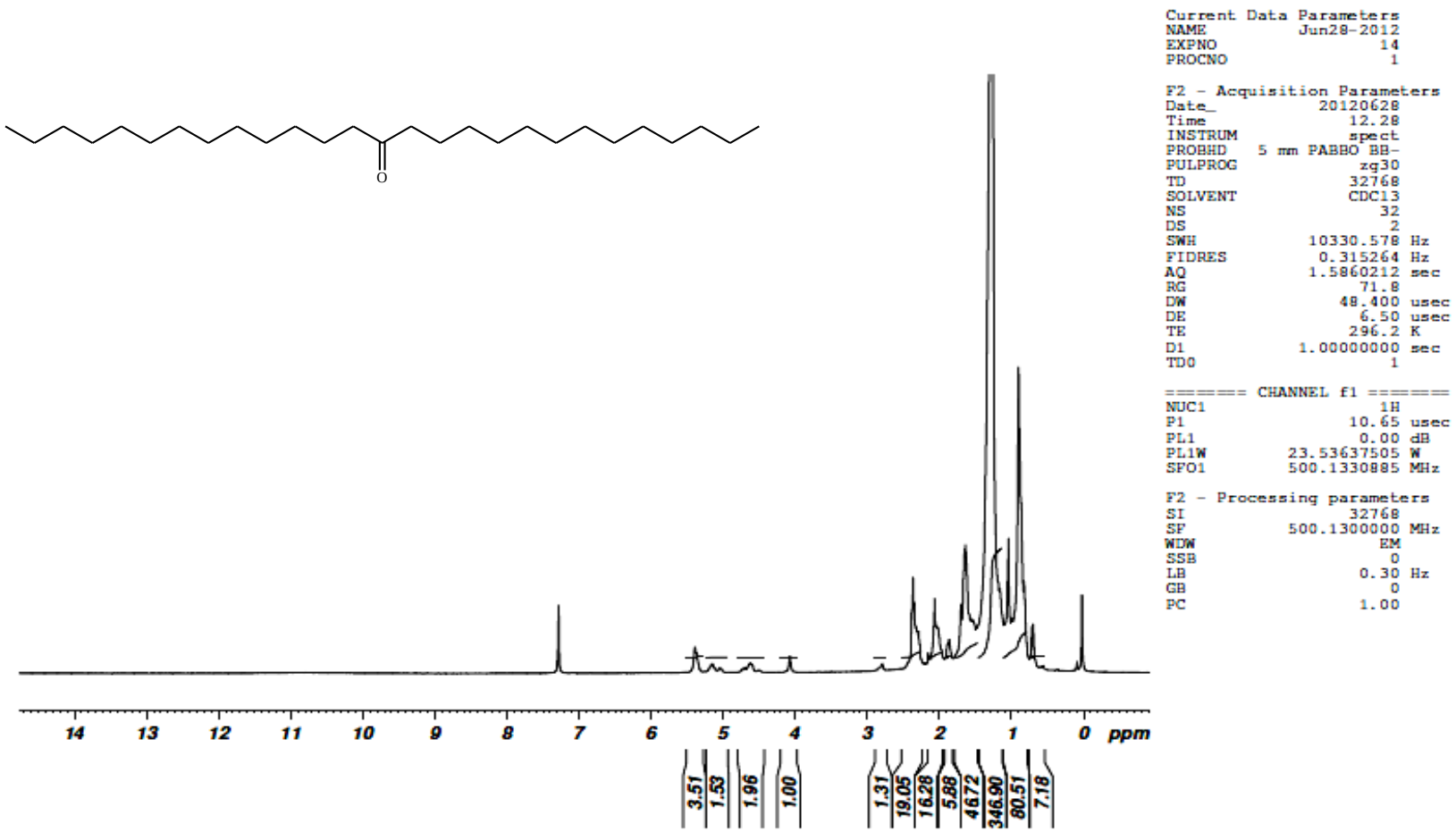


```
Current Data Parameters
NAME          Jun28-2012
EXPNO                 14
PROCNO                 1

F2 - Acquisition Parameters
Date_           20120628
Time               12.28
INSTRUM            spect
PROBHD   5 mm PABBO BB-
PULPROG             zg30
TD                 32768
SOLVENT            CDCl3
NS                    32
DS                     2
SWH           10330.578 Hz
FIDRES         0.315264 Hz
AQ             1.5860212 sec
RG                  71.8
DW                48.400 usec
DE                 6.50 usec
TE                296.2 K
D1            1.00000000 sec
TD0                    1

====== CHANNEL f1 ======
NUC1                  1H
P1                10.65 usec
PL1                0.00 dB
PL1W        23.53637505 W
SFO1        500.1330885 MHz

F2 - Processing parameters
SI                 32768
SF          500.1300000 MHz
WDW                   EM
SSB                    0
LB                 0.30 Hz
GB                     0
PC                  1.00
```

Figure 69. ^{1}H NMR spectrum of HP6

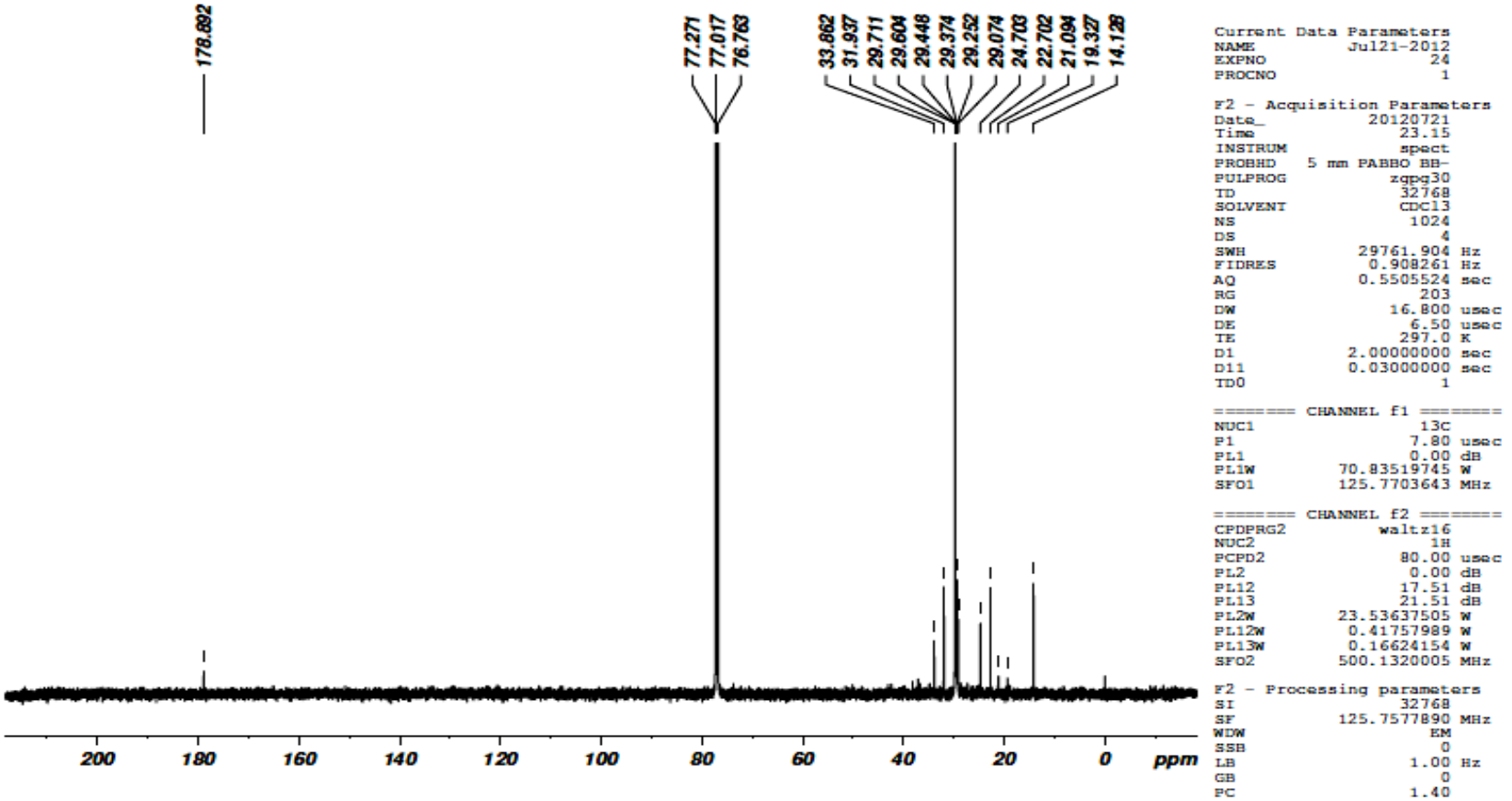

Figure 70. ^{13}C NMR spectrum of HP6

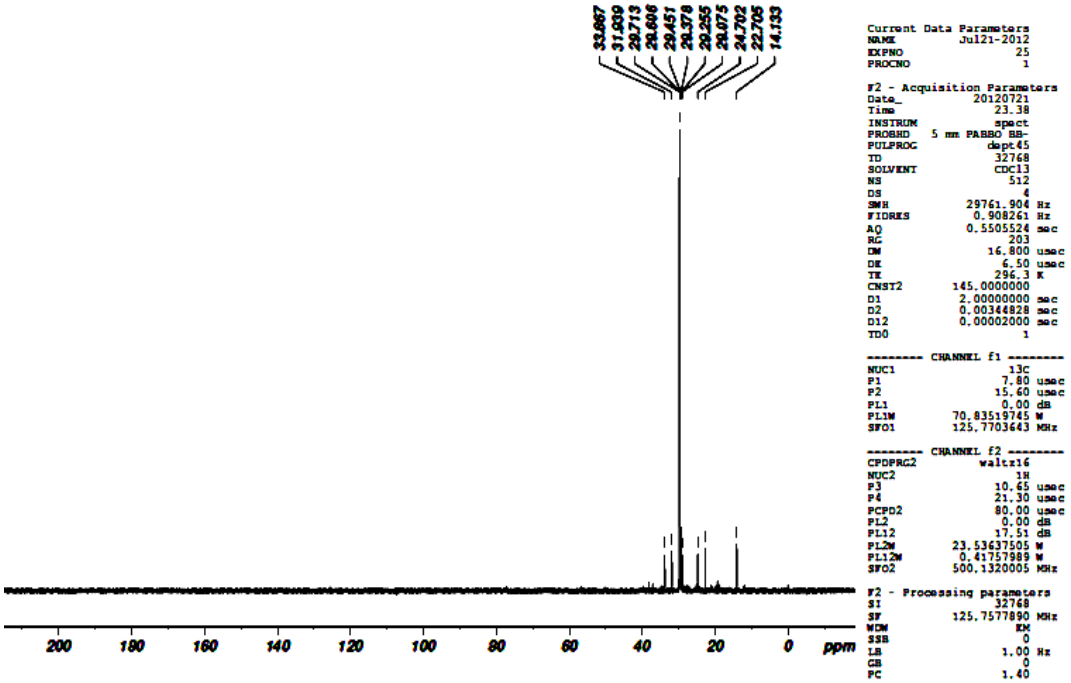

Figure 71. DEPT 45 spectrum of HP6

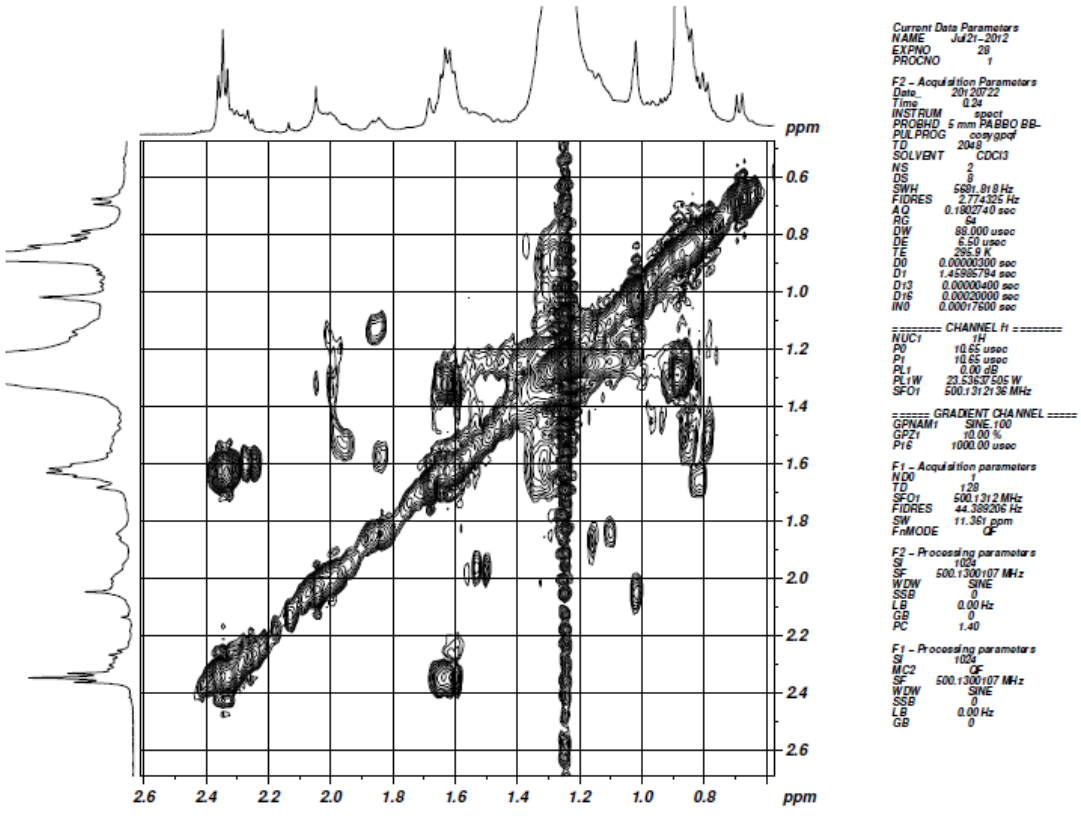

Figure 72. ^{1}H-^{1}H COSY spectrum of HP6

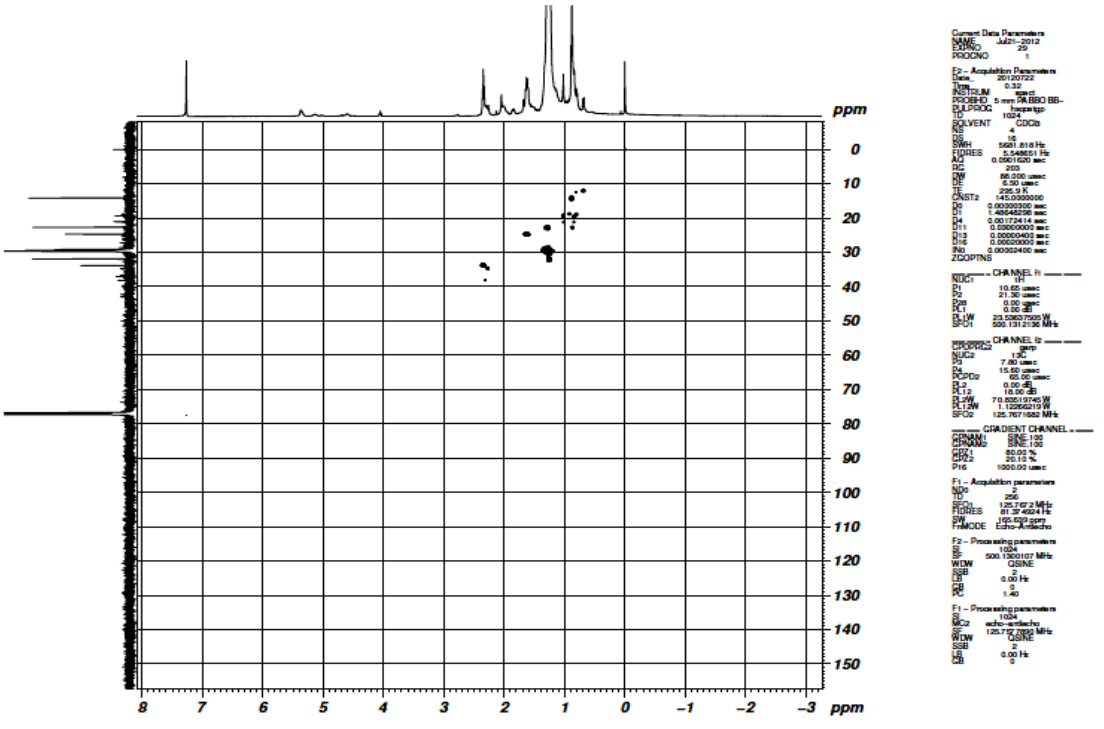

Figure 73. HSQC spectrum of HP6

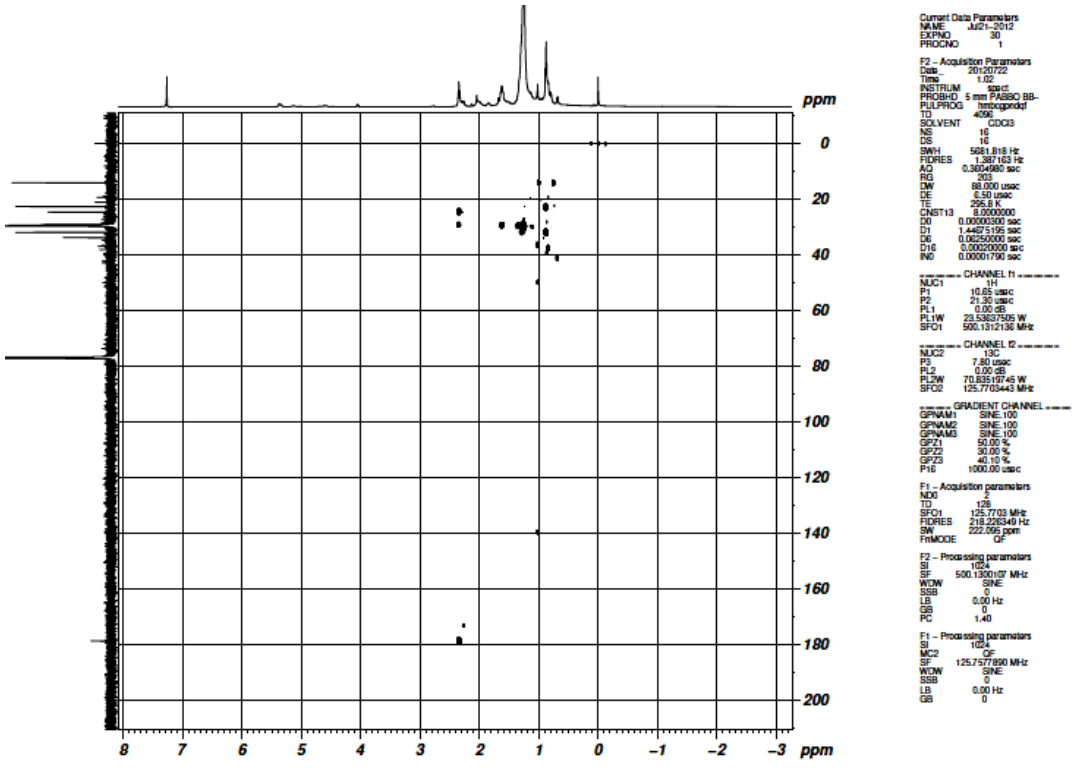

Figure 74. HMBC spectrum of HP6

4.4.5.3 Characterization of HP7

Petroleum ether fractionate on elution with 10%ethyl acetate: petroleum ether gave a brown solid.The compound was recrystallized with chloroform giving white crystal and was designated as HP7 (Yield- 2g).

Physical characteristics

(i) Appearance- White needle crystals.

Chemical characteristics

(i) Liebermann - Burchard test- Green colour indicating the presence of sterol moiety.

(ii) Salkowski test- Formation of red colour in upper layer indicating the presence of sterol moiety.

(iii) TLC - Rf -0.5 (100% chloroform), an intense brown spot in iodine vapour that remains for a longer period.

Characterization of HP7

The R_f (0.5) of the compound in 100% chloroform matches with E13 characterized as stigmasterol. Further confirmation was made by comparing the melting point, IR, ^{1}H and ^{13}C NMR spectra with that of the standard stigmasterol. Hence, the compound was characterized as stigmasterol.

Significance of isolation of compounds from *E. crassipes*

The present study aimed at the isolation of compounds from extracts of *E. crassipes* resulted in the isolation of several compounds of which 18 compounds were purified and characterized. Fresh plant (1050 kg) was collected from a local water body and dried. The plant has high moisture content (90%) and therefore, it became essential to find a suitable extraction method. Hence, different methods for extraction of dried and fresh *E. crassipes* have been carried out. Literature reports suggested the vast applicability of sonic assisted extraction for a number of plants. In addition, there were no reports on the sonic assisted extraction of *E. crassipes*. The sonic assisted extraction of *E. crassipes* was found to give a good yield of extract for fresh *E. crassipes* whereas conventional method (reflux) gave good yield for dried *E. crassipes*.

Quantitative isolation of sterols, alkaloids and terpenoids were carried out and the isolated metabolites were profiled by GC-MS revealing the pharmacological significance of the plant. Phytochemical screening test demonstrated the presence of commercially significant metabolites in the plant extracts which motivated to isolate compounds from various extracts of plants.

Open column chromatography was chosen for the isolation of the compounds as this is a convenient method of isolation which requires no expensive instruments and this can be scaled up to isolate a large quantity of compounds. Highly advanced techniques like HPLC isolation are expensive and only few milligrams to gram of the compounds could be isolated using such techniques.

Terpenoids and fatty esters were isolated from the acetone extract of *E. crassipes.* The method adopted was the first of its kind for the isolation of compounds from *E. crassipes.* The procedure involved the use of ethanolic potassium hydroxide. An exothermic reaction occurred during the process of preparation of slurry and change in the nature of the compounds was anticipated. The use of acetone and ethanolic KOH was expected to produce cyclisation and esterification.

Table 29

Compounds isolated from various extract s of *E. crassipes* in the present study

Acetone	• **Diterpene** • **Undecanoic acid 4-oxo-tetradecyl ester** • **Phthalic acid dibutyl ester** • **Phthalic acid bis-(2-methyl-tridecyl) ester**
Ethyl acetate (Silica)	• **A Long chain fatty acid ester** • **Methyl linoleate** • **Hexadecanyl 2-hydroxy 4-methoxy cinnamate** • **Mixture of campesterol, β-sitosterol and stigmasterol** • **Mixture of β-sitosterol and stigmasterol** • **Stigmasterol** • **Stigmast-22-ene-3,7-dione** • **Azacrown compound**
Aqueous	• **Carbohydrate**
Ethyl acetate (Activated Charcoal)	• **Tridecanoic acid 3-hydroxy propyl ester** • **Pentacosan-13-one**
Petroleum ether fractionate	• **Hydrocarbon** • **Heptacosan-14-one** • **Stigmasterol**

Bulk column chromatography was adopted for the isolation of compounds from the ethyl acetate and aqueous extract of *E. crassipes* as there is more recovery of the solvent. Additionally, ecofriendly solvents like ethyl acetate and water were used in the study.

Activated charcoal was used as an adsorbent for the isolation of compounds from ethyl acetate extract. This method suggested the usefulness of the activated charcoal for the isolation of compounds from *E. crassipes* as the isolated compounds were pure and required less purification techniques. **There are no reports on the isolation of compounds from petroleum ether fractionate of ethyl acetate extract of *E. crassipes*.** This fractionation procedure was found to minimize the complexity involved in the isolation of compounds. The compounds isolated from extracts of *E. crassipes* are consolidated and presented in Table 29. The isolation of pharmacologically significant compounds from *E. crassipes* throws light on the usefulness of the plant as a source of phytochemicals.

4.4.6 HPLC studies of ethyl acetate and aqueous extracts of *E. crassipes* for detection of glutathione

Glutathione has a tripeptidic structure with the formula L-γ-glutamyl-L-cysteine glycine. It is the most abundant intracellular thiol in plants and other organisms, and is involved in the synthesis of proteins, DNA, and enzyme cofactors. Glutathione plays a significant role in maintaining the protein −SH groups in the reduced state and in removing toxic peroxides formed in metabolism (**Bodo *et al,* 2004a**).

The ethyl acetate and aqueous extract of *E. crassipes* obtained by percolation method was analysed for the presence of glutathione using HPLC. The composition of the mobile phase was optimized using varying concentration of the two mobile phases. The composition 0.06 % trifluoroacetic acid (TFA) in water (v/v) (A) and 100 % acetonitrile (B) (50% A and 50% B) was chosen for the study. The HPLC of standard glutathione, ethyl acetate extract, and aqueous extract was recorded in the optimized chromatographic conditions. Glutathione showed two peaks at RT 0.37 and 2.25. Varying concentrations of the ethyl acetate extract in methanol (1 mg, 1.25 mg, 1.6 mg) were analysed. The ethyl acetate extract showed three peaks at RT 1.35, 2.52 and 2.91 (Figure 75). The area of the peak at RT 2.9 was found to increase with increase in concentration whereas the other peaks showed a decrease in area with increase in concentration indicating the predominancy of the compound. In comparison with the

standard, the peak at RT 2.9 was confirmed to be glutathione. The aqueous extract showed the presence of three peaks at RT 2.21, 2.49 and 2.96 (Figure 76). The area of the peaks was found to increase with increase in concentration. The peak at RT 2.21 was attributed to glutathione in comparison with the standard.

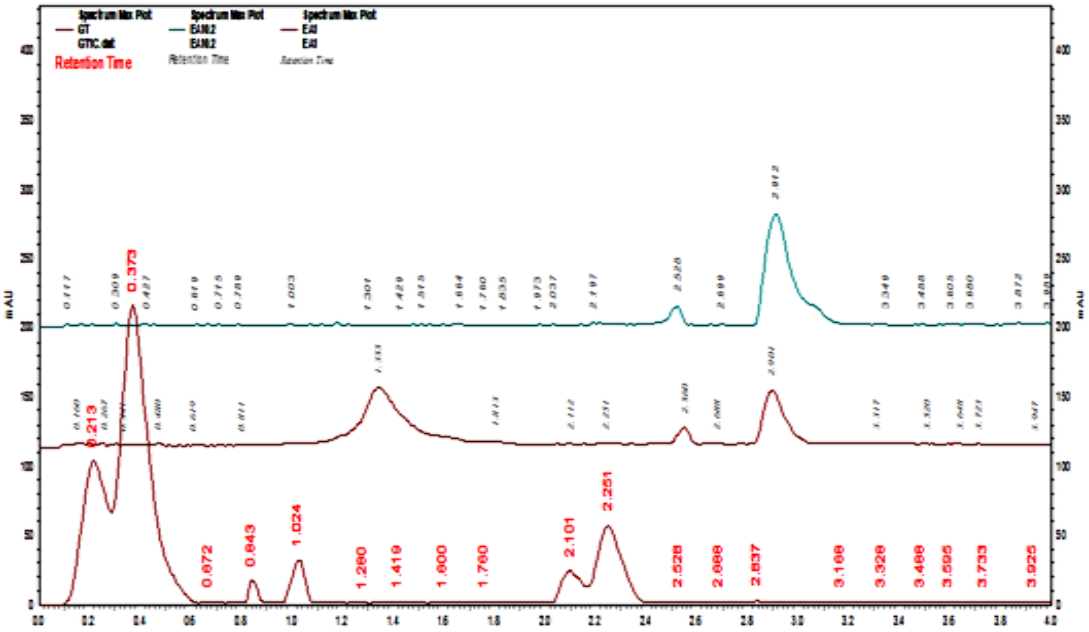

Figure 75. HPLC of the ethyl acetate extract of *E. crassipes*

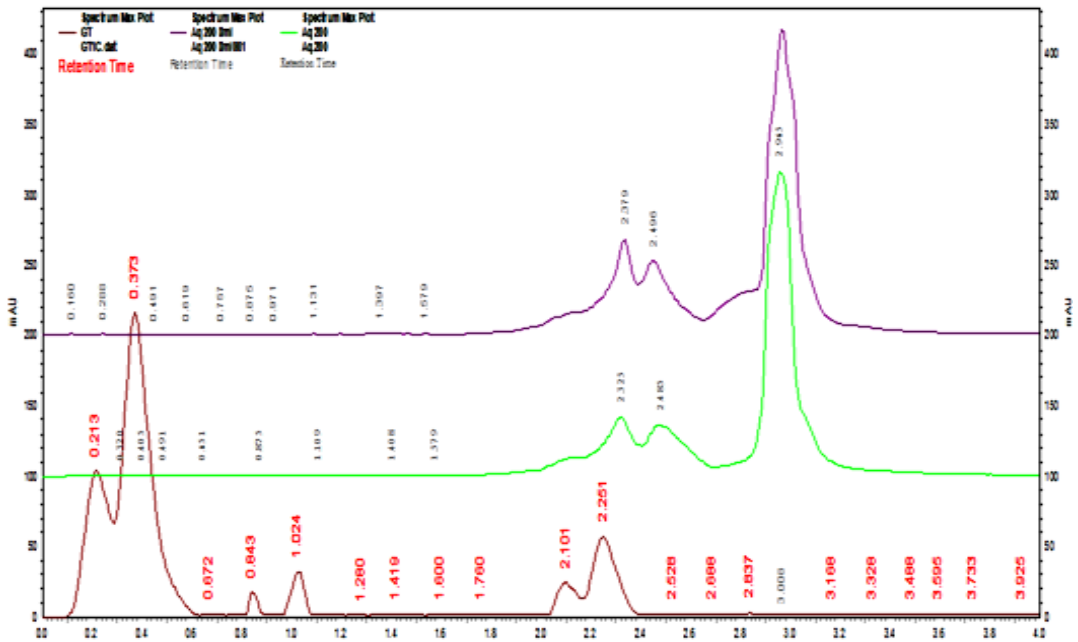

Figure 76. HPLC of the aqueous extract of *E. crassipes*

The presence of glutathione in the dry leaves of *E. crassipes* has been detected by HPLC and estimated by total glutathione assay (**Bodo *et al,* 2004a,b**). In the present study, presence of glutathione was noted in the ethyl acetate and aqueous extract of *E. crassipes.*This may provide an opportunity for the plant to be used in pharmacological and cosmeceutical industry as glutathione has been reported to possess strong antioxidant and antiageing activity. Antiageing property can be correlated to the glutathione content. The results of this study motivated us to carry out the *in vitro* and *in silico* antiageing studies.

4.5 Biological and pharmacological activity screening of extracts and fractionates of *E. crassipes*

Plants have been used for the treatment of illness from time immemorial. *E. crassipes*, even though classified as an aquatic weed has been used by the tribals for the treatment of various ailments. Pharmacological use of *E. crassipes* thus demands scientific evidence enabling the plant to be a pioneer of all other weeds to be explored for their significance.

4.5.1 Antimicrobial assay

Determination of the antimicrobial activity of the plant in recent strides is of utmost importance as every second reveals a new disease that needs to be treated with the drugs available at hand. Moreover, multidrug resistance is of concern to the medical community as the organisms in long run become resistant to the medicines used for treatment. Hence exploring plants, which is a store of several thousands of compounds of pharmacological importance is crucial. The antimicrobial activity of petroleum ether (PE), ethyl acetate (EA), chloroform (CE), ethanol (EE), methanol (ME), aqueous (AQ) and acetone extract (Ac), methanol fractionate (MFA), ethanol fractionate (EFA) of aqueous extract of *E. crassipes* and E12 has been tested against two bacteria and two fungi.

4.5.1.1 Antibacterial activity

An important characteristic of plant extracts and their components is hydrophobicity, which enable them to partition the lipid of the bacterial cell membrane and mitochondria, disturbing the cell structures and rendering them more permeable. Extensive leakage from bacterial cells or the exit of critical molecules and ions will lead to death. The variation in the effectiveness of the extract against different microorganisms depends upon the chemical composition of the extracts and membrane

permeability of the microbes for the chemicals and their metabolism (**Baral and Vaidya, 2011**).

The results of the antibacterial activity of extracts, fractionates and compound E12 isolated from ethyl acetate extract of *E. crassipes* against *Pseudomonas aeruginosa* and *Staphyloccus albus* is given in Table 30 and Figure 77. 50 µg/mL solutions of extracts, fractionates and compound were compared with standard drug gentamycin. A clear zone of growth inhibition was noted around the disc due to diffusion of drug (Figure 77). The diameter of the inhibition zone denotes the relative susceptibility of the test microorganisms to a particular test substance (**Arulpriya *et al*, 2010**).

Zone of Inhibition (mm)	Type of antimicrobe
> 13	Highly sensitive or susceptible
8-13	Moderately sensitive or intermediate
< 8	Resistant

Ac and EE were highly active against *Pseudomonas aerugniosa* and ME was active against *Staphyloccus albus* which may be due to the presence of phytochemicals like alkaloids, sterols, terpenoids, anthocyanins and anthroquinone. EA, ME and E12 showed moderate activity against *Pseudomonas aeruginosa. Staphylococcus albus* was moderately susceptible to EA, EE, Ac and E12. PE showed least activity against the two organisms tested. The organisms were resistant to CE, AQ, MFA and EFA.

Table 30. Antibacterial activity of the extracts/ fractionates and E12 of *E. crassipes*

Extract	Bacteria- Zone of inhibition (mm)	
	Pseudomonas aeruginosa	***Staphylococcus albus***
Standard	22	35
PE	6	6
EA	8	8
CE	Resistant	Resistant
EE	14	8
ME	8	**18**
AQ	Resistant	Resistant
Ac	**18**	12
MFA	Resistant	Resistant
EFA	Resistant	Resistant
E12	8	10

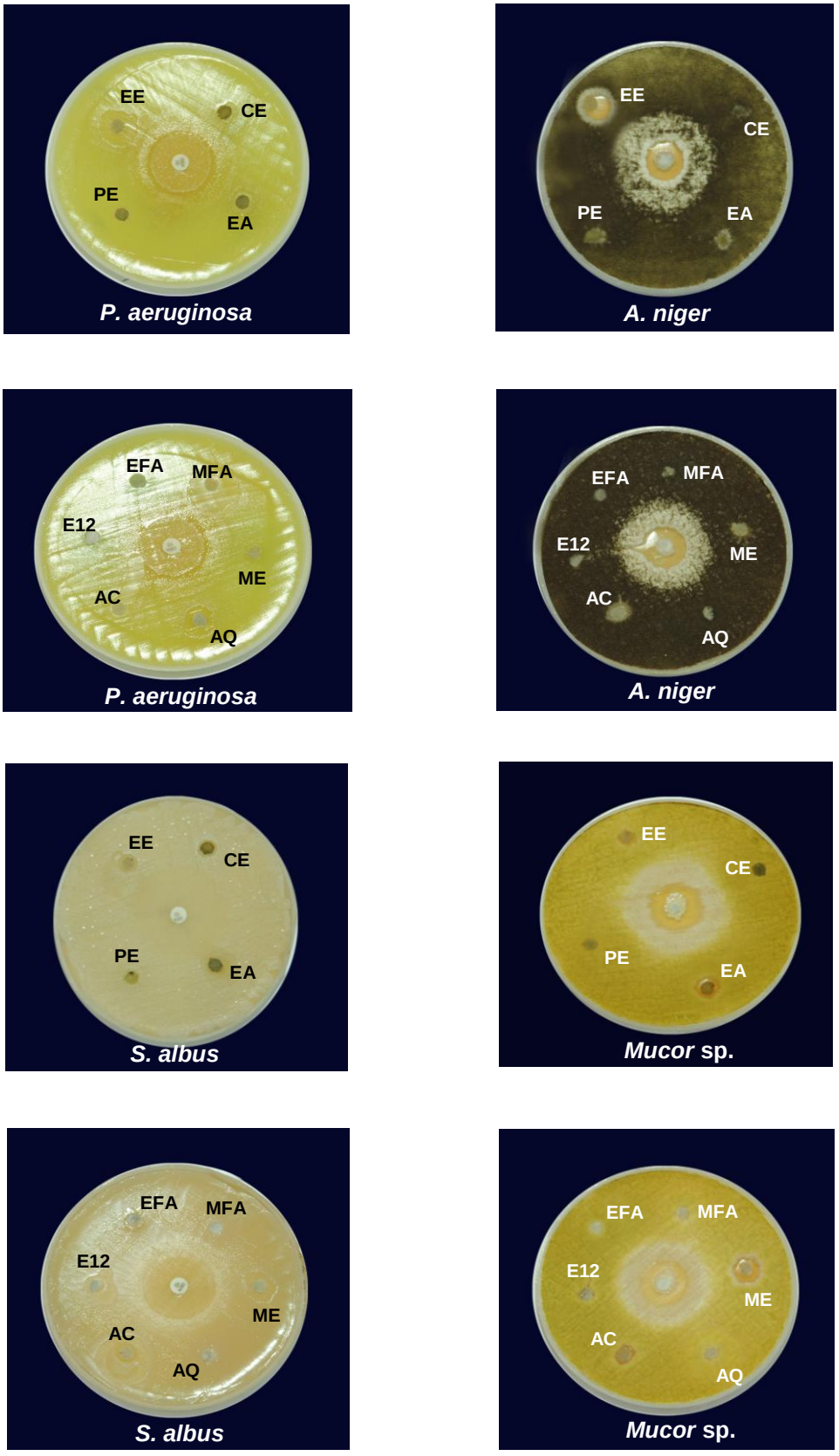

Figure 77. Plates depicting the antimicrobial activity of *E. crassipes*

4.5.1.2 Antifungal activity

The antifungal activity of the extracts of *E. crassipes* is depicted in Figure 77 and Table 31. EE showed highest antimicrobial activity against *Aspergillus niger* and was found to show three-fourth activity as that of the standard flucanozole. Both EA and Ac showed moderate activity against *Mucor* sp but was half the activity exhibited by the standard. The two fungi used in the present study were resistant to CE, AQ, MFA, EFA and E12.

Table 31. Antifungal activity of the extracts/fractionates and E12 of *E. crassipes*

Extract	Fungi - Zone of inhibition (mm)	
	Aspergillus niger	***Mucor* sp**
Standard	16	20
PE	8	6
EA	6	**10**
CE	Resistant	Resistant
EE	**12**	6
ME	8	6
AQ	Resistant	Resistant
Ac	6	**10**
MFA	Resistant	Resistant
EFA	Resistant	Resistant
E12	Resistant	6

The results of the antimicrobial activity of the extracts, fractionates and E12 of *E. crassipes* demonstrated that the acetone extract (Ac) exerted a high activity against all the microorganisms tested amongst all test substances, ME and EE showed moderate activity whereas EA showed appreciable activity.

The phytochemicals like alkaloids (**Karou *et al,* 2006; Garba and Okeniyi, 2012; Singh and Kumar, 2012**), flavonoids (**Ali and Dixit, 2012; Nessa *et al,* 2012; Vijayasanthi *et al,* 2012**), sterols (**Gowthami *et al,* 2012; Singh *et al,* 2012),** terpenoids (**Mustarichie *et al,* 2012; Sermakkani, 2012**), anthraquinones (**Mariappan and Shanthi, 2012; Muthu *et al,* 2012**), anthocyanins (**Burdulis *et al,* 2009; Cisowska *et al,* 2011**), proteins (**Fadaei, 2012; Tehrani *et al,* 2012**), phenolics (**Lamounier *et al,* 2012**) were reported to exhibit antimicrobial activity. Hence, it may be ascertained that these phytochemicals are the bioactive components exerting antimicrobial activity.

The phytochemicals like alkaloids, flavonoids, sterols, terpenoids and proteins might be responsible for the antimicrobial activity of the extracts. All the microorganisms tested in the present study were resistant to CE, AQ, EFA and MFA. The chloroform and aqueous extract contains sugars and glylcosides that might have acted as a media rather than inhibiting it. **Baral and Vaidya (2011)** has reported similar trend where methanol extract was potent than the aqueous extract. Aqueous extract of *E. crassipes* has been found to be inactive against organisms like *Staphylococcus aureus*, *Escherichia coli, Fusarium oxysporum, F. moniliforme* and *F. proliferatum*.

4.5.2 Antioxidant activity

Free radicals have in large received considerable attention due to various deleterious effects. Antioxidants reduce the adverse effects of these radicals by any one of the reported regulatory mechanisms. The phytochemicals in the plants are considered to play a crucial role in conferring the activities to the plant. Assessing the antioxidant capacity of *E. crassipes* thus becomes a key strategy to find its application in various pharmacological activities.

4.5.2.1 Reducing power assay

Reducing power of a sample serves as a significant reflection of the potential antioxidant activity (**Oktay *et al*, 2003; Nikhat *et al*, 2009**). Compounds with reducing power indicate that they are electron donors and reduce the oxidized intermediates of lipid peroxidation processes, thereby acting as primary and secondary antioxidants (**Chanda and Dave, 2009**).

The antioxidant activity of the extract and fractionates of *E. crassipes* was discernible in the reducing power assay. The reducing power of the standard ascorbic acid, extract and fractionates (Table 32) of *E. crassipes* shows a dose dependent relationship and increases with increase in concentration. Among the extracts and fractionates tested, acetone extract showed highest reducing capacity. This may be due to the presence of metabolites like alkaloids, sterols, terpenoids, anthraquinones and anthocyanins in the acetone extract. Alkaloids (**Kolak *et al*, 2006; Maiza-Benabdesselam *et al*, 2007; Rackova *et al*, 2007; Pandey *et al*, 2010; Singh *et al*, 2010; Rao *et al*, 2012**), sterols (**Rao *et al*, 2012**), terpenoids (**Patil *et al*, 2012**), anthraquinones (**Jasril *et al*, 2003**) and anthocyanins (**Pasko *et al*, 2009**) have been reported to show good antioxidant capacity.

Table 32. Reducing capacity of the extracts/fractionates of *E. crassipes* as a function of concentration

Extracts and fractionates	Absorbance					
Concentration (μg)	**10**	**20**	**30**	**40**	**50**	**100**
Ac	0.1	0.28	0.36	0.5	0.6	
Hy	0.11	0.31	0.41	0.43	0.44	
AQE	0.19	0.21	0.35	0.46	0.48	0.79
MFA	0.09	0.16	0.25	0.27	0.35	0.69
EFA	0.11	0.19	0.21	0.26	0.31	0.66
AFE	0.16	0.18	0.21	0.25	0.28	0.50
Concentration (μg)	**100**	**200**	**300**	**400**	**500**	**1000**
AA	0.20	0.39	0.56	0.65	0.86	-
AFM	0.12	0.18	0.28	0.35	0.44	0.72
Concentration (μg)	**50**	**100**	**150**	**200**	**250**	**1000**
PE	0.12	0.14	0.17	0.19	0.22	
EA	0.34	0.40	0.48	0.66	0.82	

Table 33. Reducing capacity of the extracts/fractionates of *E. crassipes* as a function of time at 50 μg/mL and 500 μg/mL for AFM

Extracts and fractionates	Absorbance				
Time	**10**	**15**	**20**	**25**	**30**
PE	0.16	0.16	0.22	0.22	0.25
EA	0.42	0.6	0.82	1.04	1.48
Ac	0.37	0.5	0.6	0.52	0.54
Hy	0.32	0.34	0.44	0.46	0.55
AQE	0.19	0.29	0.49	0.50	0.50
MFA	0.14	0.20	0.30	0.35	0.39
EFA	0.14	0.21	0.31	0.37	0.41
AFE	0.14	0.23	0.28	0.33	0.42
AFM	0.13	0.29	0.44	0.48	0.61

The reducing capacity of the extracts of *E. crassipes* is in the order Ac>Hy>AQE>MFA>EFA>AFE>EA>PE>AFM. The reducing capacity of all the extracts except PE and AFM are higher than the standard ascorbic acid. The marked antioxidant activity of extracts and fractionates may be probably due to the presence of secondary metabolites in the plant extracts, which may act in a similar fashion as reductones by donating the electrons and reacting with free radicals to convert them to more stable product and terminate free radical chain reaction. The reducing properties are generally

associated with the presence of reductones (**Pin-Der Duh, 1998**). The antioxidant action of reductones is based on the breaking of the free radical chain by the donation of a hydrogen atom. Reductones also react with certain precursors of peroxide, thus preventing peroxide formation (**Gordon, 1990**). The presence of ascorbic acid in *E. crassipes* also contributes to the antioxidant capacity (**Lata and Dubey, 2010b**).

The reducing ability of extract and fractionates of *E. crassipes* was found to be time-dependent (Table 33). Excluding acetone extract, all the test samples showed an increase in absorbance with increasing time. After 20 min, the reducing power of the acetone extract was found to decrease. This may be due to the decrease in the reducers which would have converted the Fe^{3+}/ferricyanide complex to the ferrous form within a short time.

4.5.2.2 DPPH scavenging assay

The DPPH method is rapid, simple, accurate and inexpensive assay (**Mythili *et al*, 2011**) for measuring the ability of different compounds to act as free radical scavengers or hydrogen donors, and to evaluate the antioxidant activity of compounds. This method is independent of sample polarity for screening of many samples for radical scavenging activity (**Marinova and Batchvarov, 2011**). DPPH is a stable free radical by virtue of the delocalisation of the spare electron over the molecule as a whole, so that the molecules do not dimerize. The delocalization gives rise to a stable violet colour in ethanol/methanol solution characterized by an absorption band centred at about 520 nm (**Molyneux, 2004**).

The percentage inhibition of the extracts and fractionates of *E. crassipes* is given in Table 34. The extracts and fractionates of *E. crassipes* show a dose response relationship. Similar trend in the increase of the free radical scavenging activity of plant extracts in a concentration dependent manner has been reported by several authors (**Gowri *et al*, 2011; Li *et al*, 2011; Padmawar and Bhadoriya, 2011; Bhaskar and Avadhani, 2012; Kensa and Neelamegam, 2012**). The extracts and fractionates of *E. crassipes* show better scavenging activity than ascorbic acid. The metabolites like flavonoids, alkaloids, tannins, glycosides and phenols in the extracts and fractionates may be probably responsible for free radical scavenging activity. Phenols, flavonoids (**Akinmoladun *et al*, 2007; Prosper-Cabral *et al*, 2007; Pandey *et al*, 2010; Bhalodia *et al*, 2011; Gupta *et al*, 2011; Amir *et al*, 2012**), tannins (**Gil *et al,* 2000**), alkaloids (**Moura *et al*, 2007**), glycosides (**Cervellati *et al,* 2004**) are good antioxidant substances and prevent or control oxidative stress related disorders.

Hydrolysed extract of *E. crassipes* showed maximum inhibition percentage than other extracts and fractionates. This is because hydrolysis liberates bound antioxidant substances bound to sugars (**Prosper-Cabral *et al*, 2007**). It is obvious from the Table 34 that acetone extract (Ac) (75%) showed maximum inhibition than the chloroform extract (71%). Albeit aqueous extract contains alkaloids, flavonoids and other phytochemicals, it exhibited 69% inhibition with IC_{50} of 11.26 µg/mL. This might be because of the interaction between the phytochemicals that render the hydrogen atom unavailable for the $DPPH^{\bullet}$ radical.

Fractionates of the aqueous extract viz AFM, AFE, EFA and MFA shows lesser inhibition percentage than the aqueous extract (AQE). Synergistic effect existing between the antioxidants in the aqueous extract might be the reason for the higher inhibition percentage of the aqueous extract of *E. crassipes*. The IC_{50} values for the extracts and fractionates are given in Table 34. This study affirmed the $DPPH^{\bullet}$ scavenging ability of the extracts and fractionates of *E. crassipes*, with the results comparable to those of standard ascorbic acid.

Table 34. DPPH radical scavenging activity of the extracts and fractionates of *E. crassipes*

Extractants	Regression equation	r^2	Maximum inhibition percentage (%)	IC_{50} (µL/mL)
Hy	y = 4.5667x - 1.5	0.9689	71	5.4
Ac	y = 4.5x + 7.3	0.9478	75	9.48
PE	y = 4.7x - 1.5	0.9478	68	10.9
AQE	y = 4.6x - 1.8	0.9923	69	11.26
$CHCl_3$	y = 4.5667x - 1.5	0.9689	71	11.27
EA	y = 2.1333x + 21.4	0.9961	54	13.4
MFA	y = 3.2667x + 14.4	0.939	59	10.89
EFA	y = 4.0333x + 0.1	0.9537	63	12.37
AFM	y = 3.9667x - 4.5	0.9628	53	13.73
AFE	y = 2.4667x + 16	0.9695	54	13.78
Ascorbic acid	y = 1.6429x + 26.286	0.9716	63	14.43

In the reducing power assay, acetone extract (Ac) showed highest reducing capacity (Abs. 0.6 at 50 µg) whereas in the DPPH radical scavenging assay, hydrolysed extract (Hy) exhibited highest radical scavenging ability (IC_{50} = 5.4 µL/mL) . The order of the antioxidant activity of the extracts and fractionates differ in the two methods because of the difference in the underlying mechanisms (**Sun *et al,* 2007**).

4.5.3 Acute toxicity study

The results of the acute oral toxicity study conducted as per the OECD guidelines 423 for the ethyl acetate extract (EA), aqueous extract (AQ) and methanol fractionate of the aqueous extract (MFA) of *E. crassipes* is given in Table 35. It is obvious from the table that the extracts did not produce any mortality throughout the study period of 14 days even when the limit dose was maintained at 2000 mg/kg body weight.

Table 36 indicates the parameters observed before and after the administration of the test substance for the three extracts of *E. crassipes*. The writhing reflux was observed immediately up to 15 min after administration of the test substance at all administered doses for the extracts of *E. crassipes*. The other parameters observed were normal even at the highest dosage of 2000 mg/kg body weight of the test animal. This clearly indicates that the above extracts of *E. crassipes* do not produce oral toxicity. The medium lethal dose (LD_{50}) of the extracts is higher than 2000 mg/kg body weight and hence, in a single dose administration, the plant extracts had no adverse effect.

The statistical analysis was carried out for the dose administered to each animal on the basis of the weight. Duncan's Multiple Range Test (DMRT) was tested between the chosen parameters. The statistical analysis showed that the dose adminitstered were significant at 5 % (Table 36).

Figure 78. Photograph of Swiss Albino mice used in acute oral toxicity studies

Table 35. Effect of EA, AQ and MFA of *E. crassipes* on acute oral toxicity test in mice

S.No	Response	Unmarked		Head		Body		Tail		Head & Tail		Head & Body	
		Before	After	Before	After	Before	After	Before	After	Before	After	Before	After
1	Alertness	Normal	Normal	Normal	Normal	Normal	Normal	Normal	Normal	Normal	Normal	Normal	Normal
2	Grooming	Absent	Absent	Absent	Absent	Absent	Absent	Absent	Absent	Absent	Absent	Absent	Absent
3	Touch response	Absent	Absent	Absent	Absent	Absent	Absent	Absent	Absent	Absent	Absent	Absent	Absent
4	Torch response	Normal	Normal	Normal	Normal	Normal	Normal	Normal	Normal	Normal	Normal	Normal	Normal
5	Pain response	Absent	Absent	Absent	Absent	Absent	Absent	Absent	Absent	Absent	Absent	Absent	Absent
6	Tremors	Absent	Absent	Absent	Absent	Absent	Absent	Absent	Absent	Absent	Absent	Absent	Absent
7	Convulsion	Absent	Absent	Absent	Absent	Absent	Absent	Absent	Absent	Absent	Absent	Absent	Absent
8	Righting reflux	Present	Present	Present	Present	Present	Present	Present	Present	Present	Present	Present	Present
9	Gripping strength	Normal	Normal	Normal	Normal	Normal	Normal	Normal	Normal	Normal	Normal	Normal	Normal
10	Pinna reflux	Normal	Normal	Normal	Normal	Normal	Normal	Normal	Normal	Normal	Normal	Normal	Normal
11	Corneal reflux	Present	Present	Present	Present	Present	Present	Present	Present	Present	Present	Present	Present
12	Writhing	Absent	Present	Absent	Present	Absent	Present	Absent	Present	Absent	Present	Absent	Present
13	Pupils	Normal	Normal	Normal	Normal	Normal	Normal	Normal	Normal	Normal	Normal	Normal	Normal
14	Urination	Normal	Normal	Normal	Normal	Normal	Normal	Normal	Normal	Normal	Normal	Normal	Normal
15	Salivation	Normal	Normal	Normal	Normal	Normal	Normal	Normal	Normal	Normal	Normal	Normal	Normal
16	Skin colour	Normal	Normal	Normal	Normal	Normal	Normal	Normal	Normal	Normal	Normal	Normal	Normal
17	Lacrimation	Normal	Normal	Normal	Normal	Normal	Normal	Normal	Normal	Normal	Normal	Normal	Normal
18	Hyper activity	Absent	Absent	Absent	Absent	Absent	Absent	Absent	Absent	Absent	Absent	Absent	Absent

Table 36. Dosage of *E. crassipes* extracts administered to test animals

Concentration (mg/kg)	EA	AQ	MFA
100	2.35 ± 0.49^{f}	1.73 ± 0.57^{f}	2.16 ± 0.44^{f}
250	6.25 ± 0.73^{e}	6.12 ± 0.92^{e}	6.75 ± 0.89^{e}
500	13.58 ± 1.49^{d}	12.83 ± 1.45^{d}	12.66 ± 1.01^{d}
750	17.75 ± 1.93^{c}	18.75 ± 1.71^{c}	19.25 ± 1.79^{c}
1000	25.25 ± 2.02^{b}	27.50 ± 2.23^{b}	23.33 ± 1.70^{b}
2000	49.02 ± 3.03^{a}	47.33 ± 2.01^{a}	44.66 ± 1.72^{a}

The values of the dose administered to the animals are expressed as mean ± SD of six samples in each group. Column means followed by a common superscript are not significant at 5% by using Duncan's Multiple Range Test (DMRT).

4.5.4 Wound healing activity

Wound healing process holds several steps which involve coagulation, inflammation, formation of granulation tissue, matrix formation, remodeling of connective tissue, collagenization and aquisation of wound strength (**Ayyanar and Ignacimuthu, 2009**). Healing is a physiological process which depends on the repairing ability of the tissue in addition to type and degree of damage and general health status of the tissue. It does not normally require much help but still wounds cause discomfort and are prone to infection and other complications (**Shukla *et al*, 1999**). The objective of wound healing therefore is to heal the wound as quickly as possible with minimal pain and scarring to the patient. Besides, a flexible and fine scar with high tensile strength is desired for perfect wound closure (**Suntar *et al*, 2009**). Therefore, use of agents expediting healing is refined. The most preferable dosage form is cream as it is the most convenient for topical application (**Patil *et al*, 2012**). Therefore, the *E. crassipes* extracts were formulated into ointments and the effectiveness of these ointments tested on rats.

4.5.4.1 Rate of wound contraction

Wound contraction involves a complex and superbly orchestrated interaction of cells, extracellular matrix and cytokines. The wound area (mm^2) of all groups was measured on day 0, 1, 4, 7 and 9. The rate of wound contraction and percentage of wound healing are given in Table 37 and 38 respectively. In the present study, rate of

wound contraction in F4, F5, F6 and F7 treated rats were significantly higher. It is obvious from Table 37 that F4 shows 13% better rate of wound contraction than the untreated wound. After the application of ointment for the first four days, the vehicle showed the highest percentage wound healing (47%) than the ointments and standard. It was observed during the study that the rats licked the ointments containing extracts. After day 4, wound healing activity of the extracts started increasing. The results of wound healing activity after a week indicated the better rate of wound contraction of F4 than the untreated wound (47.5%) and other ointments. Complete wound contraction (100%) was observed for the F4 treated rats on 9th day compared to the standard F2 (98.8%).

The application of ointment was continued till 11th day after which it was attempted to remove the sutures. The sutures were unidentifiable due to the complete wound healing (Figure 79). The incised skin from the animals sacrificed on 14th day were analysed for the tensile strength and histopathology.

Figure 79. Wound healing activity of extract of *E. crassipes* in Albino Wistar rats

The additive effect of phenolics, anthraquinones in ethyl acetate extract and flavonoids, terpenoids, anthraquinones in turmeric, sandalwood and aloevera may probably have enhanced the rate of wound healing in F4. Higher wound healing (98.67%) was observed in F7 than in F6 treated rats (95%) due to the presence of proteins, flavonoids, alkaloids, phenols and sterols.

Increased rate of contraction in ointments might be due to the proliferation and transformation of fibroblast cells into myofibroblast (**Barua *et al*, 2000**) which has enhanced contractile property resulting in the increase of epithelialisation (**Sasidharan *et al*, 2012**). Moreover, the ointments were administered topically and this mode promotes faster wound contraction due to the larger availability of the wound site (**Sumithra *et al*, 2005**).

Table 37. Effect of the ointments on wound area (mm^2) in rats

Groups	Day 1	Day 4	Day 7	Day 9
F1	100.00	71.00 ± 7.55	52.50 ± 12.88	13.00 ± 1.15
F2	100.00	72.50 ± 13.22a^{ns}	23.50 ± 11.89a^{***}	1.00 ±1.50a^{***}
F3	100.00	53.0 ±13.22$a^{***}b^{***}$	26.00 ± 11.89$a^{***}b^{ns}$	10.0 ± 2.60$a^{ns}b^{**}$
F4	100.00	73.00 ± 4.76$a^{ns}b^{ns}$	2.50 ± 5.0a^{***}b***	0
F5	100.00	73.50 ±7.90$a^{ns}b^{ns}$	53.00 ± 10.13$a^{ns}b^{***}$	2.00 ±0$a^{***}b^{ns}$
F6	100.00	73.00 ± 6.0$a^{ns}b^{ns}$	10.00 ± 11.55$a^{***}b^{**}$	5.00 ± 5.77$a^{*}b^{*}$
F7	100.00	68.67 ±9.87$a^{ns}b^{*}$	25.00 ± 15.28$a^{***}b^{ns}$	1.00 ± 2.00$a^{**}b^{ns}$

Table 38. Effect of the ointments on rate of wound contraction in rats

Groups	Day 1	Day 4	Day 7	Day 9
F1	0	29	47.5	87
F2	0	26a^{ns}	73.6a^{***}	98.8a^{**}
F3	0	47$a^{***}b^{***}$	74$a^{***}b^{ns}$	90$a^{ns}b^{*}$
F4	0	27$a^{ns}b^{ns}$	97.5$a^{***}b^{***}$	100$a^{**}b^{ns}$
F5	0	26.5$a^{ns}b^{ns}$	47$a^{ns}b^{***}$	98$a^{**}b^{ns}$
F6	0	27$a^{ns}b^{ns}$	90$a^{***}b^{***}$	95$a^{*}b^{ns}$
F7	0	31.34$a^{ns}b^{*}$	66.67$a^{***}b^{**}$	98.67$a^{**}b^{ns}$

Data are expressed as mean ± S.E.M from six rats and analysed by two way ANOVA followed by Bonferroni's test. *P < 0.05, **P < 0.01, ***P < 0.001 as compared to negative control group and standard group. 'a' represents F1 vs F2,F3,F4,F5,F6,F7 and 'b' represents F2 vs F3, F4, F5, F6 and F7.

4.5.4.2 Tensile strength

The results of the measurement of tensile strength of the incised skin of Albino Wistar rats are given in Figure 80. Animals treated with aqueous extract ointment showed highest tensile strength followed by the ethyl acetate extract ointment. Higher tensile strength was noted in the incised skin on which only vehicle was applied than the incised skin applied with F6 (ointment prepared with aqueous polyherbal formulation). The phytochemicals in the aqueous polyherbal formulation probably would have softened the skin which might have resulted in the reduction of tensile strength of the animal. Treatment with the F5 and F7 significantly increased the tensile strength compared to the control and vehicle group. F4 showed better rate of wound contraction whereas tensile strength was found to be low. This might be due to the decrease in collagen concentration of the tissue treated with this ointment. Tensile strength of the animals

treated with F7 was higher than F4, F5 and F6. Enhanced tensile strength may be attributed to the increase in collagen concentration forming intermolecular cross - linking via vitamin C dependent hydroxylation (**Nagori and Solanki, 2011**) and stabilization of fibres (**Hayouni *et al*, 2011**).

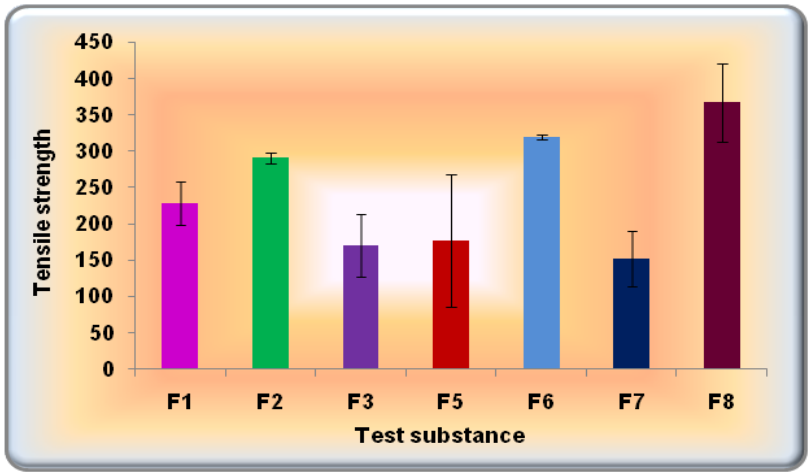

Figure 80. Effect of the ointments and formulation on the tensile strength of the animals

4.5.4.3 Histopathological evaluation

Histopathological evaluation of the control, vehicle and test group is shown in Figure 81. Wound healing process which consists of inflammation, proliferation and remodeling phase was analyzed in histopathological study. A small wound with ulcerated epidermis and moderate inflammation in dermis was observed in the control group. Vascular and fibroblast proliferation was noted indicating an inflammatory granulation tissue in control group. In F4 and F6 treated group, the fibrosis of the dermis was found to be normal indicating a healed wound. A minimal inflammation with occasional inflammatory cell was noted in these groups. A normal epidermis was noted in F5treated animals. The dermis showed extensive scar formation with fibrosis and fibroblasts. Moderate inflammation was noted in this group. In F7 treated group, the epidermis was found to be normal. The dermis shows focal scar formation and occasional epitheloid cell granuloma was seen in the scar region.

Wound healing effect of the prepared ointment may be due to the regulation of collagen I expression and increase in tensile strength (**Abdulla *et al*, 2010**) by the phytoconstituents. General phytoconstituents like alkaloids, flavonoids, sterols, proteins in plant extracts are known to promote wound healing process mainly due to their antimicrobial property (**Dash *et al*, 2011**). Also the phytoconstituents like flavonoids and phenols contribute to the antioxidative capacity (**Singh *et al*, 2002**).

A wound when exposed to external environment is prone to attack by microbes like *Staphylococcus aureus, Escherichia coli, Streptococcus pyogenes, Corynebacterium sp*. which invade through the skin delaying the natural wound healing process. Reactive Oxygen Species plays a vital part of healing and serve as a cellular messenger that drive numerous aspects of molecular and cell biology. Micromolecular concentration of Reactive Oxygen Species can trigger various pathaways of wound healing whereas higher concentration leads to deleterious effect (**Akkol *et al*, 2011**).

If the inflammatory phase does not resolve in time, oxidative stress occurs due to the increase in the concentration of reactive oxygen species than the antioxidative capacity of the cell. Oxidative stress mediated by radical ROS and non-radical ROS may inhibit cell migration and proliferation and cause tissue damage and perpetuation of inflammation. On the other hand, neutrophil defect leads to severe infections and poor wound healing (**Kanta, 2011**). Hence, if a plant extract or a compound possesses antioxidative and antimicrobial potential, it can be used as a good therapeutic agent for promoting wound healing process.

The good antioxidant potential of the extracts of *E. crassipes* due to the presence of phytochemicals like flavonoids, alkaloids, sterols, proteins in the aqueous extract and anthraquinones, phenolics in the ethyl acetate extract might have contributed to the wound healing activity of the prepared ointment. *E. crassipes* possesses metabolites like terpenoids, alkaloids, flavonoids, sterols (**Lata and Dubey, 2010a**) which are found to possess wound healing activity (**Sasidharan *et al*, 2010; Venkatanarayana *et al*, 2010**). Also the antimicrobial study carried out with these extracts against *Pseudomonas aeruginosa, Staphylococcus albus, Aspergillus niger* and *Mucor* sp. showed the appreciable antimicrobial activity of ethyl acetate extract.

Hence the external application of the ointments prepared with ethyl acetate extract, aqueous extract and polyherbal formulation with these two extracts might have prevented the invasion of the microbes in the wound thereby protecting the wound. At the same time, external application of the ointments might have entrapped the free radicals liberated by the cells, which at low concentration have inherent machinery to protect the cells from microbes (**Vijaya Bharathi *et al*, 2010**).

E. crassipes contains ascorbic acid (**Ogulensi *et al*, 2010; Lata and Dubey, 2010b; Lata *et al*, 2010e**) which is reported to have scavenging activities and inhibition of lipid peroxidation (**Nithya *et al*, 2011**). Any drug that inhibits lipid peroxidation

increases the viability of collagen fibres by enhancing its strength, preventing cell damage, promoting DNA synthesis and by aiding in circulation (**Dash *et al*, 2011**).

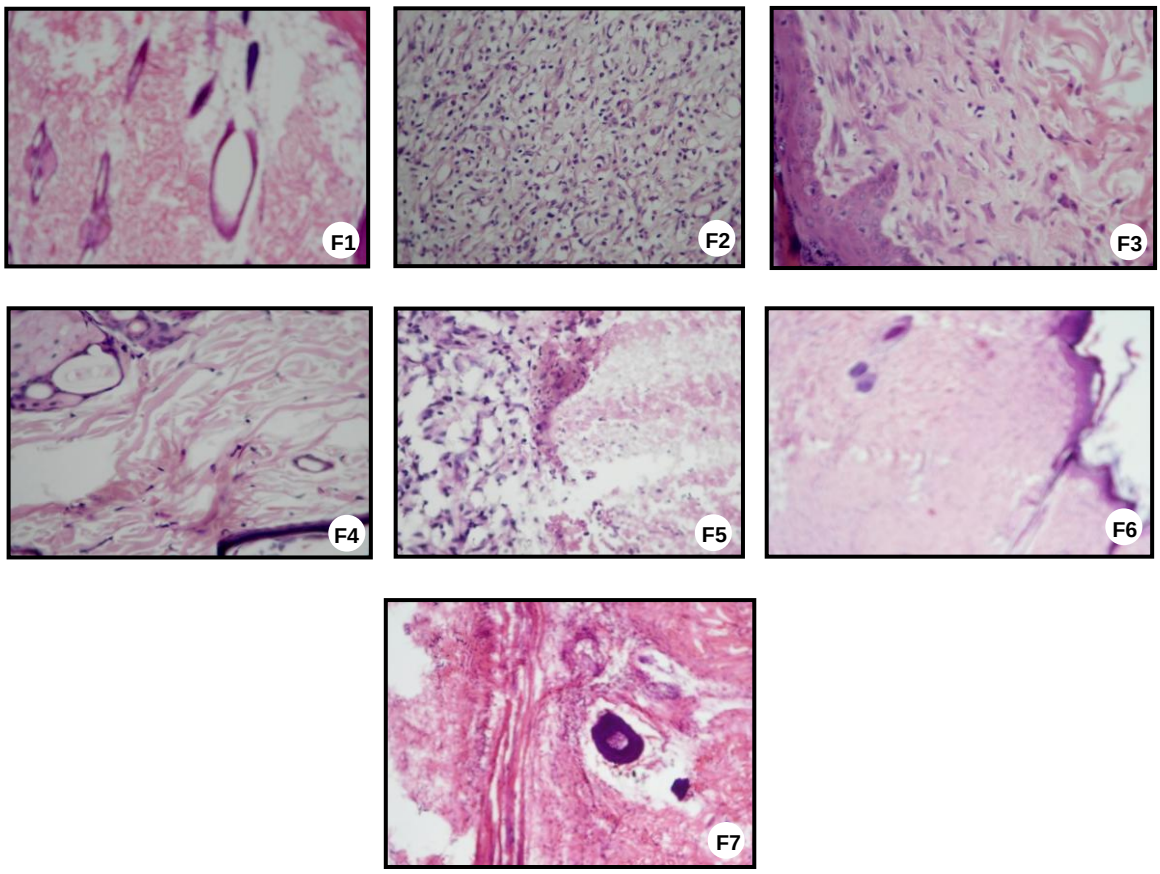

Figure 81. Photomicrographs of sections of the skin from treated rats stained with hematoxylin and eosin. Skin microscopic image of F1, F2, F3, F4 F5, F6 and F7

Besides its antioxidative and antimicrobial potential, the plant contains zinc (**Lata and Dubey, 2010f**) which is one of the essential trace elements. Zinc serves as a cofactor in various enzyme systems, including zinc dependent matrix, metalloproteinases, which augment autodebridement and keratinocyte migration during wound repair process. It also provides resistance to epithelial apoptosis, probably through antioxidative activity of cysteine rich metallothioneins, against ROS and bacterial toxin. Topical application of zinc rather than oral administration aids in wound healing because of its effect in reducing superinfections (**Suntar *et al*, 2009**). Topical application of the ointments prepared with *E. crassipes* which contained zinc would have helped in the healing process by moisture holding capacity of the skin, cell migration and regeneration.

The isolation of compounds from plants may either potentiate the wound healing activity or that single compound becomes toxic compared to the whole plant extract (**Akkol *et al*, 2011**). Plant extracts when used as such have beneficiary effects. The secondary compounds acts synergistically with primary active compounds and eases the side effects caused by them. Thus the synergistic effect of the phytoconstituents, antioxidative and antimicrobial activity might have accelerated the wound healing process in the test animals.

4.5.5 Skin whitening and antiageing assay of the skin cream prepared with ethyl acetate extract of *E. crassipes*

Skin whitening products are commercially available for cosmetic purposes in order to obtain a lighter skin appearance. They are also utilized for clinical treatment of pigmentary disorders such as melasma or postinflammatory hyperpigmentation. Whitening agents act at various levels of melanin production in the skin. Many of them are known as competitive inhibitors of tyrosinase, the key enzyme in melanogenesis. Others inhibit the maturation of this enzyme or the transport of pigment granules (melanosomes) from melanocytes to surrounding keratinocytes (**Smit, 2009**). Skin aging is a complex and dynamic process which involves genetic, hormonal and environmental factors. In a biochemical level, the aging process is just an inevitable process of oxidation and cellular death. A balanced diet, exercise and basic care such as using antiageing creams will be reflected in the delay of ageing (**Loandos and Cabral, 2010**).

Skin whitening and antiageing creams can be prepared as per the standard procedures and any prepared skin cream in India should adhere to the specifications given in IS 6608:2004. The skin cream was prepared in the present study with the ethyl acetate extract of *E. crassipes* because of the presence of compounds like cinnamate esters, long chain fatty acid esters, stigmasterol, glutathione, etc., in this extract. Cinnamate esters are used as sunblock in sunscreen lotions and creams (**Alexander and Chaudhuri, 1996**), long chain fatty acid esters are used for the skin cream preparation (**Mausner, 1995; 1999**), sterols possess antimicrobial (**Chakraborty and Shah, 2011**), anti-inflammatory (**Gaspari and Rietschel, 1985**) and other pharmacological properties. Hence, the ethyl acetate extract was chosen among other extracts for the preparation of the skin cream (LPR1). The skin cream made out of ethyl acetate extract, selected quantities of lime and musk (LP3) was prepared to study the synergistic skin whitening action of the composition in the skin cream.

4.5.5.1 Stability and Chemical tests for the skin cream

The pH of human skin ranges from 4.5 to 6.0 and 5.5 is considered to be average pH of the skin. Therefore, the formulations intended for application to skin should have pH closer to this range. pH has an imperative character in the stability of pharmaceuticals and in case of products intended for skin application, these must be compatible with the skin (**Rasul and Akhtar, 2012**). The pH of the skin cream LP3 prepared using ethyl acetate extract of *E. crassipes* was 5.15 which is the normal pH for the cream. The total fat and total residue of LP3 is 39.26% and 73.20% which is ideal for any skin cream formulation. Heavy metals like lead and arsenic were absent in the skin cream formulation. The skin cream prepared was found to be devoid of any microorganisms which indicate that the skin cream prepared abides by the specification mentioned in the skin cream testing procedure IS 6608:2004. The physico chemical parameters of the skin creams LPR1 and LP3 are given in Table 39.

Table 39. Physico chemical parameters of the skin cream

Analytical Parameters	LPR1	LP3
pH	-	5.15
Total Fat %	-	39.26
Total Residue %	-	73.20
Thermal Stability	Pass	Pass
Heavy metals		
Lead (ppm)	Nil	Nil
Arsenic (ppm)	Nil	Nil
Microbial Load		
Total Bacterial Count	Nil	Nil
Total Fungal Count	Nil	Nil
Specific Pathogen		
Escherichia coli	Nil	Nil
Salmonella sp	Nil	Nil
Staphylococcus aureus	Nil	Nil
Pseudomonas aeruginosa	Nil	Nil

4.5.5.2 *In vitro* skin whitening property of the skin cream by Tyrosinase assay

The results of the percentage inhibition of tyrosinase inhibition showed that skin cream containing only ethyl acetate tested for its activity at 0.5 mg to 20 mg showed no inhibition while for the skin cream containing musk at 0.5 and 1.0 mg, 8.25 and 11.10% inhibition respectively was noted. Melanin biosynthesis is a multistep pathway and the extracts may not show tyrosinase inhibition if it had acted on other enzymes in the

pathway rather than directly on tyrosinase. The synergistic effect of lime and musk in LP3 probably might have contributed to the tyrosinase inhibitory activity of LP3.

Quercetin is reported to be good tyrosinase inhibitor (**Kubo *et al*, 2000; Choi *et al*, 2007; Kubo *et al*, 2007**) which is present in *E. crassipes* (**Lata and Dubey, 2010c**). In certain cases, this flavone may act as a strong inductor of melanogenesis in normal and malignant human melanocytes and in reconstituted three-dimensional human epidermis models (**Solano *et al*, 2006**). This might also contribute to the decreased tyrosinase inhibition activity of the skin creams.

4.5.5.3 *In vitro* anti-ageing property of the skin cream

4.5.5.3.1 Free radical medicated DNA damage inhibition assay

Cellular metabolism has been shown to generate the reactive oxygen species such as hydrogen peroxide, hydroxyl radical, and superoxide radical. Trace metals such as copper and iron that are present in biological systems may interact with active oxygen species, ionizing radiation, or microwaves to damage macromolecules. The cleavage of metalloproteins by oxidative damage may lead to increase in the levels of metal ions in biological cells (**Kim and Kang, 2006**). DNA is one of the major targets of free-radical-induced damage. Under physiological conditions, the constant and endogenous rate of production of free radicals may lead to minimal DNA damage, which is needed to induce the defensive systems and DNA repair mechanisms. However, if the production of free radicals increases, they may attack DNA at either the sugar (deoxyribose) or the base level, giving rise to a large number of toxic products. Attack at the sugar level ultimately leads to a strand break with terminal fragmented sugar residues (**Desmarchelier *et al*, 1997; Acharya *et al*, 2011; Devi *et al*, 2012**). Some of the fragmentation products can be detected by adding thiobarbituric acid (TBA) to the reaction mixture, resulting in formation of a pink (TBA) 2-MDA chromogen (**Halliwell and Gutteridge, 1981**). The Fenton reaction generates hydroxyl radicals (OH•), which degrade DNA deoxyribose, using Fe^{2+} salts as an important catalytic component (**Kim and Kang, 2006; Bhaumik *et al*, 2008**). Hydroxyl radicals are the most reactive radicals that are produced via the Fenton's reaction in living systems. These radicals are mainly implicated in the pathology of several diseases such as Parkinson's disease, rheumatoid arthritis, and carcinogenesis (**Bhaumik *et al*, 2008**).

For any skin cream to possess good ageing capacity it should possess efficient antioxidant activity. Free radical medicated DNA damage inhibition of the skin cream

LPR1 and LP3 assay is given in Table 40. The DNA damage inhibition offered by the skin creams LPR1 and LP3 (Table 40) increases with increase in concentration (1 mg to 20 mg). The DNA damage inhibition offered by the skin creams LPR1 and LP3 reached a maximum at 5 mg and then decreased gradually afterwards. Increase in percentage DNA damage was noted upto 5 mg concentration for LP3. The variation in the pH/concentration of LP3 probably might have reduced the percentage of DNA damage inhibition.

Table 40. Percentage inhibition of DNA damage of LPR1 and LP3

Concentration of cream (mg)	% Inhibition of DNA Damage	
	LPR1	LP3
1	8.07	12.39
2	17.36	14.14
5	27.78	17.26
10	6.78	1.27
20	4.18	Negative

4.5.5.3.2 DPPH radical scavenging activity of the skin cream

The percentage inhibition of the DPPH radical scavenging activity of skin creams LPR1 and LP3 is given in Table 41. The DPPH radical scavenging activity of LPR1 and LP3 shows that with increase in concentration (2 to 50 mg), the radical scavenging activity increases (1 to 6%). This indicates the increase in concentration of the compounds responsible for radical scavenging activity with increasing concentration of the skin cream. Both LPR1 and LP3 shows comparable percentage of DPPH radical scavenging activity which indicates that the constituents added (Lemon and Musk) do not alter the nature of the skin cream in terms of its activity.

Table 41. DPPH radical scavenging activity of LPR1 and LP3

Concentration of cream (mg)	% DPPH scavenged	
	LPR1	LP3
2	1.15	1.23
10	2.57	2.71
20	3.45	3.77
50	6.12	5.19

The skin creams LPR1 and LP3 were certified by T.Stanes & Company Limited with the number TSPPTL/5409/2012.

4.6 Larvicidal, pupicidal and repellent studies

The results of the percentage mortality of the larvae and pupae of *C. quinquefasciatus* by petroleum ether (PE), acetone (Ac), ethyl acetate (EA), aqueous extract (AQ), methanol (MFA) and ethanol fractionate (EFA) of aqueous extract of *E. crassipes* are given in Figure 82, 83 respectively and Table 42.

The ethanol fractionate of *E. crassipes* showed highest larvicidal activity (LC_{50}= 71.43, 94.68, 120.42 and 152.15 ppm) followed by methanol fractionate (LC_{50} = 84.64, 138.36, 192.53 and 252.41 ppm) for I - IV instar larvae. The larval toxicity values of *E. crassipes* extracts and fractionates based on LC_{50} and LC_{90} is in the order EFA>MFA>AQ>EA>PE. The results show that the extracts and fractionates exhibit better larvicidal activity at higher concentrations. A positive correlation was seen between the larvicidal activity and the extract concentrations (50 to 375 ppm), the rate of mortality being proportional to the concentration indicating a dose dependent effect on mortality. Mortality was not observed in the control for four different instar larvae and pupae.

The present study indicated that the toxicity of the extracts and fractionates of *E. crassipes* when extended to pupae, showed appreciable pupal mortality. The decreasing order of pupal mortality based on the comparison of LC_{50} and LC_{90} values are EFA>AQ>MFA>EA>PE.

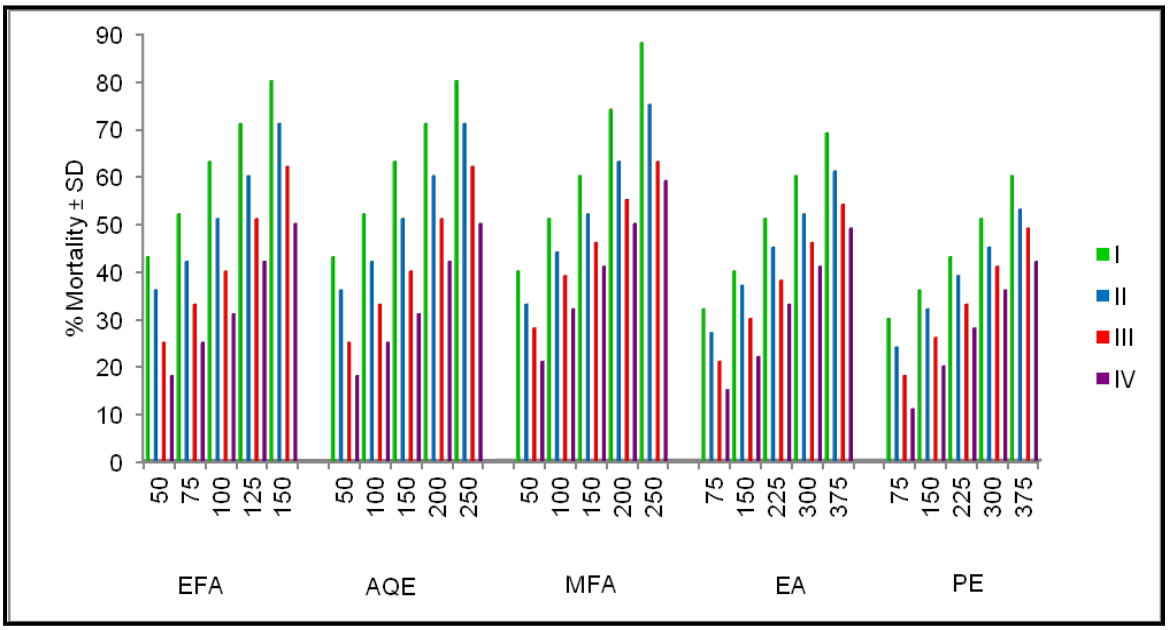

Figure 82. Percentage mortality of *Culex quinquefasciatus* larvae on treatment with extracts and fractionates of *E. crassipes*

Table 42. Toxicity of extracts and fractionates of *E. crassipes* on larvae (I, II, III and IV) and pupae of *C.quinquefasciatus* at 24 h of exposure

	Larvae and pupae mortality (%)																								
Extract / Fractionate	**EFA**					**AQE**					**MFA**					**EA**					**PE**				
Conc. (ppm)	50	75	100	125	150	50	100	150	200	250	50	100	150	200	250	75	150	225	300	375	75	150	225	300	375
I instar larvae	43	52	63	71	80	40	51	60	74	88	43	52	63	71	80	32	40	51	60	69	30	36	43	51	60
II instar larvae	36	42	51	60	71	33	44	52	63	75	36	42	51	60	71	27	37	45	52	61	24	32	39	45	53
III instar larvae	25	33	40	51	62	28	39	46	55	63	25	33	40	51	62	21	30	38	46	54	18	26	33	41	49
IV instar larvae	18	25	31	42	50	21	32	41	50	59	18	25	31	42	50	15	22	33	41	49	11	20	28	36	42
Pupae	12	20	29	36	43	15	23	31	40	48	12	20	29	36	43	9	13	19	26	34	6	12	17	22	31

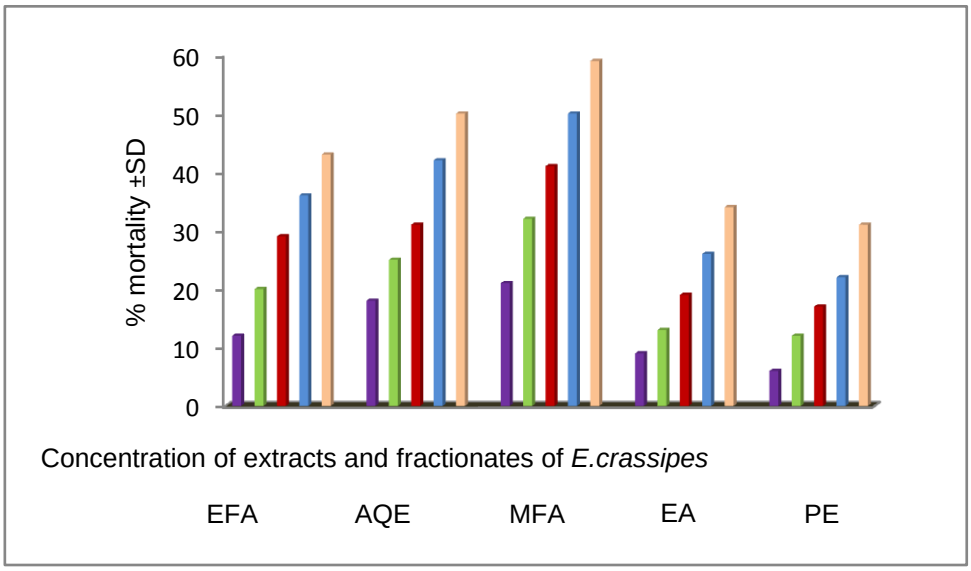

Figure 83. Percentage mortality of *Culex quinquefasciatus* pupae on treatment with extracts and fractionates of *E. crassipes*

The statistical data pertaining to the LC_{50}, LC_{90}, regression equation, chi-square and 95% fiducidal limits of the larvae and pupae of *Culex quinquefasciatus* were calculated and are presented in Table 43. The concentration of the extract that has killed 50% and 90% of the larvae and pupae of *C. quinquefasciatus* and its upper and lower fiducidal respectively is represented as LC_{50} and LC_{90} and 95% confidence limit. The regression and correlation analysis was done between the parameters larvicidal activity and concentration of the extract.

The larvicidal and pupicidal activity of the extracts might be due to the synergistic or additive effect of the phytochemicals present in the extract. Presence of flavonoids in petroleum ether extract, anthraquinone and phenolics in ethyl acetate extract, alkaloids, flavonoids, sterols, anthraquinones, anthocyanins, proteins and quinones in aqueous extract of *E. crassipes* has been noted. Methanol fractionate of *E. crassipes* contains flavonoids, anthraquinones, anthocyanins, carbohydrates. Ethanol fractionate possess alkaloids, flavonoids, anthraquinones, anthocyanins and quinones. The column chromatography of acetone extract of *E. crassipes* resulted in the isolation of sterol mixture which was identified by Gas Liquid Chromatography as stigmasterol, campesterol, β-sitosterol (**Goswami *et al*, 1983**). Sterols in particular β-sitosterol have been reported to possess larvicidal activity (**Rahuman *et al*, 2008**). Except PE, all the extracts and fractionates of *E. crassipes* tested for its larvicidal and pupicidal toxicity against *Culex*

quinquefasciatus contains anthraquinones. Anthraquinone class of compounds has been reported to exhibit larvicidal and pupicidal activity (**Cheng *et al*, 2008**).

Table 43. Larvicidal and Pupicidal activity of extracts and fractionates of *E. crassipes* against *Culex quinquefasciatus*

Larval instar	LC_{50}	LC_{90}	Reg. Equation	95% Confidence limit				Chi square value*
				LL		UL		
				LC_{50}	LC_{90}	LC_{50}	LC_{90}	
EFA								
I	71.43	176.12	y = 0.372x + 24.6	87.29	251.52	109.41	284.94	5.302
II	94.68	213.56	y = 0.352x + 16.8	123.36	312.11	148.52	349.69	1.532
III	120.42	234.96	y = 0.368x + 5.4	161.17	389.71	186.35	424.13	3.674
IV	152.15	277.82	y = 0.324x + 0.8	187.45	393.55	214.85	433.28	3.419
Pupae	173.35	198.57	y = 0.312x - 3.2	250.26	485.64	275.10	526.31	6.396
MFA								
I	84.64	301.49	y = 0.186x + 33.9	76.17	281.34	89.10	321.63	1.926
II	138.36	366.18	y = 0.176x + 25.6	128.52	343.56	147.19	382.79	5.801
III	192.53	407.26	y = 0.184x + 14.6	177.28	376.53	205.78	432.98	3.080
IV	252.41	499.24	y = 0.162x + 8.9	237.16	469.31	267.65	532.16	3.419
Pupae	292.75	548.51	y = 0.156x + 4.6	272.47	518.65	312.02	583.36	4.099
AQE								
I	99.40	269.23	y = 0.238x + 26.9	87.29	251.52	109.41	284.94	5.25
II	135.51	331.62	y = 0.206x + 22.5	123.36	312.11	148.52	349.69	1.805
III	172.38	405.21	y = 0.172x + 20.4	161.17	389.71	186.35	424.13	1.664
IV	200.56	412.27	y = 0.188x + 12.4	187.45	393.55	214.85	433.28	6.621
Pupae	262.75	505.32	y = 0.08x - 0.4	250.26	485.64	275.10	526.31	5.225
EA								
I	224.17	537.46	y = 0.1253x + 22.2	206.75	504.46	231.58	568.20	2.392
II	275.68	636.54	y = 0.1107x + 19.5	259.11	598.78	297.24	691.18	3.358
III	333.67	696.25	y = 0.1093x + 13.2	309.20	654.52	357.03	736.97	1.547
IV	376.82	722.37	y = 0.116x + 5.9	357.13	678.26	404.50	754.60	1.988
Pupae	577.14	1051.3	y = 0.084x + 1.3	549.42	996.18	60.4.18	1096.4	1.803
PE								
I	278.16	681.64	y = 0.1x + 21.5	252.94	647.47	293.34	709.80	3.847
II	348.26	770.68	y = 0.0947x + 17.3	326.41	741.84	362.52	798.26	2.556
III	385.41	782.59	y = 0.1027x + 10.3	359.16	763.42	405.36	814.59	1.872
IV	440.34	831.79	y = 0.104x + 4	427.62	80.5.74	463.84	859.51	5.229
Pupae	628.42	1135.18	y = 0.08x - 0.4	604.38	1106.13	646.23	1162.59	1.285

* Significant at p<0.05; LL-Lower Limit; UL-Upper Limit

The higher larvicidal and pupicidal efficacy of EFA of *E. crassipes* compared to aqueous extract might be attributed to the separation of phytochemicals during fractionation which might have rendered those phytochemicals the higher efficacy. The difference in activity between EFA and MFA may be due to the presence of alkaloids and quinones in EFA. The mode of action of the phytochemicals on the mosquito larvae are not certain whereas it has been reported that one or all of the phytochemicals interfere with proper functioning of the mitochondria of mosquito larvae more specifically at the proton transferring sites. Phytochemicals are also reported to affect the midgut epithelium, gastric area and malphigian tubules in the larvae (**Rajkumar and Jebanesan 2009**).

The toxicity of the *E. crassipes* extracts and fractionates to *C. quinquefasciatus* was found to decrease (50 ppm to 375 ppm) with increase in the larval stage (I to IV) and pupal stage. This has been attributed to several factors including alteration in the thickness and composition of larvae, higher detoxification potential and the difference in the surface area (**Waliwitiya *et al*, 2008**).

Several plant extracts have been tested against *C. quinquefasciatus* and a survey of literature on the use of plant extracts for the control of different instars of *C. quinquefasciatus* revealed that this vector is susceptible to almost all the tested extracts.

In Bangladesh, the dried whole plant of *E. crassipes* has been used to ward off insects in animal sheds (**Rahmatullah *et al*, 2010**). Hence, repellent activity for the plant against *C. quinquefascitus* was studied. *E. crassipes* extracts and fractionates tested at the particular concentration did not exert repellent activity towards the filarial vector. The use of any plant as an efficient insect repellent depends on the concentration of the extract used. Testing of the extracts and fractionates at higher concentration may reveal the repellent activity of the plant. Similar results were reported where the acetone extract of *E. crassipes* has not exerted repellent activity towards maize weevil *Sitophilus zeamais* whereas it has shown an attractant property towards the test insects (**Chakradhar *et al*, 2010**).

4.7 *In silico* molecular docking

The need for *in silico* prediction of the selected drug molecules prior to *in vivo studies* is crucial. Hence, in the present study, molecular docking of chosen stigmasterol derivatives were carried out with receptors COX-1(1EQG), COX-2 (1CVU) and SIRT1

(2HJH) using the *Hex* software 6.3. The prediction of the or affinity of the ligand to the receptor can analyzed by considering parameters such as docking score, the energy of binding molecules with the receptor, van der Waals interactions, hydrophobic interactions and rare charge interactions. The more the negative value of the energy of binding, the better is the affinity of the molecule to the receptor.

The crystal structure of the receptors used for molecular docking in the present study was retrieved from Protein Data Bank. The ligands used for docking are given in Figure 84. Indomethacin (S1) and argireline (S2), well known anti-inflammatory and antiageing agents respectively were used as standards for comparison. Energy scores of the docking of ligands to the receptors COX-1, COX-2 and SIRT1 is given in Table 44.

Figure 84. Ligands chosen for the molecular docking

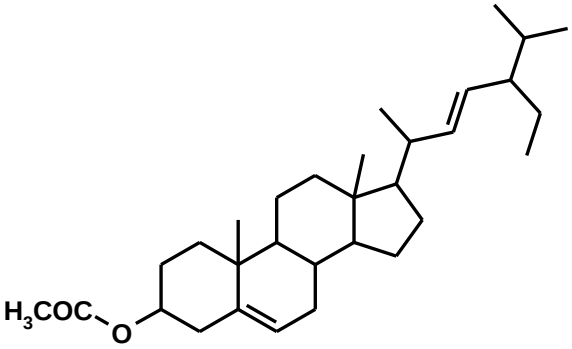

Stigma 5,22 diene-3 acetate (1)

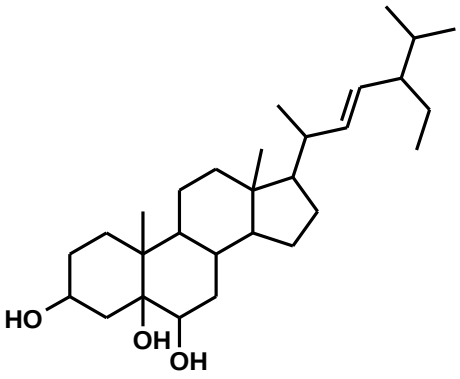

Stigmast 22-ene-3,5,6-triol (2)

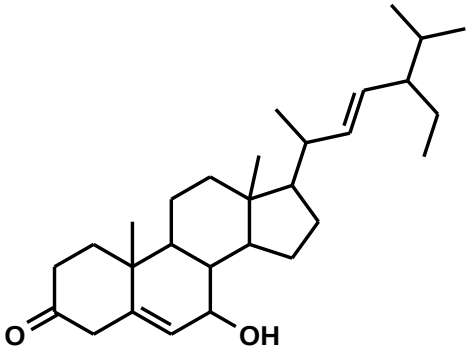

Stigma 5,22-ene-7 hydroxy-3-one (3)

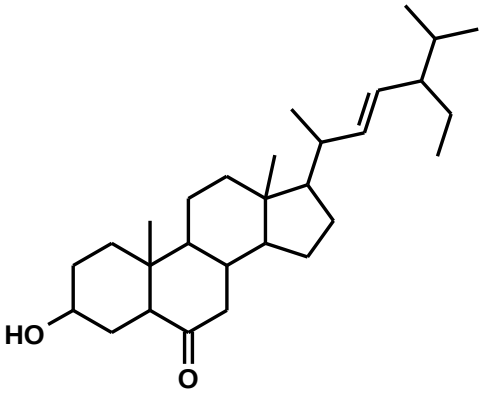

Stigma 22-ene-3, hydroxy-6-one (4)

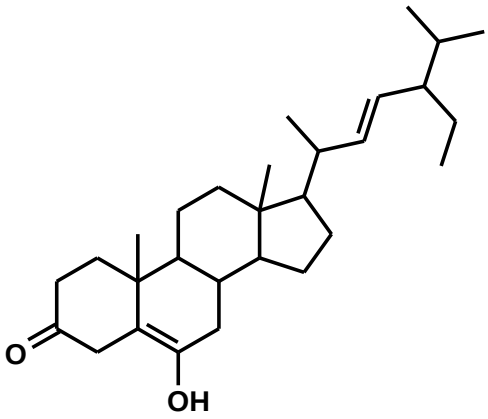

Stigma 5,22-ene-6 hydroxy-3-one (5)

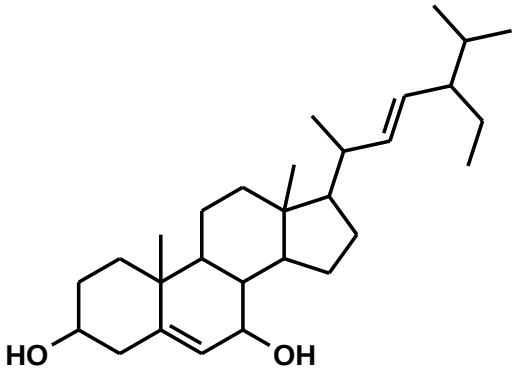

Stigma 5,22-diene-3,7-diol (6)

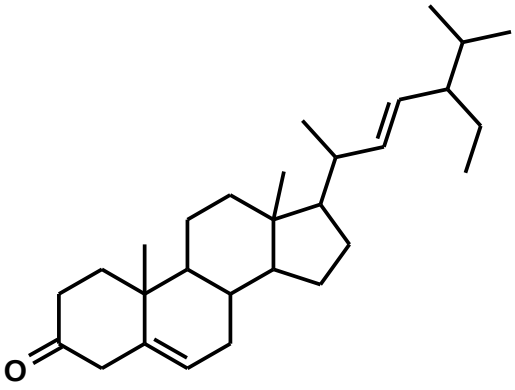

Stigma 5,22-diene-3-one (7)

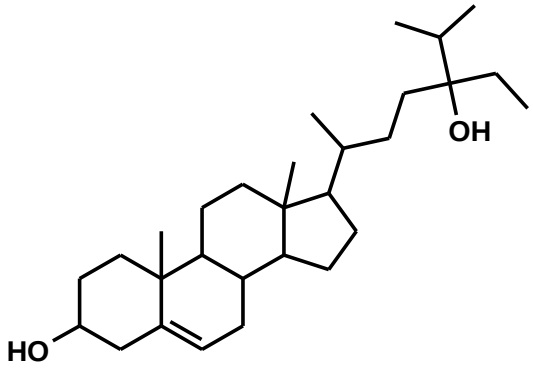

Stigmast-5ene-3 β-24 diol (8)

Table 44. Docking energy score of ligands against the receptors COX-1, COX-2 and SIRT1

Ligand	-E value (kcal/mole)		
	COX-1	COX-2	SIRT1
1	271.81	208.13	219.87
2	261.78	208.18	223.33
3	248.65	187.01	239.87
4	242.02	198.24	234.93
5	238.89	218.33	227.40
6	245.61	178.93	221.45
7	251.26	234.64	219.41
8	251.28	238.84	224.56
9	154.24	234.35	206.60

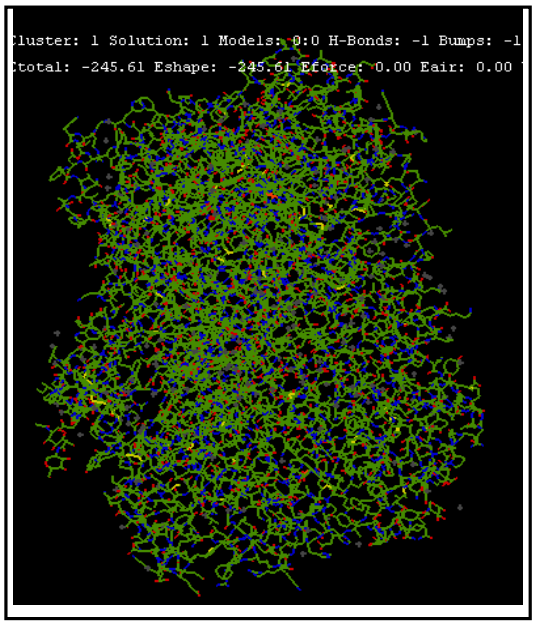

S1	208.64	169.42	-
S2	-	-	329.23

Figure 85. Representative docking of the ligand stigma 5,22-diene-3,7-diol to the receptor COX-1

It is quite obvious from the results that, when compared to the standard indomethacin at the specified orientation and docking control, all the ligands studied docked with COX-1, showed higher energy score. Maximum energy score (271.81) is showed by stigma 5,22 diene-3 acetate. In the case of docking of ligands with COX-2, stigmast-5ene-3 β-24 diol gave maximum energy score (238.40). The presence of acetate group enhances the lipophilic nature and hence the increased energy score (**Estour *et al,* 2007; Missel *et al,* 2010**) for the stigma 5,22 diene-3 acetate. The docking of ligands with SIRT1 showed almost equal energy score. Representative docking of stigma 5,22-diene-3,7-diol to the receptor COX-1 is given in Figure 85.

The results depict that the stigmasterol derivatives are involved in the anti-inflammatory activity of the extracts. These chemical constituents can be used in anti-inflammatory and antiageing drugs. The presence of stigmasterol in *E. crassipes* hence suggests anti-inflammatory activity for the extracts. Based on the results of *in* silico docking, research on anti-inflammatory activity of solvent extracts of *E. crassipes* (**Sujitha *et al,* 2012**) carried out in our laboratory was successful.